Aus der Berufsgenossenschaftlichen Unfallklinik

Klinik für Unfall- und Wiederherstellungschirurgie an der
Universität Tübingen

Role of neutrophil extracellular traps in delayed fracture healing of type 2 diabetics

Inaugural-Dissertation
zur Erlangung des Doktorgrades
der Humanwissenschaften

der Medizinischen Fakultät
der Eberhard Karls Universität
zu Tübingen

Vorgelegt von

Linnemann, Caren

2022

Dekan:	Professor Dr. B. Pichler
1. Berichterstatter:	Professor Dr. A. Nüssler
2. Berichterstatter:	Professor Dr. R. Lukowski

Tag der Disputation: 15.07.2022

To all the healthy volunteers

Table of contents

Abbreviations

ANOVA	Analysis of variance
AP	Alkaline phosphatase
ARDS	Acute respiratory distress syndrome
ARMS-PCR	Amplification refractory mutation system polymerase chain reaction
ATRA	All-*trans* retinoic acid
AUC	Area under the curve
BMI	Body mass index
BSA	Bovine serum albumin
CCL	CC chemokine ligand
CCR	CC chemokine receptors
cfDNA	Circulating free DNA
CI	Calcium ionophore A23187
Cit-H3	Citrullinated histone H3
CRP	C-reactive protein
DAMP	Danger-associated molecular patterns
DCs	Dendritic cells
DCFH-DA	Dichloro-dihydro-fluorescein diacetate
DEPC	Diethyl pyrocarbonate
DFS	Diabetic foot syndrome
DHE	Dihydroethidium
DHR	Dihydrorhodamine
DM	Diabetes mellitus
DMSO	Dimethyl sulfoxide
ECIS	Electric cell-substrate impedance sensing
ECL	Enhanced chemiluminescence
EDTA	Ethylenediaminetetraacetic acid
ETs	Extracellular traps
FCS	Fetal calf serum
fMLP	*N*-Formylmethionine-leucyl-phenylalanine

GM-CSF	Granulocyte-macrophage colony-stimulating factor
HbA1c	Hemoglobin A1c
HG	High glucose
HUVECs	Human umbilical vein endothelial cells
NE	Neutrophil elastase
HPRT	Hypoxanthine-guanine phosphoribosyl transferase
hTERT	human telomerase reverse transcriptase
ICU	Intensive care unit
IFN	Interferon
IL	Interleukin
Ins	Insulin
LDH	Lactate dehydrogenase
Leu	Leupeptin
LPS	Lipopolysaccharide
MAPK	Mitogen-activated protein kinase
MMP	Matrix metalloproteinase
MOF	Multi-organ failure
MPO	Myeloperoxidase
MSCs	Mesenchymal stem cells
mtDNA	mitochondrial DNA
NETs	Neutrophil extracellular traps
NF-κB	Nuclear factor kappa B
NOX	NADPH oxidase
NSAIDs	Nonsteroidal anti-inflammatory drug
PAD4	Peptidyl arginine deiminase type IV
PBMC	Peripheral blood mononuclear cell
PBS	Phosphate buffered saline
Pep A	Pepstatin A
p-ERK	Phospho-extracellular signal-regulated kinases
p-GSK3β	Phospho-glycogen synthase kinase-3β
PKC	Protein kinase C
PMA	Phorbol 12-myristate 13-acetate

PMNs	Polymorphonuclear leukocytes
PMSF	Phenylmethylsulfonyl fluoride
p-p38	Phospho- p38 MAPK
RA	Rheumatoid arthritis
RIPA	Radioimmunoprecipitation assay
ROS	Reactive oxygen species
PCR	Polymerase chain reaction
SDS-PAGE	Sodium dodecyl sulfate polyacrylamide gel electrophoresis
SLE	Systemic lupus erythematosus
SNP	Single nucleotide polymorphism
SRB	Sulforhodamine B
T2DM	Type 2 diabetes mellitus
TBE	Tris/Borate/Ethylenediaminetetraacetic acid
TBS-T	Tris-buffered saline with tween
TGF	Transforming growth factor
TLR	Toll-like receptor
TNF	Tumor necrosis factor
UGT1A6	UDP-glucuronosyltransferase 1-6

List of tables

List of figures

1. Introduction

1.1 Diabetes

Diabetes is a prominent disease whose prevalence is increasing worldwide. More than 415 million people are affected, and the number is estimated to double during the next decade (Federation, 2019). In Germany, about 9 million people have been diagnosed with diabetes, from which about 90% have type 2 diabetes mellitus (T2DM) (Heidemann *et al.*, 2017).

T2DM is associated with several secondary diseases like cardiovascular complications, nephro- and neuropathies, and micro- and macroangiopathies. Additionally, T2DM patients show abnormal wound (Baltzis *et al.*, 2014) and fracture healing and an increased risk for falls (Hamann *et al.*, 2012).

Besides diagnosed T2DM patients, there is a high estimated number of undiagnosed cases and prediabetic patients. Before T2DM can manifest, a long prediabetic state occurs. Glucose levels are higher in this state, and insulin resistance develops (Greiner *et al.*, 2020). These patients already show altered bone structure and an increased risk of developing complications during fracture healing (Chen *et al.*, 2020). In a study at the University Hospital Tübingen, where all hospitalized patients were monitored for 1 month, nearly half of them were reported to have prediabetes (24%) or diabetes (22%) (Kufeldt *et al.*, 2018). At the BG Unfallklinik Tübingen, 13% of all investigated patients had a documented T2DM. In the septic and geriatric ward of the Unfallklinik, this number increased up to 20% (Pscherer *et al.*, 2017a). Moreover, T2DM patients also represent a relevant group with more complications and prolonged hospital stay (Sharma *et al.*, 2013).

Due to the high number of diabetic patients, complications in diabetic fracture healing are a highly relevant socio-economic burden (Kahm *et al.*, 2018).

1.1.1 Diabetes and bone

The reasons for delayed fracture healing in T2DM patients are still not fully understood. Despite having a higher bone mineral density, the fall and fracture

risk in T2DM patients is higher than in non-diabetics. Their bone stability is reduced (Dede *et al.*, 2014, Schwartz *et al.*, 2011), and lower bone turnover is observed (Sassi *et al.*, 2018). Additionally, the fall risk is increased (Carnevale *et al.*, 2014).

Diabetic fracture healing is associated with a prolonged hospital stay (Sharma *et al.*, 2013) due to higher complication rates (Hernandez *et al.*, 2012, Pscherer *et al.*, 2016, Pscherer *et al.*, 2015). The prolonged stay has two negative effects: T2DM patients have twice the medical costs compared with non-diabetics (Ulrich *et al.*, 2016), and patients have a reduced (subjective) quality of life (Wintermeyer *et al.*, 2019). Additionally, diabetes is still the main reason for non-traumatic amputations of the lower limb (Kröger *et al.*, 2017) due to the high rate of diabetic patients developing diabetic foot syndrome (DFS) or Charcot-osteoarthropathy (Sämann *et al.*, 2008). Interesting in this regard, the costs and 5-year survival rate of DFS treatment are generally similar to those of cancer (Armstrong *et al.*, 2020).

Bone cells are also directly affected by diabetes. The altered factors in the blood of diabetics directly affect bone cells by inducing proliferation instead of differentiation (Ehnert *et al.*, 2015b, Pscherer *et al.*, 2013). Further, the recruitment of hematopoietic stem cells and proangiogenic cells is altered (Fadini *et al.*, 2013, Ferraro *et al.*, 2011), and microangiopathy can be found in bone (Oikawa *et al.*, 2010).

In recent years, the role of the immune system in bone healing has received more attention. T2DM patients show a constant inflammatory state (Alexandraki *et al.*, 2008) and a reduced response to pathogenic stimuli (Jin *et al.*, 2020). Changes in cytokine levels in the blood also directly affect bone cells leading to reduced osteoblast maturation (Ehnert *et al.*, 2015b).

1.2 Fracture healing

Three different types of fracture healing are generally distinguished: intramembranous, endochondral, and primary. Intramembranous and primary bone healing only apply for particular locations and very small defects. This process is driven by mesenchymal stem cells (MSCs), which directly differentiate

into osteoblasts (Rutkovskiy *et al.*, 2016). Most bones heal via endochondral fracture healing, where cartilage formation is the first step in the bone defect, which is then remodeled into bone.

Endochondral fracture healing can be divided into three main phases. First, in the inflammatory phase, a hematoma is formed, and immune cells invade the damaged tissue (first days after fracture). A soft callus is then built within the first weeks, which is then remodeled into the hard callus (3 weeks up to several years) (Einhorn and Gerstenfeld, 2015). In optimal cases, the bone reaches its original stability.

1.2.1 Fracture hematoma

The conditions in the fracture hematoma characterize the beginning of fracture healing: low pH, increased lactate, and oxygen deficiency (Hoff *et al.*, 2016, Pfeiffenberger *et al.*, 2019).

The hematoma is formed directly after the fracture due to ruptured blood vessels (Kolar *et al.*, 2011, Lu *et al.*, 2008). In the beginning, it consists mainly of a fibrin network (Loi *et al.*, 2016) formed by fibroblasts (Brighton, 1984). The fracture hematoma is crucial for fracture healing (Grundnes and Reikerås, 1993). In general, the fracture hematoma is a potent inducer of bone formation and can trigger ectopic bone generation (Mizuno *et al.*, 1990).

The invading immune cells (Hoff *et al.*, 2016) induce inflammation, which is essential for the regeneration process (Schmidt-Bleek *et al.*, 2012). Neutrophils, the first immune cells arriving in the hematoma, help to stabilize the fibrin network (Varjú and Kolev, 2019).

Several important factors are secreted by the fracture hematoma in a highly orchestrated manner. Initially, inflammatory cytokines (interleukin [IL]-6, tumor necrosis factor [TNF]-α, IL-1β) are released, and polymorphonuclear leukocytes (PMNs), especially neutrophils, are recruited. Then, in a second step, more anti-inflammatory cytokines (IL-10, transforming growth factor [TGF]-β) are secreted, and macrophages replace neutrophils (Maruyama *et al.*, 2020). Revascularization of the bone is the next essential step in fracture healing

(Ramasamy *et al.*, 2014), where factors released from leukocytes play an important role (Schmidt-Bleek *et al.*, 2009). In the subsequent step, MSCs are recruited (Pfeiffenberger *et al.*, 2019), which differentiate into the cells essential for the bone matrix: chondrocytes and osteoblasts (Knight and Hankenson, 2013). The chemokine cocktail from the fracture hematoma recruits MSCs (Hoff *et al.*, 2016) and induces their proliferation and osteogenic differentiation (Wasnik *et al.*, 2018).

One of the first factors secreted by platelets and released from the bone by the acidic environment is TGF-β (Crane and Cao, 2014). This cytokine is essential for the recruitment of MSCs and their proliferation (Tang *et al.*, 2009). TGF-β levels rapidly decline after the beginning of fracture healing (Sarahrudi *et al.*, 2011). When the decline does not occur, increased TGF-β can be harmful for osteogenic differentiation (Bosetti *et al.*, 2007, Ehnert *et al.*, 2010). TGF-β is increased in T2DM patients (Ehnert *et al.*, 2015b).

Other factors secreted by the fracture hematoma are chemokines (chemokine ligand 2 [CCL2], CCL5, CCL7, CCL8, CXCL1-3, CXCL12, IL-8) that help to attract MSCs and immune cells (Förster *et al.*, 2016, Hoff *et al.*, 2016, Ishikawa *et al.*, 2014, Wintges *et al.*, 2013, Xing *et al.*, 2010). Additionally, classical inflammatory cytokines like IL-6, IL-1β, interferon [IFN]-γ, and TNF-α are released from the fracture hematoma (Hoff *et al.*, 2016). The invading MSCs first differentiate into chondrocytes in endochondral fracture healing and later into osteoblasts (Einhorn and Gerstenfeld, 2015). Cell types interacting with MSCs are osteoclasts, which are responsible for bone remodeling and degradation of the soft callus (Einhorn and Gerstenfeld, 2015).

Alterations in the differentiation or migration of MSCs can negatively affect fracture healing. Factors that may negatively influence migration and differentiation of MSCs—and, consequently, fracture healing—include smoking (Aspera-Werz *et al.*, 2019, Castillo *et al.*, 2005), Nonsteroidal anti-inflammatory drugs (NSAIDs) (Hernandez *et al.*, 2012), poor nutrition (Calori *et al.*, 2007), rheumatoid arthritis (RA), or osteoporosis (Nikolaou *et al.*, 2009).

1.3 The immune system in bone healing

At the beginning of the healing process, the inflammatory process substantially affects the clinical outcome (Einhorn and Gerstenfeld, 2015, Schmidt-Bleek *et al.*, 2012). The most abundant cells in the early fracture hematoma are neutrophils (Kovtun *et al.*, 2016), later followed by monocytes and macrophages and cells of the adaptive immune system (Julier *et al.*, 2017); Figure 1). Those cells stay longer in the fracture gap (Konnecke *et al.*, 2014), whereas neutrophils are only present during the first days after the fracture in normal fracture healing (Förster *et al.*, 2016). However, this can be different in delayed fracture healing, which is often characterized by a persistent inflammatory response (Toben *et al.*, 2011) and altered polarization of macrophages (Ackerman *et al.*, 2017, Schlundt *et al.*, 2018). This polarization of macrophages into the inflammatory ("M1") or anti-inflammatory ("M2") type strongly influences the healing outcome (Schlundt *et al.*, 2018, Wasnik *et al.*, 2018). Macrophages further support bone healing by releasing growth factors for the induction of angiogenesis (Debels *et al.*, 2013).

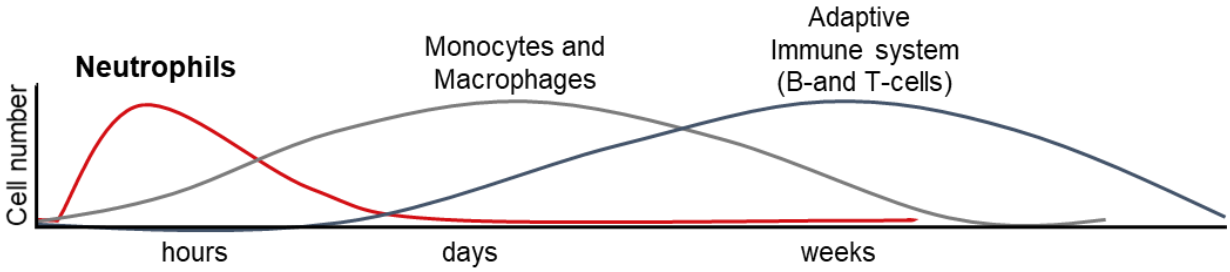

Figure 1: Time course of immune cells in the fracture gap. Neutrophils (red line) are the first cells in the fracture gap, followed by monocytes and macrophages (grey line). Cells of the adaptive immune system (blue line) invade the fracture gap after some days. Neutrophils reach their peak after some hours and decline in number until some days after the fracture. Monocytes and macrophages and the cells of the adaptive immune system stay longer in the fracture gap. Adapted from Julier *et al.*, 2017.

The role of neutrophils in fracture healing is not so clear. Neutrophils display a strong phagocytic activity and are solid promoters of an inflammatory response (Mantovani *et al.*, 2011), thus being crucial for clearance of debris and pathogen defense (Mantovani *et al.*, 2011). Neutrophils are attracted by the forming fracture hematoma (Bastian *et al.*, 2018b, Timlin *et al.*, 2005), most likely by damage-associated molecular patterns (DAMPs) like mitochondrial DNA (mtDNA (Li *et al.*, 2016)). Those mitochondrial components induce a systemic inflammatory

reaction (Zhang *et al.*, 2010) and the release of additional inflammatory cytokines like IL-8 or IL-1α (Chen and Nuñez, 2010, Heijink *et al.*, 2015).

In this regard, it is interesting that depletion of neutrophils in animal models leads to different results. In a rat model, depletion of neutrophils induced higher bone stiffness after a certain time of healing (Grøgaard *et al.*, 1990). On the contrary, in a mouse fracture model, neutrophil depletion induced delayed healing (Kovtun *et al.*, 2016). In another model, neutrophils improved fracture healing by inducing CCL2 secretion from monocytes, and depletion of neutrophils reduced healing abilities (Chan *et al.*, 2015). Neutrophils can promote healing by the production of a supporting matrix for MSC infiltration into the fracture gap (Bastian *et al.*, 2016), but can inhibit matrix formation by MSCs themselves *in vitro* (Bastian *et al.*, 2018a).

Overall, some modifications of the immune system have been suggested to treat delayed healing (Maruyama *et al.*, 2020). The peripheral blood mononuclear cell (PBMC) has been used successfully in animal models to improve tissue healing (Hacker *et al.*, 2016, Laggner *et al.*, 2020, Simader *et al.*, 2019) but *in vitro* studies suggest that this could be ineffective under diabetic conditions (Linnemann *et al.*, 2021).

These findings underline the importance of the immune system with the right balance of inflammatory and anti-inflammatory reactions.

1.4 The specific role of neutrophils and neutrophil extracellular traps

Neutrophils exhibit intense phagocytosis, oxidative burst, and cytokine release and can strongly influence other cell types (Amulic *et al.*, 2012). Thus, they play a crucial role in many inflammatory processes in the human body. Additionally, they can release DNA as a defense mechanism to trap pathogens (Brinkmann *et al.*, 2004). The released DNA is covered with antimicrobial proteins and histones and builds large structures, so-called neutrophil extracellular traps (NETs) (Bruschi *et al.*, 2019). The released proteins can vary, but some are conserved (myeloperoxidase [MPO], cathepsin G, histones, granzyme G, cathelicidin, catalase; Bruschi *et al.*, 2019, Petretto *et al.*, 2019). NETs are a highly potent

defense mechanism against large pathogens and those evading phagocytosis (von Köckritz-Blickwede *et al.*, 2016). Still, excessive NETs are involved in the pathogenesis of many inflammatory diseases like RA or systemic lupus erythematosus (SLE) (Mitsios *et al.*, 2016). Natural inducers of NET release are bacterial or fungal components (Kenny *et al.*, 2017), cytokines (An *et al.*, 2019), or crystal structures (Tatsiy *et al.*, 2019).

Other immune cell types can also release extracellular traps (ETs) (*e.g.*, macrophages, dendritic cells) under similar stimuli such as IL-8, phorbol 12-myristate 13-acetate (PMA), or reactive oxygen species (ROS) (Rayner *et al.*, 2018), but to a lesser extent (Goldmann and Medina, 2012).

The effect of NET formation in fracture healing and the impact of NETs on MSCs has not yet been investigated and is the topic of this study.

1.4.1 Neutrophils, NETs, and monocyte interaction

Monocytes are the second cell type arriving in the fracture gap, and they stay there longer than neutrophils (Stefanowski *et al.*, 2019). However, monocytes are strongly affected by the activation status of neutrophils. NETs induce a significant release of inflammatory cytokines (TNF-α, IL-6, IL-1β) by macrophages, which can further phagocytose and degrade NETs (Braian *et al.*, 2013, Lazzaretto and Fadeel, 2019). This activity depends on the stimulus inducing the NETs: Pathogen-induced NETs activated macrophages, whereas PMA-induced NETs did not (Braian *et al.*, 2013). Macrophages can support the clearance of NETs. Pre-treatment of NETs with DNase I facilitates this clearance. NET uptake itself does not necessarily augment inflammation, but in combination with a second stimulus (*e.g.*, lipopolysaccharide [LPS]), the inflammatory response can be boosted (Farrera and Fadeel, 2013). Similarly, NET induction by titanium surfaces leads to inflammatory macrophage polarization (Abaricia *et al.*, 2020). The neutrophil-monocyte interaction also plays a role in the pathogenic wound healing of diabetic patients: Overactivation of NETs leads to consistent activation of macrophages, which contributes to delayed wound healing (Liu *et al.*, 2019a).

The interaction between neutrophils (and NETs) with monocytes is essential at the beginning of fracture healing.

1.4.2 Mechanisms of NET formation

There are two different forms of NETs: suicidal NETs (also called NETosis) and vital NET formation. In suicidal NETosis, dying neutrophils release their genomic DNA (Brinkmann and Zychlinsky, 2007), whereas in vital NET formation, neutrophils release mitochondrial or nuclear DNA in vesicles (de Buhr and von Kockritz-Blickwede, 2016, Pilsczek *et al.*, 2010). Vital NET formation allows neutrophils to maintain their phagocytic activity (Yipp *et al.*, 2012).

Several cellular processes are involved in NET formation, and the used pathways are highly stimulus-dependent. For NETosis, ROS formation is essential (Al-Khafaji *et al.*, 2016). MPO is activated and, together with neutrophil elastase (NE), leads to actin and nuclear envelope degradation (Metzler *et al.*, 2014). Cell cycle proteins (Amulic *et al.*, 2017) and peptidyl arginine deiminase type IV (PAD4) (Lewis *et al.*, 2015) are also involved. *In vitro*, calcium ionophores (such as A23187 [CI]) or PMA (Protein kinase C activator) are often used as activators of NET formation in model systems (Linnemann *et al.*, 2020).

Calcium ionophores induce NET formation by high calcium levels in the cells. Calcium influx activates PAD4 and mitochondrial ROS release (Douda *et al.*, 2015). Inhibition of mitochondrial ROS prevents NET formation by calcium ionophores (Douda *et al.*, 2015). PAD4 itself is translocated to the nucleus, where it contributes to chromatin decondensation by citrullination of histones (Thiam *et al.*, 2020). During Ca^{2+}-induced NET formation, ROS are less relevant than during NETosis (Pieterse *et al.*, 2018).

PMA-induced NETosis is strongly dependent on ROS formation by NADPH oxidase (NOX; Al-Khafaji *et al.*, 2016) and requires activation of MPO (Kenny *et al.*, 2017). The LPS-activated NET formation relies on similar pathways as PMA-induced NET formation but leads to slower ROS production (de Bont *et al.*, 2018). Inhibition of PAD4 prevents NET formation of diverse stimuli (Tatsiy and McDonald, 2018).

Common pathways activated for NET formation involve mitogen-active protein kinases (MAPKs), namely extracellular signal-regulated kinase (ERK) or p38. ERK and p38 are essential for NET formation by different stimuli —for example,

immobilized immune complexes (Behnen *et al.*, 2014), *N*-Formylmethionyl-leucyl-phenylalanine (fMLP), granulocyte-macrophage colony-stimulating factor (GM-CSF), PMA, and TNF-α (Tatsiy and McDonald, 2018). Phospho-p38 (p-p38) but not phospho-ERK (p-ERK) was shown to be essential for calcium-induced NET formation (Douda *et al.*, 2015).

Early after NET activation, inhibition of signaling pathways successfully prevents NET formation, whereas at later stages, inhibition of NET formation is difficult when a point of no return is reached (Neubert *et al.*, 2018). In general, a crosstalk between the different pathways is not excluded. An overview of the possible signaling pathways with the stimulants PMA, CI, and LPS can be found in Figure 2.

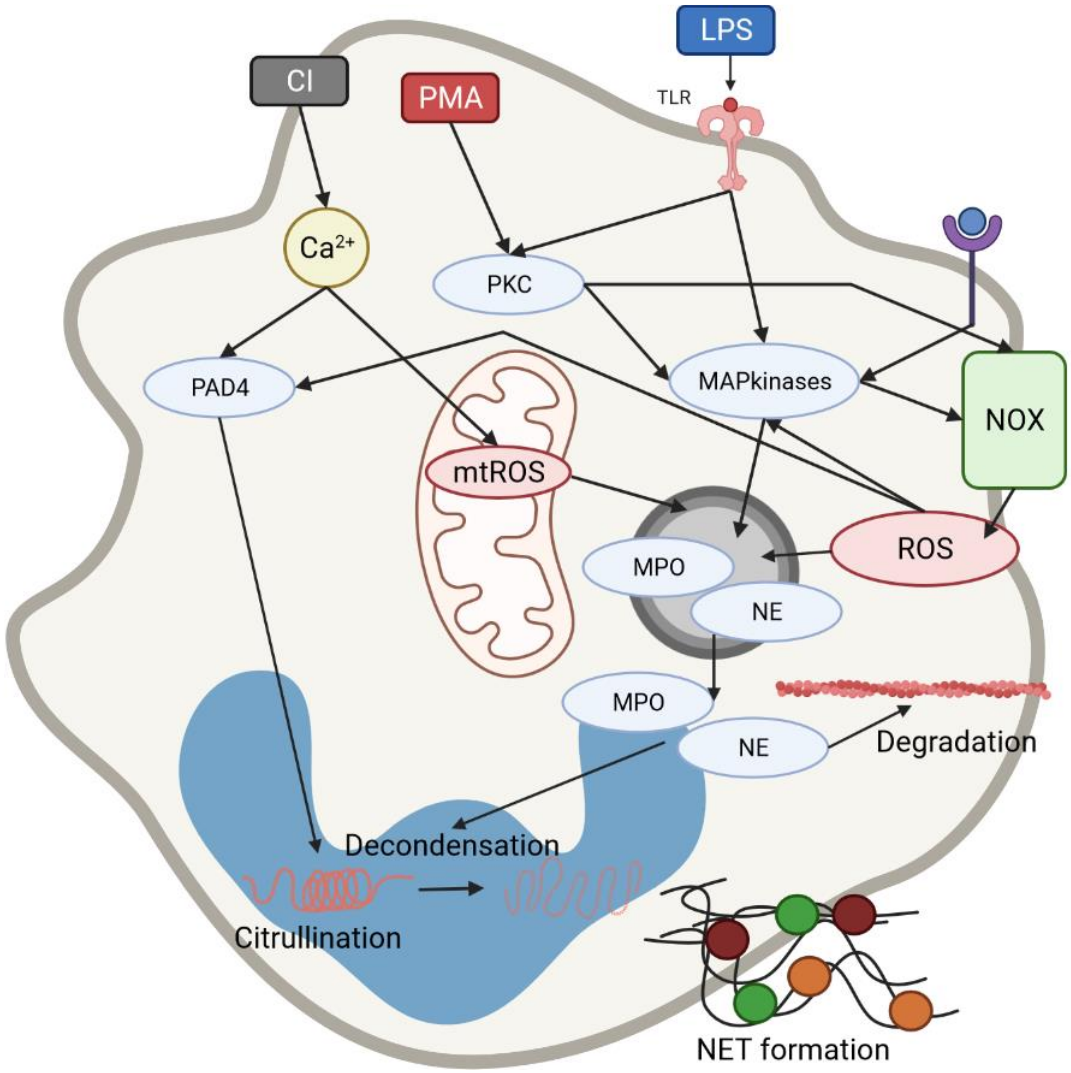

Figure 2: Overview of the main signaling pathways involved in NET formation by PMA, CI, or LPS stimulation. PMA: phorbol 12-myristate 13-acetate; CI: calcium ionophore A23187; LPS: lipopolysaccharide; PKC: protein kinase C; ROS: Reactive oxygen species; mtROS: mitochondrial ROS; NOX: NADPH oxidase; NE: neutrophil elastase; MPO: myeloperoxidase; PAD4: peptidyl arginine deiminase 4; TLR: Toll-like receptor. Modified from Denning *et al.*, 2019, Neubert *et al.*, 2018, Papayannopoulos *et al.*, 2010, Speziale and Pietrocola, 2021, Vorobjeva, 2020, Vorobjeva and Chernyak, 2020. Created with Biorender.com.

1.4.3 Peptidyl arginine deiminase 4 (PAD4)

PAD4 is one of the main drivers of NET formation, namely by inducing chromatin decondensation (Neubert *et al.*, 2018). PAD enzymes catalyze the modification of arginine residues to citrulline. In humans, there are five PAD isoforms (PAD1-4 and PAD6; Wang and Wang, 2013). PAD2 has the broadest range of targets, whereas PAD4 is mainly expressed in immune cells and targets histones (Mondal and Thompson, 2019).

Several studies have shown the importance of PAD4 for NET formation (Hemmers *et al.*, 2011, Tatsiy and McDonald, 2018). PAD4 citrullinates histones in the nucleus and directly drives chromatin expansion (Leshner *et al.*, 2012, Neubert *et al.*, 2018). The primary marker for PAD4 action on histones is citrullinated histone H3 (cit-H3).

The main regulator of PAD4 is calcium. With its five calcium binding sites, PAD4 needs high calcium concentrations for activation and subsequent nuclear translocation (Arita *et al.*, 2004, Mastronardi *et al.*, 2006). In neutrophils, activation of PAD4 by high intracellular calcium is directly correlated to increased ROS production (Zhou *et al.*, 2018), which is an additional direct prerequisite for NET formation (Al-Khafaji *et al.*, 2016).

PAD4 plays an important role in various pathologies such as wound healing (Wong *et al.*, 2015) and reduction of RA (Seri *et al.*, 2015). A scaffold loaded with a PAD4 inhibiting peptide improved wound healing *in vitro* and in an *in vivo* diabetic rat model (Kaur *et al.*, 2020). Moreover, PAD4 is relevant in thrombosis formation (Martinod *et al.*, 2013, Sorvillo *et al.*, 2019), multiple sclerosis (Mastronardi *et al.*, 2006), and mortality after sepsis (Costa *et al.*, 2018). In the same line of evidence, researchers recently showed that chemical inhibition of PAD4 prevented the development of autoimmune type 1 diabetes in a mouse model (Sodré *et al.*, 2021).

1.4.4 *PADI4* and its single nucleotide polymorphisms

Single nucleotide polymorphisms (SNPs) are single base changes in the genome that can be found in every human. SNPs are commonly defined as base changes that occur in > 1% of a defined population, so they are different from individual mutations (Consortium *et al.*, 2015). Possible changes are deletions, base pair changes, or insertions. SNPs cannot affect the final mRNA or lead to shifts in the reading frame or amino acid changes. They determine characteristics such as our hair color or our blood group. However, SNPs in specific genes can also lead to diseases (such as cystic fibrosis; Wright *et al.*, 2011), increase the risk to develop certain diseases (variants in the ApoE gene in the development of Alzheimer's disease; Namboori *et al.*, 2011), or alter the response to certain drugs

by changes in the cytochrome P450 enzymes of the liver (Shastry, 2007). Combinations of certain SNPs in one person are called a haplotype.

There are 89 SNPs of *PADI4* cited in PubMed articles; they can be found in the dbSNP database (dbSNP database, search term “PADI4”, NCBI, October 22, 2021). A haplotype has been associated with increased risk for RA in a Japanese population (rs11203366, rs11203367, rs874881, rs1748033; Suzuki *et al.*, 2003) and three of those SNPs have been associated with RA in a German population (rs11203366, rs11203367, rs874881; Hoppe *et al.*, 2006). Another SNP (rs2240335) has been associated with increased PAD4 levels (Naranbhai *et al.*, 2015) and correlated to RA development (Mergaert *et al.*, 2019). Two other SNPs (rs1748033, rs1635564) have been associated with the development of SLE or lupus nephritis (Massarenti *et al.*, 2019).

Three *PADI4* SNPs are known to affect PAD4 stability and activity directly and have a major allele frequency >45%: 163 A>G, 245 C>T, and 335 C>G (Horikoshi *et al.*, 2011). All three variants lead to an amino acid change in the PAD4 protein. These three SNPs show a linkage disequilibrium from nearly 1 (LDLink database, January 23, 2022; Bang *et al.*, 2010, Ehnert *et al.*, 2019). In the minor haplotype, the PAD4 protein has three altered amino acids. The role of the three *PADI4* SNPs in NET formation shall be investigated here. Details for the three variants can be found in Table 1.

Table 1: Characteristics of the three investigated *PADI4* SNPs. Modified from Ehnert *et al.*, 2019.

	163 A>G	**245 C>T**	**335 C>G**
Reference	rs11203366	rs11203367	rs874881
Major allele frequency (Ensembl)	47.5% (G)	46.7% (T)	47.8% (G)
Amino acid mutation	Gly55Ser	Val82Ser	Gly112Ala

1.4.5 NETs and diseases

In recent years, NETs have been implicated in the pathogenicity of various diseases. Increased neutrophil counts and NET-associated genes have been found in severe COVID-19 cases (Middleton *et al.*, 2020, Wang *et al.*, 2020). COVID-19 is associated with a high risk of developing thrombotic events (Middleton *et al.*, 2020). Such events are also associated with increased morbidity and mortality in trauma patients (Lichte *et al.*, 2015, Paffrath *et al.*, 2010). In the same line of evidence, NETs have been shown to contribute to the formation of deep vein thrombosis in mice after trauma (Dyer *et al.*, 2018), and high circulating NET markers (circulating free DNA [cfDNA] and cit-H3) were predictive for the development of thrombosis (Liu *et al.*, 2021). Considering these findings NET formation could be highly relevant for trauma patients.

Furthermore, NE-DNA complexes and nucleosome levels have been correlated with mortality in sepsis patients (Kaufman *et al.*, 2017). Isolated neutrophils from septic patients release more NETs, and serum from sepsis patients induced more NETs in healthy neutrophils (Yang *et al.*, 2017), highlighting a dysregulation of NET formation as a possible strong contributor to complications.

In autoimmune diseases like SLE and RA, NETs contribute to the immunogenicity of the diseases (Khandpur *et al.*, 2013, Pieterse *et al.*, 2015). Specifically in RA, NETs have been shown to directly contribute to cartilage destruction (Carmona-Rivera *et al.*, 2020). NETs worsen the disease by directly damaging tissue damage and boosting inflammation.

Overall, NETs have been shown to be involved in tissue damage, immunogenicity, and thrombosis in several conditions (an overview is shown in Figure 3).

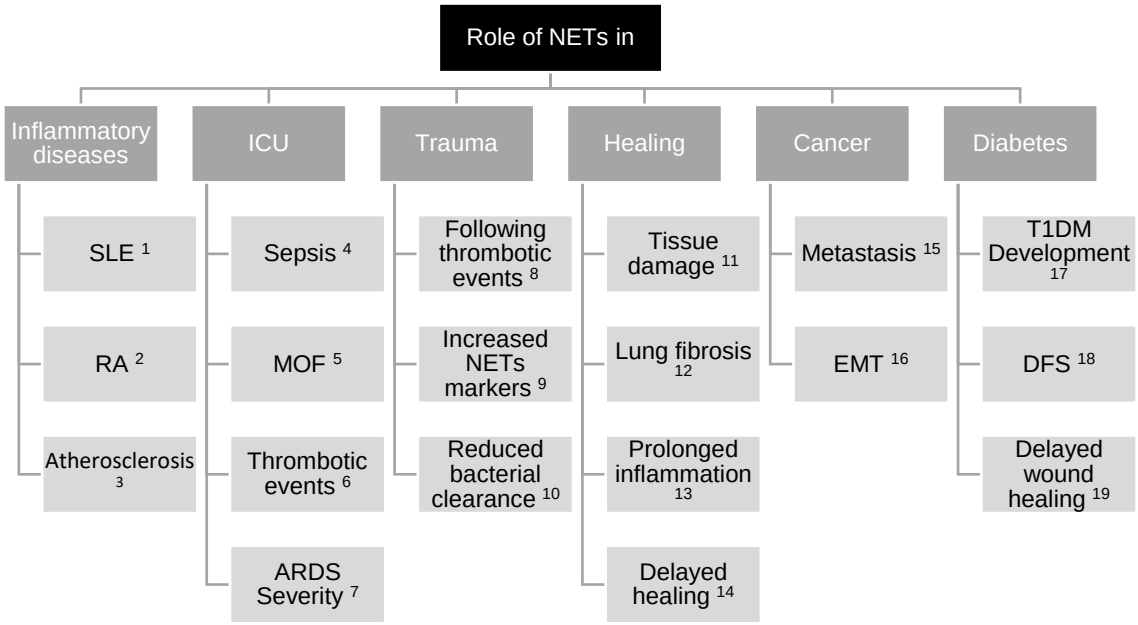

Figure 3: Overview of NET-associated pathologies.
SLE: systemic lupus erythematosus; RA: rheumatoid arthritis; ICU: intensive care unit; MOF: multi-organ failure; ARDS: acute respiratory distress syndrome; EMT: epithelial to mesenchymal transition; DFS: diabetic foot syndrome. [1] (Pieterse *et al.*, 2015), [2] (Khandpur *et al.*, 2013), [3] (Stakos *et al.*, 2015), [4] (Kaufman *et al.*, 2017), [5] (Margraf *et al.*, 2008), [6] (Yang *et al.*, 2017), [7] (Lefrancais *et al.*, 2018), [8] (Liu *et al.*, 2021), [9] (Goswami *et al.*, 2021), [10] (Li *et al.*, 2015), [11] (Agarwal *et al.*, 2019), [12] (Chrysanthopoulou *et al.*, 2014), [13] (Liu *et al.*, 2019a), [14] (Heuer *et al.*, 2021), [15] (Yang *et al.*, 2020), [16] (Pieterse *et al.*, 2017), [17] (Sodré *et al.*, 2021), [18] (Liu *et al.*, 2019a), [19] (Wong *et al.*, 2015).

1.4.6 NETs in healing processes

As mentioned above, NETs have been associated with tissue damage and overshooting inflammation. Inflammation is a potent modulator of successful healing, and prolonged inflammation is related to a delay in recovery (Toben *et al.*, 2011). After tissue injury, NETs are formed in response to released mtDNA (Liu *et al.*, 2019b), and NET markers in the blood (nucleosomes, free DNA) are elevated (Goswami *et al.*, 2021). Released NETs after trauma could be made of mtDNA (McIlroy *et al.*, 2014), which further promotes inflammation (Lood *et al.*, 2016). Such persistent circulating NETs could be found in septic patients (Otawara *et al.*, 2018), and increased levels of cfDNA are predictive for mortality in burn patients (Altrichter *et al.*, 2010), showing a negative effect of overshooting circulating NETs.

Another purpose of inflammation after trauma is clearance of contamination in injured areas. Trauma/tissue injury directly affects the clearance potential of neutrophils and NETs: Neutrophils from trauma patients spontaneously release more NETs, but the clearance of *Staphylococcus aureus* is reduced in the lungs (Li *et al.*, 2015); thus, the antimicrobial activity of neutrophils could be reduced (Hazeldine *et al.*, 2019).

However, for tissue, a reduction in NET formation could be rather beneficial. In wound models, reduced NET formation is associated with faster healing (Heuer *et al.*, 2021). Especially in diabetic wounds, NETs prolong inflammation and inhibit wound repair (Liu *et al.*, 2019a). Nevertheless, in combination with toll-like receptor (TLR) 4-activated MSCs, NETs seem to be beneficial in wound healing (Munir *et al.*, 2020).

1.4.7 Neutrophils and NETs in diabetes

T2DM is characterized by a constant faint inflammatory state (Randeria *et al.*, 2019). Major complications in T2DM patients after trauma are tissue damage, thrombotic events (Paffrath *et al.*, 2010), delayed healing (Pscherer *et al.*, 2017b), and vascular damage in general (Rhee and Kim, 2018), all of which are associated with NET formation.

Increased levels of circulating NET factors in T2DM patients are not surprising (Bryk *et al.*, 2019, Carestia *et al.*, 2016). Furthermore, increased levels of cit-H3 and cfDNA have been associated with increased risk for thrombotic events in T2DM patients (Bryk *et al.*, 2019), and increased levels of MPO-DNA complexes have been associated with microvascular complications in T2DM patients (Miyoshi *et al.*, 2016).

When analyzing isolated neutrophils from T2DM patients, the response of the cells to stimuli is altered (Joshi *et al.*, 2013), and the composition of the released NETs is changed (Soongsathitanon *et al.*, 2019), leading to reduced bactericidal activity (Arampatzioglou *et al.*, 2018, Parackova *et al.*, 2020). Additionally, T2DM neutrophils show an increased basal rate of NET formation (Joshi *et al.*, 2016), supporting clinical data with increased circulating NET markers in T2DM patients (Carestia *et al.*, 2016).

These findings are in line with earlier published work demonstrating that high glucose (HG) exposure of healthy neutrophils induced NET formation (Wang *et al.*, 2018). Furthermore, glucose pre-treatment of healthy neutrophils altered the response to various stimuli (Joshi *et al.*, 2013), indicating a strong dysregulation of NET formation in diabetes.

Regarding the effects on tissue, NETs participate in the destruction of the endothelial glycocalyx in *db/db* mice (Hirota *et al.*, 2020), and increased NET formation was found to be responsible for the delayed wound healing in diabetic mice (Wong *et al.*, 2015, Wong and Wagner, 2018).

Because the mechanisms of wound and fracture healing are similar, NETs could be involved in the delayed fracture healing of T2DM patients.

1.5 Aim of this work

In a mouse model of diabetes, increased NET formation and increased PAD4 levels led to a delay in wound healing (Wong *et al.*, 2015). Because wound and fracture healing mechanisms are somehow similar, this study aimed to investigate the effects of NETs on fracture healing in an experimental model of diabetes. The following questions were addressed:

1. Do T2DM patients release more NETs than controls?
2. What is the effect of diabetic conditions (high glucose, insulin) on NET release? How do fracture hematoma conditions (low pH, hypoxia) affect neutrophils and NET formation?
3. What is the effect of NETs on other cell types involved in fracture healing, namely MSCs and monocytes?
4. How is PAD4 involved in NET formation in humans, and how do *PADI4* variants influence NET formation?

The overall hypothesis is displayed in Figure 4. Neutrophils and monocytes get recruited by factors released after the fracture due to the fracture gap conditions (low oxygen, blood vessel rupture, low pH). Recruited neutrophils get activated. Here, the difference between diabetic and control conditions shall be analyzed regarding NET formation. The effect of NETs and MSCs shall then reveal whether NETs themselves can influence the attraction and differentiation of MSCs, leading to delayed bone healing in T2DM patients.

The overshooting formation of NETs could markedly harm the fracture healing process in T2DM patients. Several factors are hypothesized to be dysregulated: recruitment of neutrophils and MSCs, soluble factors, and PAD4 (see Figure 4 right side). Finding out more about the role of these factors could allow for new treatment options in T2DM fracture healing.

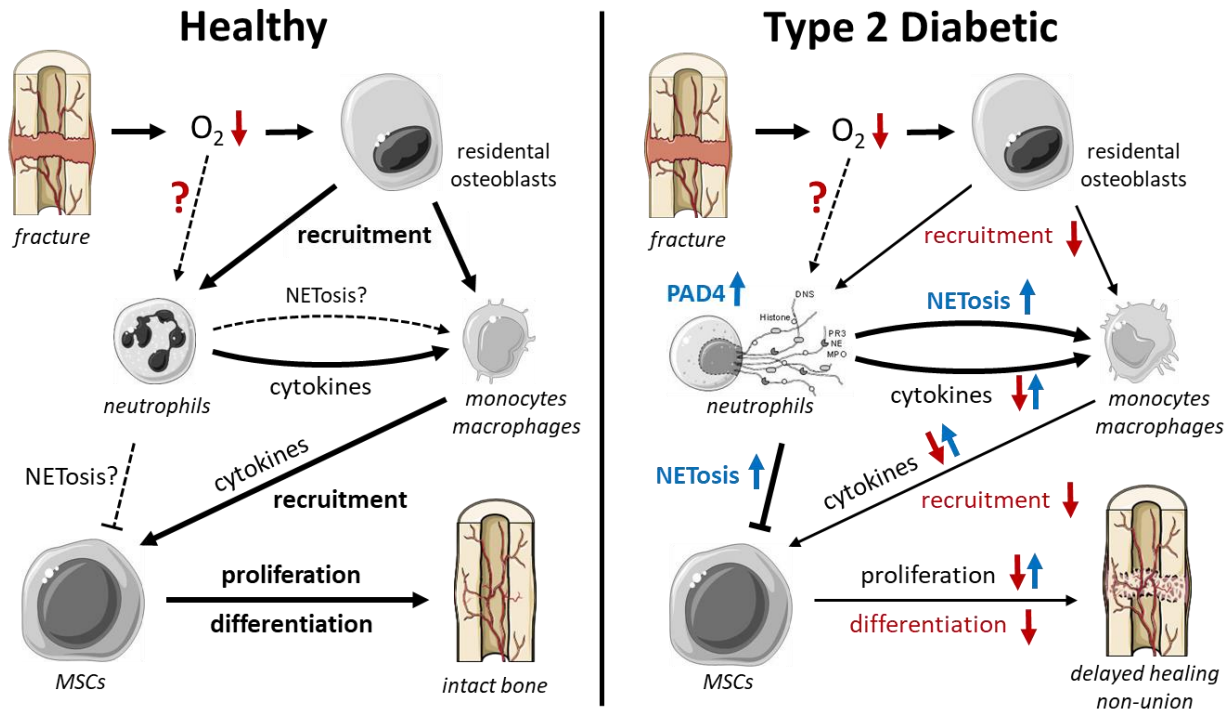

Figure 4: Hypothesis for the role of NETs in diabetic fracture healing. The left part of the figure shows the potential fracture healing process in healthy people, and the right part of the image shows the process in T2DM patients, with differences indicated by arrows. Red arrows indicate reduction; blue arrows indicate an increase.

Primary neutrophils from diabetic patients and healthy volunteers will be used to evaluate NET formation. The NET release will be analyzed by using the Sytox Green Assay and immunofluorescence analysis. The underlying mechanisms will be investigated by western blot analysis. An MSC line will be used to analyze the effect on bone cells, and a monocytic cell line will mimic the monocyte contribution. Migration and differentiation will be evaluated as the functional readout of osteogenic cells.

2. Material and Methods

2.1 Human samples

All samples were collected with the informed consent of the donors according to the Declaration of Helsinki. The experiments were approved by the Ethics Committee of the University Hospital Tübingen (666/2018B02).

2.1.1 Diabetic patients

To analyze NET formation, blood samples were collected from diabetic (T2DM and one viral-induced T1DM) patients and age-matched controls. NET release was analyzed after stimulation with PMA (50 or 100 nM), CI (4 µM), or 0.03% H_2O_2 by the Sytox Green Assay (see section 2.3.1). Protein levels (PAD4, cit-H3, MPO) were determined in neutrophils, which were stimulated for 1 h with 4 µM calcium ionophore A23187.

2.1.2 Patients with wounds

Samples were collected from patients with acute wounds (wound duration <30 days), sub-chronic wounds (wound duration 30-90 days), and chronic wounds (wound duration >90 days) after obtaining written informed consent. To analyze NET formation, venous blood samples were collected, neutrophils were isolated, and NET release in response to different concentrations of PMA (25, 50, 100 nM) or CI (0.5, 1, 4 µM) was evaluated by using the Sytox Green Assay.

2.2 Cell culture

All cell lines were regularly tested for mycoplasma contamination.

2.2.1 SCP-1 cells

SCP-1 cells, an immortalized bone-marrow-derived MSC cell line, were kindly provided by Prof. Matthias Schieker (Bocker *et al.*, 2008). SCP-1 cells were immortalized by lentiviral insertion of human telomerase reverse transcriptase (hTERT). SCP-1 cells were cultured in modified MEM-α medium with 5% FCS at 37°C in a humified atmosphere of 5% CO_2. The medium was changed twice a week, and cells were sub-cultured at 80%-90% confluence.

2.2.2 THP-1 cells

THP-1 cells are a monocytic cell line derived from an acute monocytic leukemia patient. Cells were purchased from the DSMZ (German Collection of Microorganisms and Cell Cultures GmbH, Braunschweig, Germany). They were cultured from 2×10^5 to 1×10^6 cells/mL in RMPI 1640 medium supplemented with 5% FCS.

2.2.3 Neutrophil isolation

Neutrophils were isolated as described previously (Linnemann *et al.*, 2020). Briefly, 6 mL of freshly collected venous blood was layered on 6 mL of Lympholyte-poly cell separation medium. After centrifugation at 500 *g* for 35 min without break, the different layers (plasma, PBMCs, granulocytes) were separated. Neutrophils were washed twice with 15 mL of phosphate-buffered saline (PBS; centrifugation at 400 *g*, 10 min, acceleration 5, deceleration 4). The neutrophil cell pellet was resuspended in RPMI plain medium (without phenol red, for the Sytox Green Assay), and cells were counted in a Neubauer counting chamber. Residual erythrocytes were not counted. Depending on the setup, neutrophils were diluted, and 2% of autologous plasma was added. The experiments with LPS as a stimulant were performed without adding autologous plasma because this component prevented activation. The cell concentrations used for the different assays can be found in Table 2.

Table 2: Concentration of neutrophils used for different assays.

Assay	**Cell concentration [cells/mL]**
Sytox Green Assay	2×10^5
Immunofluorescence	3×10^5
MPO activity	1×10^6
Protein isolation	1×10^6
Bio-impedance measurement	2×10^5
DCFH-DA/DHE/DHR	1×10^6

2.2.4 Diabetic conditions

Diabetic culture conditions were simulated as described previously (Freude *et al.*, 2012). The addition of up to 25 mM glucose to basal glucose in the medium simulated HG conditions. Insulin was added at a concentration of 160 IU/L if not otherwise indicated.

2.3 Analysis of NET formation

2.3.1 Sytox Green Assay

Isolated neutrophils were diluted to 2×10^5 cells/mL in RPMI without phenol red and stained with Sytox Green at a concentration of 1 µM. Cells were distributed to a pipetting reservoir, the stimuli added, and then the cells were plated into a 96-well culture plate. The plate was directly measured at Ex 485 nm/Em 520 nm to determine the 0-h value. Subsequently, the plate was measured every 30 min for 5-20 h, depending on the experimental setup. The cells were incubated continuously at 37°C with 5% CO_2. Measurements over a time course of 20 h were performed in the BMG LabTech ClarioStar (BMG Labtech, Ortenberg, Germany) with internal CO_2 and temperature control. At 3-5 h, depending on the used stimuli, microscopy images of each condition were taken with a fluorescence microscope (EVOS FL microscope, Thermo Fisher Scientific, Darmstadt, Germany) to confirm the results from fluorescence measurements. The standard concentrations of the used stimuli are listed in Table 3.

Table 3: Standard concentrations of different stimulants used in the Sytox Green Assay.

Stimulant	Standard concentration	Other concentrations used
PMA	100 nM	25 nM, 50 nM
CI	4 µM	0.5 µM, 1 µM
LPS	25 µg/mL	-
Insulin	160 IU/L	Dilution series
HG	25 mM	-
H_2O_2	0.03%	-

The area under the curve (AUC) was calculated to determine the total amount of released NETs. Modulation of the curve allowed for calculating the half-maximal stimulation time (EC_{50}) as a marker for the dynamics of NET release as described previously (Linnemann *et al.*, 2020).

2.3.2 MPO activity

MPO activity was determined by using the Myeloperoxidase Activity Assay Kit II (Promocell, Heidelberg, Germany). Isolated neutrophils were diluted to 1×10^6 cells/mL and stimulated for 1 h. After stimulation, cells were scratched in the culture dish and collected by centrifugation at 600 *g* for 10 min at 4°C. The cell pellet was resuspended in assay buffer (approximately 5×10^5 cells/10 µL of buffer) and incubated on ice for 10 min. To remove debris, the solution was centrifuged at 10000 *g* for 10 min at 4°C; the supernatant subjected to measurement. The activity was determined according to the manufacturer's instructions but with half of the sample volume in half-well 96-well plates (Greiner). The total protein content was determined by Lowry measurement (see section 2.5) to normalize the enzyme activity. The amount of formed fluorescein during the reaction was determined by a standard curve.

The enzyme activity was determined as recommended in the manufacturer's instructions. The detailed calculation can be found in Equation 1 and Equation 2 (see below).

$$MPO\ Activity = \frac{Amount\ of\ formed\ fluorescin}{(40\ min - 10\ min) \times sample\ volume\ in\ reaction\ [mL]} \times sample\ dilution\ factor = \frac{\mu U}{mL} \qquad \text{Equation 1}$$

$$Normalized\ to\ protein\ content = \frac{\frac{\mu U}{mL}}{Protein\ concentration\ of\ sample\ [\frac{\mu g}{mL}]} = \frac{mU}{mg\ Protein} \qquad \text{Equation 2}$$

2.3.3 Immunofluorescence

To analyze NET formation by immunofluorescence, microscopy slides were coated with poly-L-lysine as described previously (Linnemann *et al.*, 2020). Briefly, cells were diluted to 3×10^5 cells/mL and seeded onto self-made cover slides. Cells were then stimulated for 2-5 h, depending on the stimulus. The incubation time was derived from the Sytox Green Assay measurements. After incubation, cells were fixed with 4% paraformaldehyde and permeabilized with

1% Triton-X-100. Cells were stained with anti-MPO antibody overnight at 4°C and, after washing, incubated with Alexa Fluor 488–conjugated secondary antibody for 2 h at room temperature. Cells were counterstained with Hoechst 33342 and analyzed by fluorescence microscopy (EVOS FL microscope, Thermo Fisher Scientific, Darmstadt, Germany). At least five images were taken for each condition at 100× total magnification. For the quantification, all cells were counted in the DAPI channel (Hoechst 33342 staining), and only cells that were not round and exceeded a specific size were counted in the GFP channel (MPO staining). The ratio of cells counted in the GFP channel to all cells in the DAPI channel was taken as the ratio of NETosed cells (Equation 3). The macro for the automated quantification of the images can be found in Supplementary information V.

$$NETosed\ cells = \frac{Cells\ counted\ in\ the\ GFP\ channel}{All\ cells\ counted\ in\ the\ DAPI\ channel} \qquad \text{Equation 3}$$

2.3.4 Bio-impedance measurement

Bio-impedance was measured as described previously (Linnemann *et al.*, 2020) to evaluate the early activation of neutrophils by using electric cell-substrate impedance sensing (ECIS). Briefly, 80 µL of medium (RPMI without phenol red) with Sytox Green and stimulants (PMA, CI) was added into a 96-well xCelligence measurement plate (Omni Life Sciences, OLS, Bremen, Germany) in quadruplicates. The plate was used to measure the blank in the RTCA eSight device (OLS) in an incubator at 37°C, 5% CO_2 in a humidified atmosphere. After blank measurement, 20 µL of a concentrated neutrophil cell suspension was added to the xCelligence plate (final cell concentration 2×10^5 cells/mL), and the measurement started. Bio-impedance was measured at least every 15 min, and fluorescence microscopy images were taken every 30 min. The bio-impedance measurement was normalized as described previously (Linnemann *et al.*, 2020), and the peak times of the single donors with the different *PADI4* SNP variants were determined. The fluorescence microscopy images were also analyzed as described previously (Linnemann *et al.*, 2020), and the amount of NETosed cells at 245 min was taken as the readout for the NETosis rate.

2.4 ROS measurements

ROS were determined as described previously (Ehnert *et al.*, 2017).

2.4.1 DCFH-DA

To determine total ROS, isolated neutrophils were incubated for 25 min in 10 µM dichloro-dihydro-fluorescein diacetate (H_2DCFH-DA; Sigma, Darmstadt, Germany) in plain RPMI medium. After incubation, cells were washed once with PBS (400 *g*, 10 min, acceleration 5, deceleration 4) and resuspended in PBS. Cells were directly stimulated and distributed into a fresh 96-well plate. Fluorescence was measured over 20 min at Ex 485 nm/Em 520 nm. The positive control was 0.03% H_2O_2. For analysis, values were normalized to the control value.

2.4.2 Dihydrorhodamine 123 and dihydroethidium

Dihydrorhodamine 123 (DHR) is a non-fluorescent dye converted to the fluorescent rhodamine 123 in the presence of ROS, especially superoxide anions. To detect superoxide anions, neutrophils were stained with 10 µM DHR (Cayman Chemical, Ann Arbor, MI, USA). Staining and measurement were performed identically to detect ROS by DCFH-DA. The negative control was 0.03% H_2O_2. For analysis, values were normalized to the control value. Fluorescence was measured over 20 min at Ex 485 nm/Em 520 nm.

Dihydroethidium (DHE, Cayman Chemical) is converted to ethidium in the presence of H_2O_2. Neutrophils were stained with 10 µM DHE and then treated similarly to the procedure for DCFH-DA measurement. The positive control was 0.03% H_2O_2. Values were normalized to the untreated control for analysis. Fluorescence was measured over 20 min at Ex 544 nm/Em 590 nm.

2.5 Western blot

Western Blot was performed as described previously (Linnemann *et al.*, 2021). For protein detection, neutrophils were seeded at a density of 1×10^6 cells/mL. After stimulation, cells were collected with a cell scraper. The suspension was centrifuged at 600 *g* for 10 min, and the pellet was resuspended in freshly prepared radioimmunoprecipitation assay (RIPA) buffer (approximately 10 µL per 3×10^6 cells). The protein content was determined by using the Lowry assay

(Lowry *et al.*, 1951). First, 2 µL of sample or bovine serum albumin (BSA) standard was added into a 96-well plate in triplicates. Next, 150 µL of solution A was added to the samples and incubated for 10 min. Then, 30 µL of solution B was added and directly mixed. After 2-3 h of incubation, the absorbance was measured at 750 nm, and the protein concentration was determined from the standard. Samples were diluted with ddH_2O and 1x Lämmli buffer. For denaturation, the samples were incubated for 10 min at 98°C. Next, 35 µg of protein was loaded onto a 12% bis-acrylamide gel and separated by sodium dodecyl sulfate–polyacrylamide gel electrophoresis (SDS-PAGE) at 100 V for approximately 3 h. Separated protein was transferred to a nitrocellulose membrane by wet blot transfer for 3 h at 100 mA. Protein transfer was controlled by Ponceau S staining, and the membrane was cut according to the size of the target proteins.

Membranes were incubated with primary antibody overnight at 4°C (antibodies and dilutions are listed in Table 4), washed three times with Tris-buffered saline with tween (TBS-T), and incubated with appropriate secondary antibody for 2 h at room temperature. After washing, signals were detected by enhanced chemiluminescence (ECL) solution with a CCD-camera (Chemocam, INTAS, Göttingen, Germany). The stability of the chosen loading control proteins was analyzed before usage (Supplementary Figure 2).

Table 4: Antibodies used for western blot, dot blot, and immunofluorescence.

Target	Isotype	Manufacturer	Product number	Dilution
PAD4	Mouse	Santa Cruz Biotechnology	sc-365369	1:500
MPO	Mouse	Santa Cruz Biotechnology	sc-52707	1:500 (WB) 1:200 (IF)
p-p38	Rabbit	Cell Signaling	4511	1:1000
p-ERK	Rabbit	Cell Signaling	4370	1:1000
p-Akt	Mouse	Santa Cruz Biotechnology	sc-271966	1:500
p-GSK3β	Rabbit	Cell Signaling	5558	1:1000
Cit-H3	Rabbit	Abcam	ab5103	1:790 (WB) 1:100 (IF)
HPRT	Mouse	Santa Cruz Biotechnology	sc-376938	1:500
β-Actin	Rabbit	Cell Signaling	4970	1:10000
Mouse IgG	Horse	Cell Signaling	7076	1:10000
Rabbit IgG	Goat	Santa Cruz Biotechnology	sc-2004	1:10000

2.6 NET isolation

NETs were isolated as described previously by Schedel *et al.* (2020). Briefly, neutrophils were isolated from the blood of healthy volunteers as described in section 2.2.3. Cells were diluted to 5×10^6 cells/mL and stimulated with 500 nM PMA for 4 h in plain RPMI medium. Subsequently, cells were collected by scraping and removed from the medium by centrifugation (500 *g*, 10 min). The supernatant was distributed to 1.5 mL tubes and centrifuged again at 18000 *g* for 15 min at 4°C. The supernatant was removed, and each formed pellet was resuspended in 10 µL of PBS. The content of all tubes was pooled together, and the DNA content was determined by absorbance measurement with the LVIS plate in the Omega plate reader (BMG Labtech). The DNA concentration was taken as the reference value for dilutions in experiments.

To compare the effects of isolated NETs with genomic DNA, DNA was isolated from PBMCs as described in section 2.10.

2.6.1 Toxicity tests with SCP-1 cells

SCP-1 cells were seeded in 96-well plates at a density of 7.5×10^4 cells/mL. After overnight attachment, the medium was changed, and isolated NETs were added in a serial dilution series from 2 to 0.0625 ng/µL. After 48 h, mitochondrial activity was determined by resazurin conversion, total protein content by sulforhodamine B (SRB) staining, and cell death by lactate dehydrogenase (LDH) release. The supernatant was collected for further analysis by dot blot and determination of DNA content by polymerase chain reaction (PCR).

2.6.2 Inhibitor tests

To evaluate toxic components of isolated NETs, different substances were tested to reduce the toxicity of NETs on SCP-1 cells. Resazurin conversion and SRB staining were performed after 48 h, and the supernatant was collected and kept for analysis by PCR or dot blot.

DNase I (from bovine pancreas, Genaxxon, Ulm, Germany) was added directly to SCP-1 cells ± isolated NETs. Concentrations of 100, 200, 400, and 800 U/mL were tested (Supplementary Figure 3), and for the final experiments 200 U/mL was used.

Heat treatment was used to generally denature proteins and proteases in isolated NETs. Specifically, isolated NETs were exposed to heat treatment at 75°C for 20 min (the manufacturer's recommendation for inhibition of proteinase K) or 99°C for 10 min (the manufacturer's recommendation for inhibition of DNase) before being added to SCP-1 cells.

Proteinase K (Carl Roth, Karlsruhe, Germany) was added directly to the SCP-1 cells ± isolated NETs at a concentration of 0.5 µg/mL. Higher concentrations of proteinase K showed toxicity to the cells (Supplementary Figure 3).

Three protease inhibitors—leupeptin (Leu), pepstatin A (Pep A), and phenylmethylsulfonyl fluoride (PMSF)—were tested singularly or in combinations with each other. The concentrations used were the same as in the RIPA buffer

(Pep A 1 µg/mL [14.58 µM], Leu 5 µg/mL [11.72 µM], PMSF [1 mM]), which is also comparable to concentrations that have been used in cell cultures (Briant *et al.*, 2015, Liton *et al.*, 2008, von der Helm *et al.*, 1989, Yui *et al.*, 2014).

Leu inhibits serine, threonine, and cysteine proteases; PMSF inhibits serine proteases and partly inhibits cysteine proteases; and PepA inhibits aspartic acid proteases. All three inhibitors are known to inhibit neutrophil-specific defense enzymes, which can be released with NETs (e.g., serine-protease like cathepsin G; Majewski *et al.*, 2016).

2.6.3 Sytox Green staining of added NETs

To prove DNA addition to SCP-1 cells, Sytox Green (final concentration 1 µM) was added directly into the culture medium of SCP-1 cells treated with NETs after 48 h or after washing with PBS twice. Sytox Green is a DNA-binding dye that increases fluorescence up to 500-fold when bound to DNA (Thakur *et al.*, 2015). Fluorescence at Ex 485 nm/ Em 520 nm was measured, and microscopy images were taken with a fluorescence microscope.

2.6.4 Recovery test of SCP-1 cells after incubation with NETs

To determine the possible attachment of isolated NETs on SCP-1 cells, NET-treated SCP-1 cells were subjected to a recovery experiment. SCP-1 cells were treated for 48 h with NETs as described in the toxicity test (only concentrations of 0.25, 0.5, and 1 ng/µL). After 48 h, one plate was subjected to the following analyses: mitochondrial activity was analyzed by resazurin measurement, total protein content was determined by SRB staining, DNA was measured with Sytox Green staining, and the supernatant was analyzed by dot blot and PCR. The other plate was washed three times with PBS and incubated for another 48 h in growth medium without NETs. Then, the same tests were performed again. The experimental setup is illustrated in Figure 5.

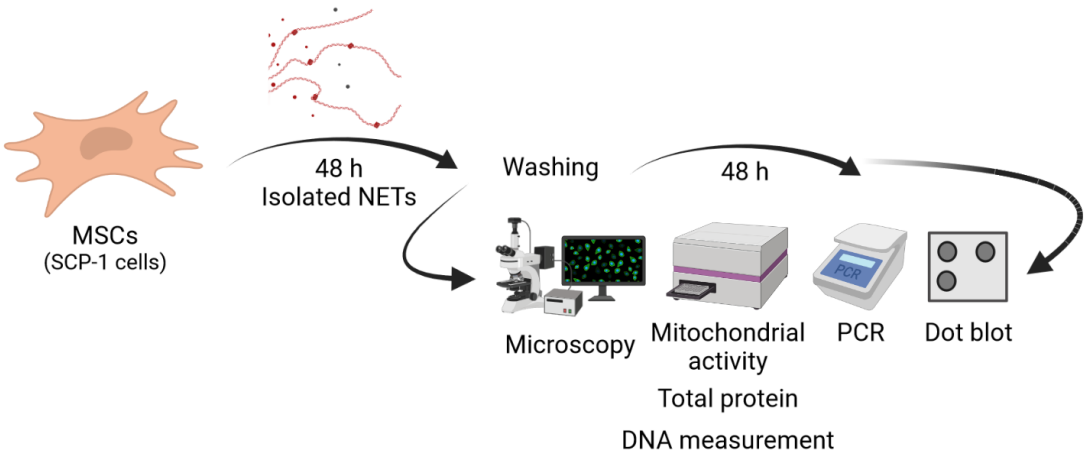

Figure 5: Experimental setup for the test of the recovery of SCP-1 cells after incubation with NETs. Created with Biorender.com.

2.6.5 TLR4 activation measurement

TLR4 activation was measured by using the commercially available HEK Blue TLR4 reporter cell line. HEK Blue TLR4 reporter cells were cultivated in DMEM with 10% FCS and 1% Pen/Strep (100 U Penicillin and 0.1 mg Streptomycin per mL). For experiments, HEK Blue cells were cultivated in the selection medium (Cultivation medium with 1x HEK Blue selection solution, Invivogen, Toulouse, France) for two passages and then seeded in 96-well plates at 1×10^5 cells/mL in 200 µL/well. After 4 h of settling, stimuli were added. The positive control was 100 ng/mL LPS. NETs were added at 0.25, 0.5, or 1 ng/µL. After 72 h of incubation, 20 µL of cell supernatant were transferred to a new 96-well plate with 180 µL of alkaline phosphatase (AP) solution. Absorbance was measured at 405 nm after 2 h of incubation (Wittmann *et al.*, 2016). For normalization, the protein was isolated from the 96-well plates by using RIPA buffer, and the protein content was determined by using the Lowry assay (see section 2.5). Absorbance values at 405 nm were normalized to the protein amount and untreated controls.

2.6.6 Incubation with THP-1 conditioned NETs

THP-1 cells were incubated with NETs or genomic DNA at a concentration of 0.5 ng/µL for 48 h. The supernatant was collected, and SCP-1 cells were incubated with the supernatant or isolated NETs/genomic DNA alone. After 48 h, resazurin conversion and total protein content of SCP-1 cells were determined. The experimental setup is shown in Figure 6.

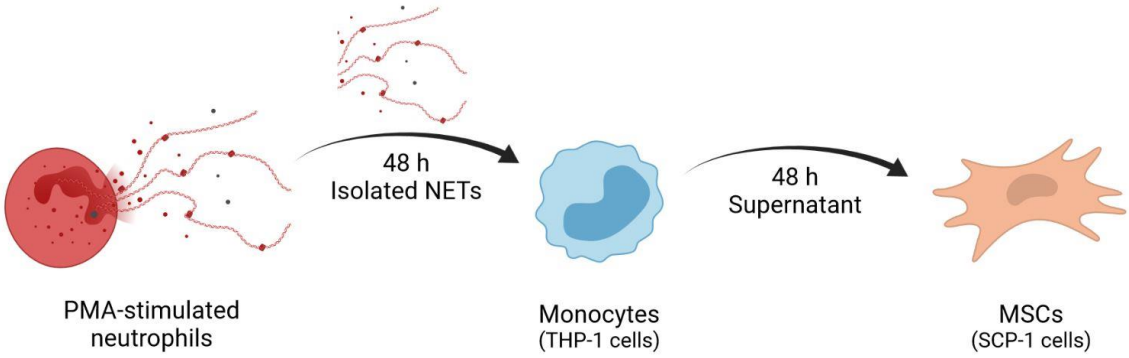

Figure 6: Experimental setup for the incubation of SCP-1 cells with THP-1-conditioned NETs. Created with Biorender.com.

2.6.7 PCR of cell culture supernatant

PCR was performed to evaluate the DNA content more precisely in supernatants of NET-treated SCP-1 cells. Primer UGT1A6 was used; it was designed to also amplify genomic DNA (Table 5). Four microliters of supernatant with different treatments were added to 7.5 µL of Mastermix (Red HS Taq,Biozym, Hessisch Oldendorf, Germany) , 0.75 µL of each forward and reverse primer, and 2 µL of diethyl pyrocarbonate (DEPC)-treated water. PCR was run with initial denaturation for 2 min at 95°C, followed by 35 cycles of denaturation for 15 s at 95°C, annealing for 15 s at 60°C, and elongation for 72°C for 30 s. In the end, a final denaturation step was performed for 10 min at 95°C. PCR products were separated on a 1.6% agarose gel with 0.07% ethidium bromide.

Table 5: Details of UGT1A6 primer.

Primer	**Forward sequence 5'→3'**	**Reverse sequence 5'→3'**	**Gene bank accession number**	**Amplicon size**
UGT1A6	TGG TGC CTG AAG TTA ATT TGC T	GCT CTG GCA GTT GAT GAA GTA	NM_001072.3	209 bp

2.6.8 Dot blot

To analyze in more detail whether isolated NETs could be quantified in treated SCP-1 cells, supernatant of SCP-1 cells treated with NETs for 48 h was collected and stored at -20°C. Eighty microliters of supernatant was transferred to a nitrocellulose membrane with the help of a dot blotter (Carl Roth, Karlsruhe,

Germany). Pure isolated NETs were diluted to 10 ng/µL in PBS as a positive control. The transfer was controlled by Ponceau S staining, and membranes were incubated for 1 h with 5% BSA in TBS-T (to block nonspecific protein binding), followed by overnight incubation with primary antibodies (see Table 4). Membranes were washed three times with TBS-T and incubated with the secondary antibody for 2 h. After washing, signals were detected by chemiluminescence detection with ECL by the CCD-camera (Weng *et al.*, 2020).

2.7 Analysis of THP-1 cells treated with isolated NETs

THP-1 cells were seeded at a density of 4×10^5 cells/mL. NETs were added at a concentration of 0.1, 0.25, 0.5, 1, or 2 ng/µL. As a control, genomic DNA was added at a concentration of 0.5, 1, or 2 ng/µL. After 48 h, mitochondrial activity was measured (see section 2.8.1).

2.7.1 Hoechst measurement and life staining

To measure the attachment of THP-1 cells, which can be seen as an indicator of cellular activation into macrophage types, wells were washed twice with 100 µL of PBS. Cells were incubated with staining solution (Hoechst 33342 2 µg/mL, Calcein AM 2 µM in plain medium) for 30 min, and the fluorescence intensity at Ex 355/Em 460 nm was measured directly. Subsequently, microscopy images were taken with an EVOS Fl fluorescence microscope in the GFP (Calcein AM) and DAPI (Hoechst) channels to confirm cell attachment and to check cell viability.

2.8 Cell analysis

2.8.1 Resazurin conversion

Cells were washed once with PBS and 0.0025% resazurin solution added in the respective culture medium. Conversion of resazurin to resorufin was determined by fluorescence measurement at Ex 544 / Em 590 nm after 60 min incubation at 37°C (Ehnert *et al.*, 2015a).

2.8.2 SRB staining

As described previously (Linnemann *et al.*, 2021), cells were fixed with 99% ethanol at -20°C for at least 1 h. After fixation, cells were washed once with tap water, dried, and incubated with 0.4% SRB solution for 30 min. Unbound stain was removed by washing three times with 1% acetic acid. Microscopy images and scans were obtained after drying. For quantification, the staining was dissolved in 10 mM unbuffered Tris solution. Absorbance was measured at 565 and 690 nm (impurities), and the 690 nm value was subtracted from the 565 nm value.

2.8.1 LDH release

SCP-1 cells were cultured for 48 h. Three wells were incubated with 1% Triton-X-100 for 30 min to lyse the cells (for the positive control). Fifty microliters of supernatant from all conditions were collected and distributed to a new 96-well plate. Fifty microliters of the reaction mixture (CyQUANT™ LDH Cytotoxicity Assay, Thermo Fisher Scientific, Heidelberg, Germany) were added, and the absorbance (490 nm) was measured at 37°C for 30 min. The slope was determined, and the percentage of dead cells was calculated by normalization to the value of lysed cells (maximum possible LDH release).

2.8.1 Migration assay

The migration of SCP-1 cells was analyzed by using the Oris cell migration assay (Platypus Technologies, Madison, WI, USA) as described previously (Linnemann *et al.*, 2021). Migration assay inserts were sterilized with 70% ethanol, washed with PBS, and dried. Inserts were placed into 96-well plates, and SCP-1 cells were seeded at a density of 2×10^4 cells/well. After overnight attachment, the inserts were removed, the wells were washed with PBS, and the medium was changed. Images of the cell-free area were taken to determine the 0-h time point. After 45 h, cells were fixed with ethanol and stained with SRB (see section 2.8.2). Images of the former cell-free area were taken. Migration was determined by the ratio of the cell-free area at 45 h to the cell-free area at 0 h (Equation 4).

$$Migration\ [\%] = \frac{Cell\text{-}free\ area_{45\ h}}{Cell\text{-}free\ area_{0\ h}} \times 100\% \qquad \text{Equation 4}$$

2.9 Differentiation of SCP-1 cells

SCP-1 cells were seeded at a density of 4,000 cells/well in 96-well plates. As described previously, SCP-1 cells were differentiated to osteogenic cells in MEMα medium supplemented with 1% FCS, 200 µM L-ascorbate-2-phosphate, 5 mM β-glycerol-phosphate, 25 mM HEPES, 1.5 mM $CaCl_2$, and 100 nM dexamethasone (Ehnert *et al.*, 2015b). The experimental setup is shown in Figure 7.

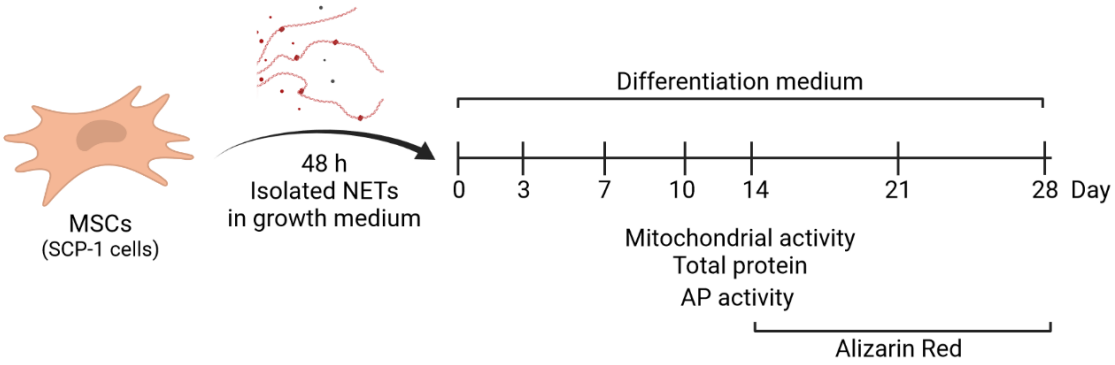

Figure 7: Experimental setup for the differentiation of SCP-1 cells with isolated NETs. Created with Biorender.com.

2.9.1 AP activity

AP activity was measured as an early osteogenic differentiation marker. SCP-1 cells were washed once with PBS and 100 µL AP substrate solution was added to each well. Absorbance at 405 nm was measured after 40 min (Ehnert *et al.*, 2010, Ehnert *et al.*, 2012).

2.9.2 Alizarin Red Staining

SCP-1 cells were fixed with 99% ethanol at -20°C after 14, 21, and 28 days of differentiation. After washing with tap water three times, the wells were covered with 0.5% Alizarin Red solution for 30 min in the light with shaking. Unbound stain was removed by washing three times with tap water. The plates were scanned, and microscopy images were taken. For quantification, the staining was dissolved with 10% cetylpyridinium chloride solution. Absorbance was measured at 560 nm (Ehnert *et al.*, 2010, Ehnert *et al.*, 2012).

2.10 DNA Isolation

DNA was isolated to determine SNPs of *PADI4*. DNA was isolated from PBMCs during neutrophil isolation. The PBMC fraction was washed simultaneously to isolate neutrophils. The PBMC pellet was taken up in 500 µL of 50 mM NaOH and optionally frozen until DNA was isolated. For DNA isolation, samples were heated at 98°C for 10 min and subsequently neutralized by adding 500 µL of demineralized water and 50 µL of 1 M Tris buffer (pH 8.0). To remove debris, samples were centrifuged at 14000 *g* for 10 min. The DNA content of the supernatant was determined photometrically with the LVIS Plate for the Omega Plate Reader (BMG Labtech). The protocol was adapted from Ehnert *et al.* (2019).

2.11 Amplification-refractory mutation system-PCR

SNPs of *PADI4* were determined by using amplification-refractory mutation system-PCR (ARMS-PCR), as described previously (Ehnert *et al.*, 2019). With the help of four primers (inner reverse, outer reverse, inner forward, and outer forward), the genotype was determined. The inner primers have one mismatch each for the *PADI4* variants so that amplification of the smaller amplicons is only possible with the right variant. The outer primers always lead to an amplicon and are the control PCR. Heterozygous samples result in three bands, while homozygous samples produce two bands. From the size of the second band, the variant can be determined. A schematic representation of the principle is shown in Figure 8.

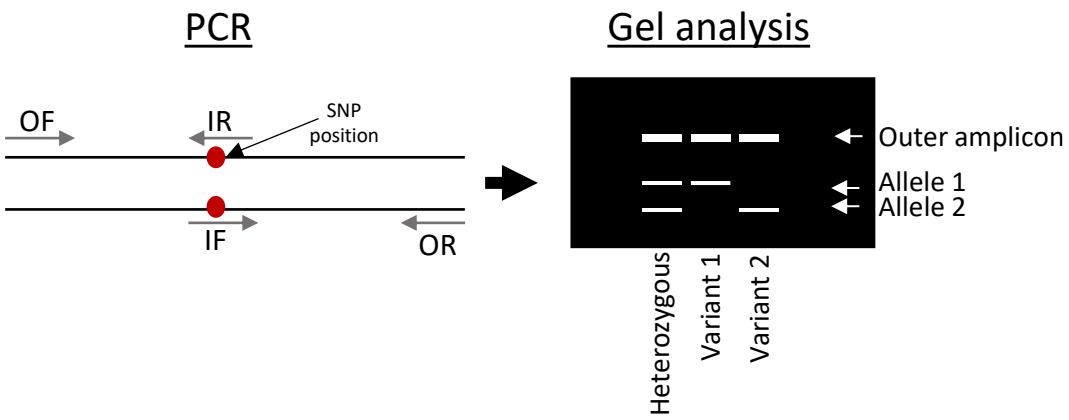

Figure 8: Principle of ARMS-PCR for the *PADI4* gene. Red dots indicate the position of a SNP, where inner primers are modified to match only one variant. Grey arrows indicate the primer position. White bands in the gel indicate visible amplicons. IR: inner reverse primer; OF: outer forward primer; IF: inner forward primer; OR: outer reverse primer.

All primer conditions were optimized to give definite results for the variants; unclear samples were repeated. The PCR program comprised initial denaturation for 2 min; 40 cycles with 15 s of denaturation, 15 s of annealing, and 15 s of elongation; and final elongation at 72°C for 10 min. 100 ng of template were used. Details for the primers are presented in Table 6. Samples were separated on a 2% agarose gel with 0.07% ethidium bromide. According to the size of the PCR products on the agarose gel, genetic variants were determined for single donors.

Table 6: Sequences of *PADI4* primers for determination of genotype by ARMS-PCR. Primer sequences are in 5'→3' direction.

***PADI4* SNP primer**	**Forward primer**	**Reverse primer**	**Annealing [°C]**	**Amplicon size [bp]**	**Amount of primer [µL] in 10 µL reaction mix**
163AG-Outer	AGGAGAAATGCTGGGAGAGCCATGGCTG	AGCTCTTCCACAGGGCAAGAGGCTCTGC	64	179	IF/IR/OF/OR 0.2
163AG-Inner	AGGGGTGGTCGTGGATATTGCCCCCA	CCTGTGGATTTCTTCTTGGCTGGAGGTCC	64	258	
245CT-Outer	GAGGACTGCACGTCCTTCAGCATCAACG	TGACCTCCATGAACCCCTGGTAGCCGTA	68	168	IF/OF/OR 0.2 IR 0.3
245CT-Inner	GGGTAGAGGTGACCCTGACGATGAACGC	CTGGTCGCCTGTGCTACCACTGGACA	68	250	
335GC-Outer	GCTTTCCCTCCATTCCCATC	ACTCCCAGATGTCTGACTGGCT	62	248	IF/OF/OR 0.1 IR 0.2
335G-Inner	CAAAGCTCTACTCTACCTCACGGG	TGGTTGTCACTTACCCAGCG	62	183	

IF: inner forward; IR: inner reverse; OF: outer forward; OR: outer reverse

2.12 Statistical analysis

All experiments were performed in triplicate in at least three independent experiments/of three donors. For statistical analysis, a non-parametric Kruskal-Wallis test with Bonferroni correction or two-way analysis of variance (ANOVA) was used for multiple comparisons. For single comparisons, the non-parametric Mann-Whitney test was used. A p-value <0.5 was considered significant. The statistical test used is indicated in the figure legends. Statistical analysis was done under the guidance of Dr. Sabrina Ehnert.

2.13 Materials

2.13.1 Chemicals

Table 7: Used chemicals

Chemical	Manufacturer
2 M NaOH	Carl Roth, Karlsruhe, Germany
2-Mercaptoethanol	Carl Roth, Karlsruhe, Germany
4-Nitrophenol solution 10 mM	Sigma-Aldrich, MO, USA
4-Nitrophenyl phosphate disodium salt hexahydrate (pNNP)	Carl Roth, Karlsruhe, Germany
Acetic Acid	Carl Roth, Karlsruhe, Germany
Agarose	Genaxxon, Ulm, Germany
Alizarin Red S	Carl Roth, Karlsruhe, Germany
Boric acid	Carl Roth, Karlsruhe, Germany
Bromphenol blue	Carl Roth, Karlsruhe, Germany
BSA (Bovine serum albumin)	Carl Roth, Karlsruhe, Germany
Calcein AM	Sigma-Aldrich, MO, USA
Calcium ionophore A23187	Sigma-Aldrich, MO, USA
Catalase	Sigma-Aldrich, MO, USA
Cetylpyridiumchloride monohydrate 98%	Carl Roth, Karlsruhe, Germany
Chloroform	Carl Roth, Karlsruhe, Germany
Cobalt chloride	Sigma-Aldrich, MO, USA
Copper sulfate pentahydrate (Cu_2SO_4*5 H_2O)	Carl Roth, Karlsruhe, Germany
DCFH-DA	Sigma-Aldrich, MO, USA
Demineralized water (ddH_2O)	Carl Roth, Karlsruhe, Germany
Deoxycholic Acid (DOC)	Carl Roth, Karlsruhe, Germany
DEPC (Diethlypyrocarbonate)	Carl Roth, Karlsruhe, Germany
Dihydroethidium	Cayman Chemical, MI, USA
Dihydrorhodamine 123	Cayman Chemical, MI, USA
DMSO (Dimethyl sulfoxide)	Carl Roth, Karlsruhe, Germany
DNase	Genaxxon, Ulm, Germany
Ethanol	Apotheke UKT

Ethidium Bromide	Carl Roth, Karlsruhe, Germany
CyQUANT™ LDH Cytotoxicity Assay	Thermo Fisher Scientific, MA, USA
Folin's Reagent	Sigma-Aldrich, MO, USA
Formaldehyde	Carl Roth, Karlsruhe, Germany
Glucose	Sigma-Aldrich, MO, USA
Glucose oxidase	Sigma-Aldrich, MO, USA
Glycerol	Carl Roth, Karlsruhe, Germany
Glycine	Sigma-Aldrich, MO, USA
Hoechst 33342	Sigma-Aldrich, MO, USA
Hydrogen peroxide (H_2O_2)	Carl Roth, Karlsruhe, Germany
Insulin	Flex Pen, Novo Nordisk, Denmark
Isopropanol	VWR, PA, USA
Leupeptin	Carl Roth, Karlsruhe, Germany
LPS (Escherichia coli O111:B4)	Sigma-Aldrich, MO, USA
Luminol	Carl Roth, Karlsruhe, Germany
Mannitol	Sigma-Aldrich, MO, USA
p-Coumaric Acid	Sigma-Aldrich, MO, USA
Pepstatin A	Sigma-Aldrich, MO, USA
Phenylmethylsulfonyl fluoride (PMSF)	Carl Roth, Karlsruhe, Germany
Phosphate-buffered saline (PBS) powder	Biochrom, Merck KGaA, Darmstadt, Germany
Phosphate-buffered saline (PBS) solution	Sigma-Aldrich, MO, USA
Phorbol-12-myristat-13-acetat (PMA)	Abcam, Cambridge, Great Britain
Proteinase K	Carl Roth, Karlsruhe, Germany
Ponceau S	Carl Roth, Karlsruhe, Germany
pUC19 DNA/MspI (HpaII) Marker	Carl Roth, Karlsruhe, Germany
RedTaq PCR Mastermix	Biozym, Hessisch Oldendorf, Germany
Resazurin Sodium Salt	Sigma-Aldrich, MO, USA
Roti-Mark Bicolor	Carl Roth, Karlsruhe, Germany
SDS (Sodium dodecyl sulfate)	Carl Roth, Karlsruhe, Germany
Sodium carbonate (Na_2CO_3)	Carl Roth, Karlsruhe, Germany
Sodium Chloride (NaCl)	Carl Roth, Karlsruhe, Germany

Sodium fluoride (NaF)	Carl Roth, Karlsruhe, Germany
Sodium Orthovanadate (Na_3VO_4)	Sigma-Aldrich, MO, USA
Sodium-Potassium Tartrate (Na-K-Tartrate)	Sigma-Aldrich, MO, USA
Sulforhodamine B sodium salt	Sigma-Aldrich, MO, USA
Sytox Green solution	Thermo Fisher Scientific, MA, USA
Tergitol Solution (NP40 substitute)	Sigma-Aldrich, MO, USA
TGF-β1	Peprotech, NJ, USA
Tris (hydroxymethyl) aminomethan	Carl Roth, Karlsruhe, Germany
Tris Base	Carl Roth, Karlsruhe, Germany
Triton-X-100	Carl Roth, Karlsruhe, Germany
Trypan Blue	Carl Roth, Karlsruhe, Germany
Tween 20	Sigma-Aldrich, MO, USA

2.13.2 Cell culture media and solutions

Table 8: Cell culture media and solutions for cell culture

Medium/Solution	Manufacturer/Composition
Lympholyte Cell separation medium	Cedarlane, Ontario, Canada
RPMI 1640	Sigma-Aldrich, MO, USA
RPMI 1640 without phenol red	Sigma-Aldrich, MO, USA
DMEM	Sigma-Aldrich, MO, USA
α-ascorbate-2-phosphate	Sigma-Aldrich, MO, USA
β-glycerophosphate	Sigma-Aldrich, MO, USA
Penicillin/Streptomycin	Sigma-Aldrich, MO, USA
α-MEM Modification with Glutamine w/o nucleosides	Gibco, Thermo Fisher Scientific, MA, USA
FCS (Fetal calf serum)	Gibco, Thermo Fisher Scientific, MA, USA
Trypsin/EDTA	Gibco, Thermo Fisher Scientific, MA, USA
THP-1 medium	RPMI 1640, 5% FCS
SCP-1 medium	α-MEM Modification, 5% FCS

SCP-1 differentiation medium	MEM-α, 1% FCS, 10 mM β-glycerol-phosphate, 200 µM L-ascorbate-2-phosphate, 25 mM HEPES, 1.5 mM calcium chloride, 100 nM Dexamethasone

2.13.3 Buffers and solutions

Table 9: Buffers and solutions

Buffer/Solution	Composition
TBE (Tris/Borate/EDTA) buffer	TRIS 0.89 M, Boric acid 0.89 M, 20 mM, pH 8.3
Trypan Blue Solution	0.125% Trypan Blue in PBS
PBS (Phosphate buffered saline)	Gibco, Thermo Fisher Scientific (USA)
TRIS pH 8.8	1.5 M Tris in ddH_2O, pH 8.8
1 M TRIS pH 6.8	1 M Tris in ddH_2O, pH 6.8
Tris 100 mM	100 mM TRIS in ddH_2O, pH 8.5
RIPA Buffer	10 mM TRIS Base, 100 mM NaCl, 0.5% Tergitol, 0.5% DOC, 10 mM EDTA, 1 µg/mL Pepstatin A, 5 µg/mL Leupeptin, 1 mM PMSF, 5 mM Sodium fluoride, 1 mM Sodium orthovanadate
Tris 10 mM unbuffered	10 mM Tris in ddH_2O, pH 10-10.5
TBS 10x (Tris buffered saline)	100 mM TRIS, 1.5 M NaCl in ddH_2O, pH 7.6
1% Acetic Acid Solution	1% Acetic Acid in ddH_2O
Sulforhodamine B Working Solution	0.4% Sulforhodamine B in 1% Acetic Acid
p-Coumaric Acid Solution	90 mM p-Coumaric acid in DMSO
Luminol Solution	250 mM Luminol in DMSO
Western Blot ECL Solution	100 mM TRIS with 0.06% H_2O_2, 1.25 mM Luminol, 0.2 mM p-Coumaric Acid
Lämmli Loading Buffer 5x	300 mM Tris pH 6.8, 50% Glycerol, 5 mM EDTA, 10% SDS, 0.05% Bromphenol Blue, 12.5% 2-Mercaptoethanol
Ponceau S Solution	0.1% Ponceau S in 1% acetic acid solution

Western Blot Transfer Buffer	25 mM Tris, 192 mM Glycine, 20% Methanol
Western Blot Stripping Solution	200 mM NaOH in ddH_2O
TBS-T	10% TBS 10x, 0.1% Tween-20 in ddH_2O
BSA Blocking Buffer for Western Blot	5% BSA in TBS-T
Lowry Solution A	0.02% Na-K-Tartrate, 0.01% $CuSO_4$, 2% Na_2CO_3, 100 mM NaOH
Lowry Solution B	33% Folin's Reagent in ddH_2O
AP Activity Assay Buffer	50 mM Glycine, 100 mM Tris-Base, 1 mM $MgCl_2$, pH 10.5 in ddH_2O
AP substrate solution	3.5 mM pNPP in AP Activity Assay Buffer
Alizarin Red Staining Solution	0.5% Alizarin Red S in ddH_2O, pH 4.0
Cetylpyridiumchloride solution	10% Cetylpyridiumchloride in tap water

2.13.4 Equipment

Table 10: Used equipment

Equipment	Manufacturer
Small Centrifuge	Heraeus Fresco 21, Thermo Fisher Scientific, MA, USA
Blood centrifuge	Medifuge, Thermo Fisher Scientific, MA, USA
Large centrifuge	MegaFuge 40 R, Thermo Fisher Scientific, MA, USA
Light microscope	Primo Vert, Carl Zeiss, Oberkochen, Germany
Fluorescence microscope	Evos FL Imaging system, Thermo Fisher Scientific, MA, USA
Thermo cycler	Thermo Fisher Scientific, MA, USA
Agarose gel chamber	Bio-Rad, CA, USA
Cell Culture Plates	Greiner Bio-One, Kremsmünster, Austria
Cell culture flasks	Greiner Bio-One, Kremsmünster, Austria
Tubes (0.5 mL, 1mL, 1.5 mL)	Sarstedt, Nümbrecht, Germany
Tubes (2 mL)	Eppendorf, Hamburg, Germany
Tubes (13 mL, for neutrophil isolation)	Sarstedt, Nümbrecht, Germany

Tubes (15 mL, 50 mL)	Greiner Bio-One, Kremsmünster, Austria
PCR Tubes	Carl Roth, Karlruhe, Germany
Shaker	LTF Labortechnik GmbH & Co. KG, Wasserburg, Germany
Incubator Cell Culture	Carl Roth, Karlsruhe, Germany
Laminar Flow Bench	Thermo Fisher Scientific, MA, USA
SDS-PAGE chamber	Carl Roth, Karlsruhe, Germany
Western Blot Tank	Rotiphorese ProClamp Mini, Carl Roth, Karlruhe, Germany
Whatman Paper	Carl Roth, Karlsruhe, Germany
Nitrocellulose Membrane	Carl Roth, Karlsruhe, Germany
Chemocam Imager 3.2	INTAS Science Imaging Instruments GmbH, Göttingen, Germany
Plate Reader Omega	Omega plate reader, BMG Labtech, Ortenberg, Germany
Plate Reader ClarioStar	Omega plate reader, BMG Labtech, Ortenberg, Germany

3. Results

3.1 NET release in diabetic conditions

Diabetic neutrophils have been shown to react differently to stimuli and release more NETs than neutrophils from healthy people (Joshi *et al.*, 2016, Miyoshi *et al.*, 2016). The reaction of neutrophils from diabetic patients and healthy controls to *in vitro* diabetic conditions was investigated regarding NET formation.

3.1.1 Neutrophils from diabetic patients show stronger NET release

Neutrophils from DM patients and control patients were isolated from pre-operatively freshly drawn blood. Four T2DM patients and one T1DM patient (diabetes caused by a viral infection) were included. The cells were stimulated by different stimuli to analyze NET release by using the Sytox Green Assay in basal conditions and after stimulation. Basal PAD4 and protein levels upon stimulation with CI were determined. Figure 9 shows the results of NET release in DM patients. The detailed information for the two groups can be found in Table 11.

Table 11: Characteristics of control and DM patients.

	Control	**DM**	**p-Value**
Sample number	6	5	-
Age [years]	63.3±7.2	62.2±6.7	0.615
BMI [kg/m^2]	25.9±3.7	26.5±4.3	0.931
Female [%]	100	50	>0.999
Neutrophil count [×1000/µL]	4085±948	5144±828	0.082
Blood glucose [mg/dL]	104.3±6.2	201.4±56.1	0.0022
CRP [mg/L]	3.32±2.62	8.10±11.18	0.706
Number of drugs	2.83±2.79	5.20±3.90	0.362

BMI: body mass index, CRP: C-reactive protein

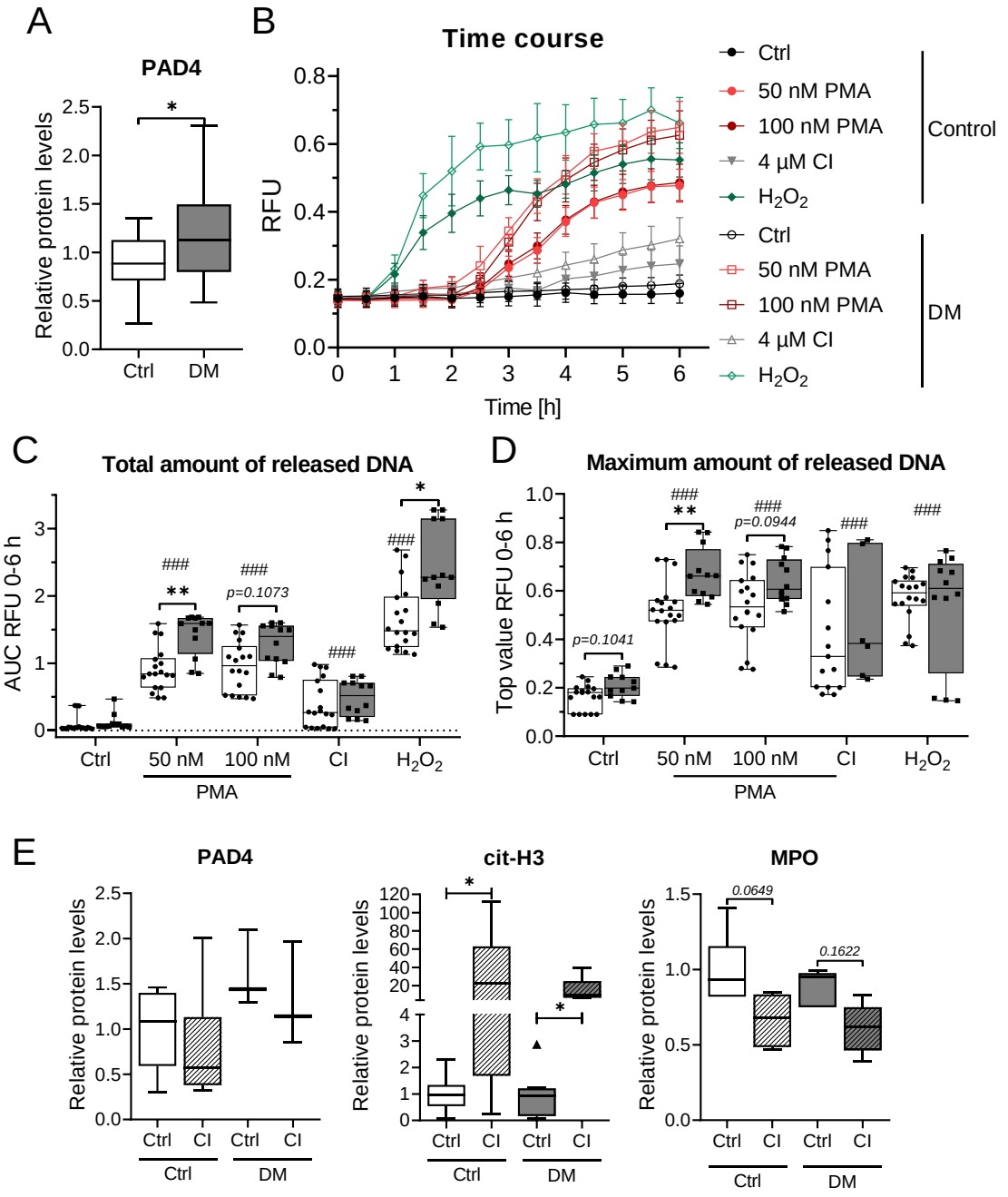

Figure 9: DM patients release more NETs. **(A)** Basal PAD4 protein levels of neutrophils determined by dot blot; N≥39, n=1. **(B)** Time course of DNA release measured by Sytox Green fluorescence; N≥4, n=3. **(C)** Total amount of DNA calculated by AUC for the 6-h time course; N(Ctrl)=6, N(DM)=4, n=3. **(D)** Maximum level of released DNA calculated by maximum fluorescence values. **(E)** Protein levels of neutrophils stimulated for 1 h; N(Ctrl)=6, N(DM)=5, n=1-2. Ctrl: control, DM: diabetes mellitus. *p<0.05, **p<0.01. ###p<0.001. # indicates significance of stimulation compared with control determined by two-way ANOVA.

DM patients showed increased basal PAD4 levels in neutrophils (Figure 9A). Upon stimulation with a low amount of PMA and H_2O_2, DM patients released significantly more NETs overall (Figure 9C), and they showed a higher maximum

amount of released NETs after PMA stimulation (Figure 9D). In unstimulated cells, the maximum amount of released NETs was elevated in neutrophils from DM patients; however, this difference was not significant (Figure 9D). The difference could also be observed in the time course of the Sytox Green Assay (Figure 9B): The curves of DM patients are overall higher than those of control patients. Upon stimulation with CI, no difference could be observed between control and DM patients (Figure 9C). Stimulation with CI significantly increased cit-H3 and showed a trend for reduced MPO, but there was no difference between control and DM patients in PAD4 (Figure 9E).

3.1.2 No basal NET formation could be observed in diabetic conditions

To find out more about the factors that increase NET formation in neutrophils of T2DM patients, neutrophils of healthy volunteers were incubated in diabetic conditions (HG and HG plus insulin [HG+Ins]) and additional with PMA and CI stimulation. NET formation was determined by using the Sytox Green Assay and immunofluorescence.

First, experiments were done with dimethyl sulfoxide (DMSO)- or all-*trans* retinoic acid (ATRA)-differentiated HL-60 cells as a model for granulocytes. However, HL-60 cells did not show appropriate differentiation into granulocyte-type cells, and no NET release occurred in response to PMA stimulation (Supplementary Figure 5). Thus, experiments were continued with freshly isolated primary neutrophils only.

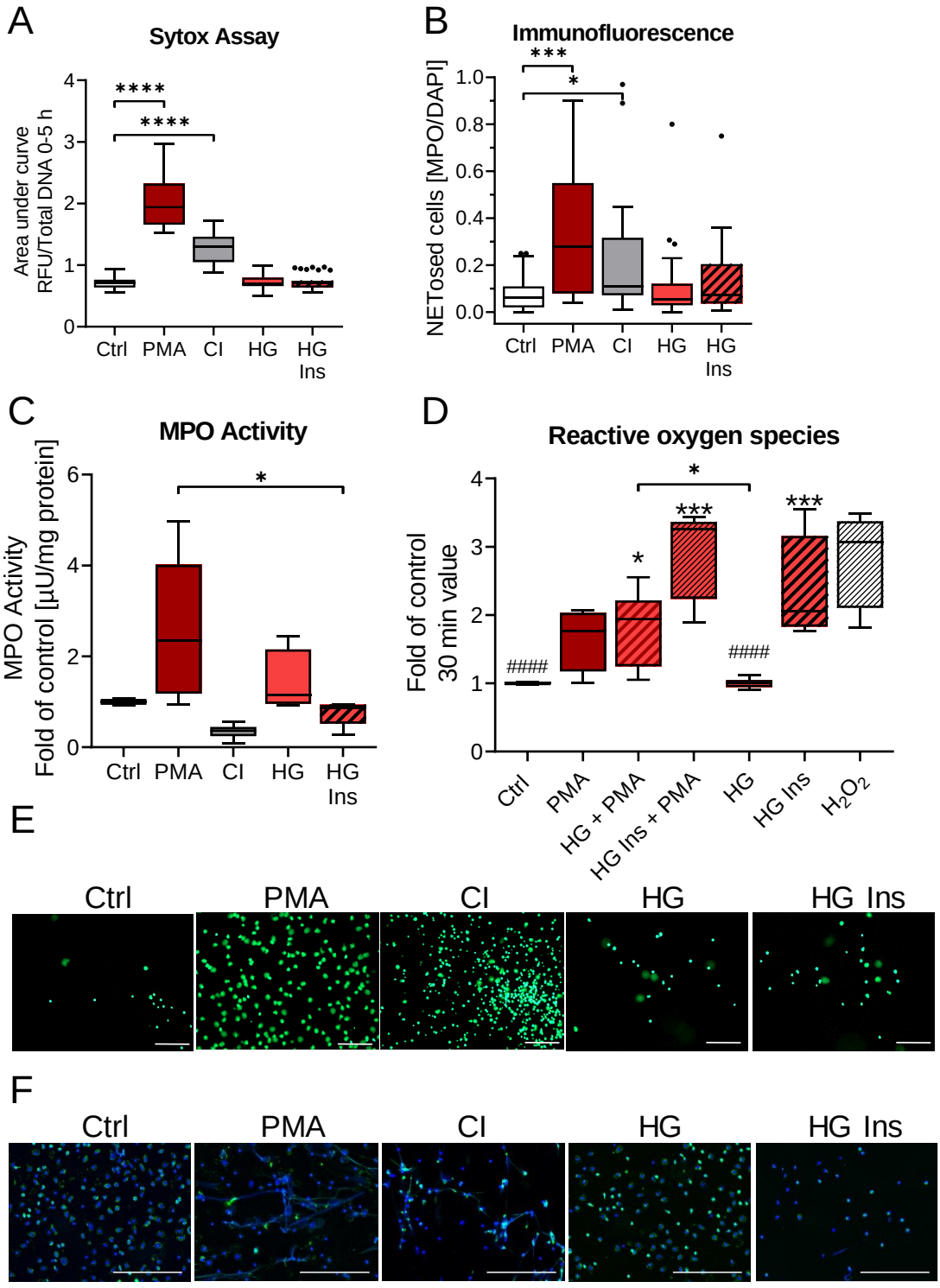

Figure 10: HG does not stimulate NET release. **(A)** Analysis of total DNA release by calculating the AUC from the Sytox Green Assay; N=15, n=3 **(B)** Analysis of NET formation by immunofluorescence; N=12, n=3 **(C)** MPO activity of stimulated neutrophils after 1 h; N=5, n=2 **(D)** Analysis of ROS formation by the DCFH-DA assay; N=4, n=3, ###p<0.001 compared with H_2O_2; an asterisk above the boxes indicates significance compared with Ctrl. **(E)** Representative images of the Sytox Green Assay; the scale bar is 200 µm. **(F)** Representative images of immunofluorescence staining. Green: MPO; blue: Hoechst 33342; the scale bar is 200 µm. *p<0.05, ***p<0.001, ****p<0.0001 determined by the Kruskal-Wallis test.

DNA release was strongly induced by PMA and by CI stimulation (Figure 10A), but neither HG nor HG+Ins triggered NET formation. Immunofluorescence analysis of the stimulated cells at 3 h showed a similar result. PMA showed the highest induction of NET formation, followed by CI stimulation, but HG or HG+Ins did not stimulate NET formation (Figure 10B). PMA induced MPO activity, but neither CI nor the diabetic conditions did (Figure 10C). ROS, one of the most important inducers of NETs, were generated by PMA and PMA in combination with diabetic conditions (Figure 10D). HG alone did not lead to ROS production, but HG+Ins strongly enhanced ROS, reaching nearly the level of the positive control (H_2O_2). However, the increased ROS formation did not lead to NET formation, although this finding is different from a previous report (Al-Khafaji *et al.*, 2016).

3.1.3 HG does not enhance CI-induced NET formation

No basal NET formation could be observed in diabetic conditions. In the DM patients, the differences were more pronounced with additional stimulation. PAD4 is increased in DM patients, and CI-induced NET formation is PAD4 dependent (Lewis *et al.*, 2015). Thus, CI was added to the diabetic conditions, and NET formation was analyzed by using the Sytox Green Assay and immunofluorescence analysis

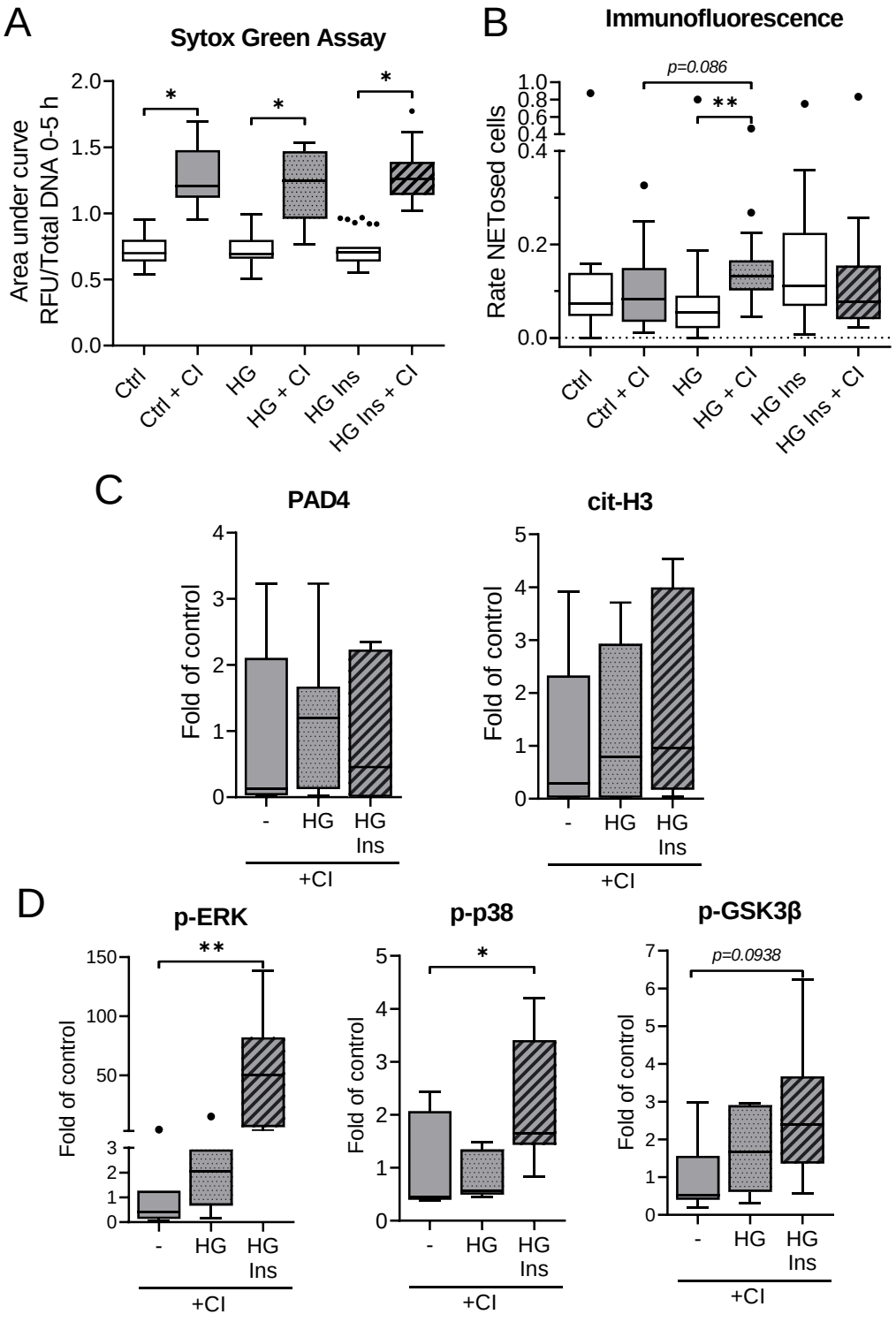

Figure 11: HG does not enhance NET release by CI. Neutrophils were stimulated for 1 h with diabetic conditions, and subsequently CI was added. **(A)** Analysis of total DNA release by calculating the AUC from the Sytox Green Assay; N=5, n=3. **(B)** Analysis of NET formation by immunofluorescence; N=5, n=3. **(C)** Analysis of NET-relevant protein levels after 2-h total incubation; N=5, n=1-2. **(D)** Analysis of NET-relevant signaling protein levels after 2-h total incubation; N=5, n=1-2, *p<0.05, **p<0.01, ***p<0.001, ****p<0.0001 determined by the Kruskal-Wallis test.

CI induced strong DNA release, but the diabetic conditions did not influence the amount of released DNA (Figure 11A). There was a slight but non-significant increase in NET formation by HG+CI compared with CI alone (Figure 11B). Overall, CI only induced low amounts of NETs. The levels of PAD4 and cit-H3 were unaffected by the diabetic conditions (Figure 11C), in contrast to PAD4 levels in T2DM patients (Figure 9A). However, HG+Ins induced significant phosphorylation of the two MAPKs, ERK and p-38, and a non-significant increase in the level of phospho-glycogen synthase kinase-3β (p-GSK3β) compared with CI alone or CI with HG (Figure 11D).

3.1.4 Insulin delays NET formation

PMA and calcium ionophores use different signaling pathways to induce NET release of neutrophils (Kenny *et al.*, 2017). Because PMA induced significantly higher NET release in neutrophils from DM patients than control patients (Figure 9), NET induction by PMA was analyzed in diabetic conditions.

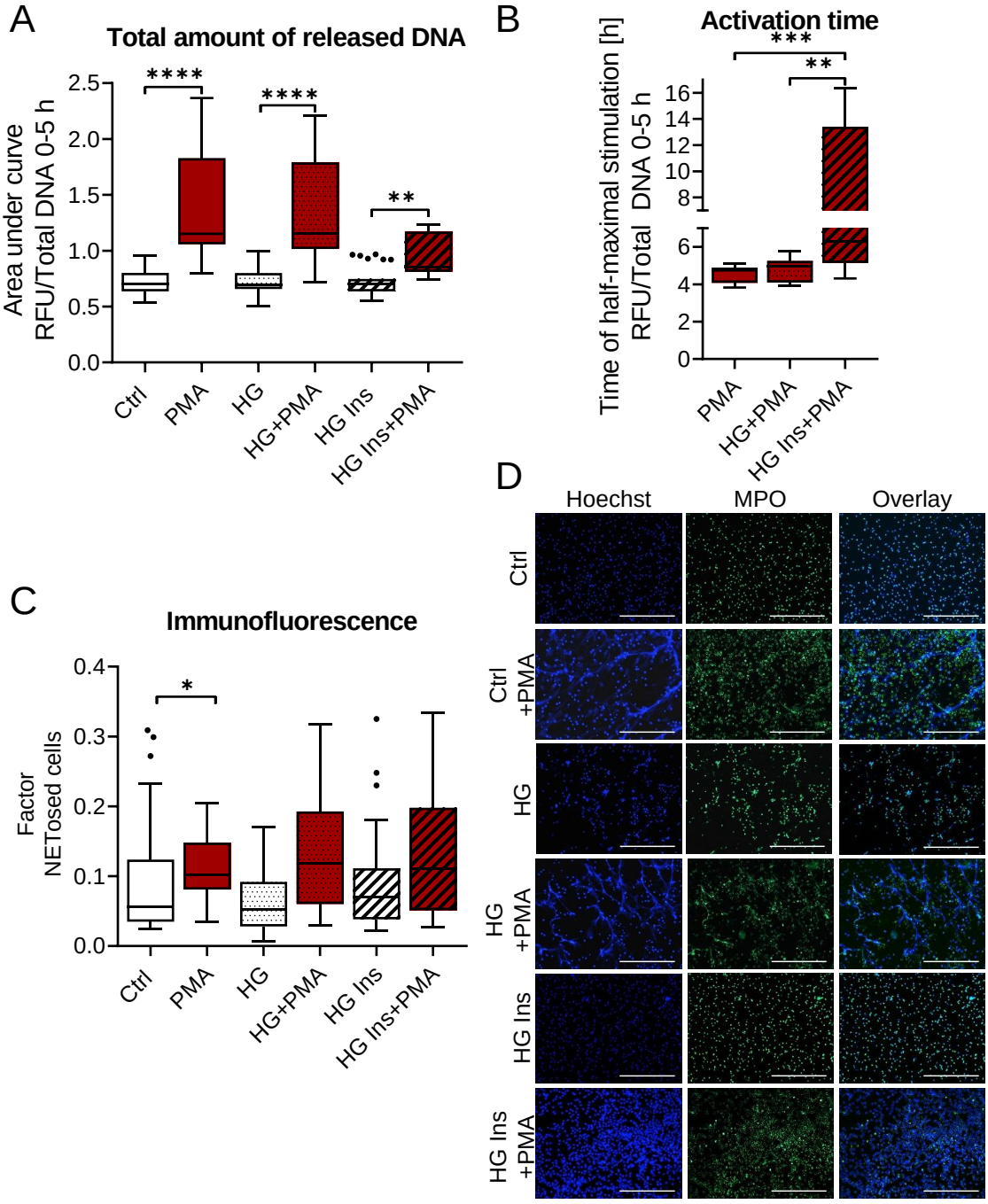

Figure 12: Insulin delays PMA-induced NET formation. Neutrophils were stimulated for 1 h in diabetic conditions, and subsequently PMA was added. **(A)** Analysis of total DNA release by calculating the AUC from the Sytox Green Assay; N=5, n=3. **(B)** Half-maximal stimulation time determined from the Sytox Green Assay; N=5, n=3. **(C)** Analysis of NET formation by immunofluorescence after 3-h total incubation; N=4, n=5. *p<0.05, **p<0.01, ***p<0.001 determined by the Kruskal-Wallis test.

HG did not influence NET release by PMA, but HG+Ins reduced the amount of released DNA (Figure 12A). The activation time of neutrophils for NET release was delayed by several hours by adding HG+Ins compared with PMA alone or

HG+PMA (Figure 12B). The difference was not as pronounced in the immunofluorescence analysis (Figure 12C+D). PMA only significantly induced NET formation in the control condition. Based on the microscopy images (Figure 12D), there are larger extracellular structures after treatment with PMA alone or HG+PMA, whereas treatment with HG+Ins and PMA decondensed chromatin, but large extracellular structures are absent.

To further analyze the effect of insulin on NET release, neutrophils were incubated with PMA and insulin alone for a longer time (20 h).

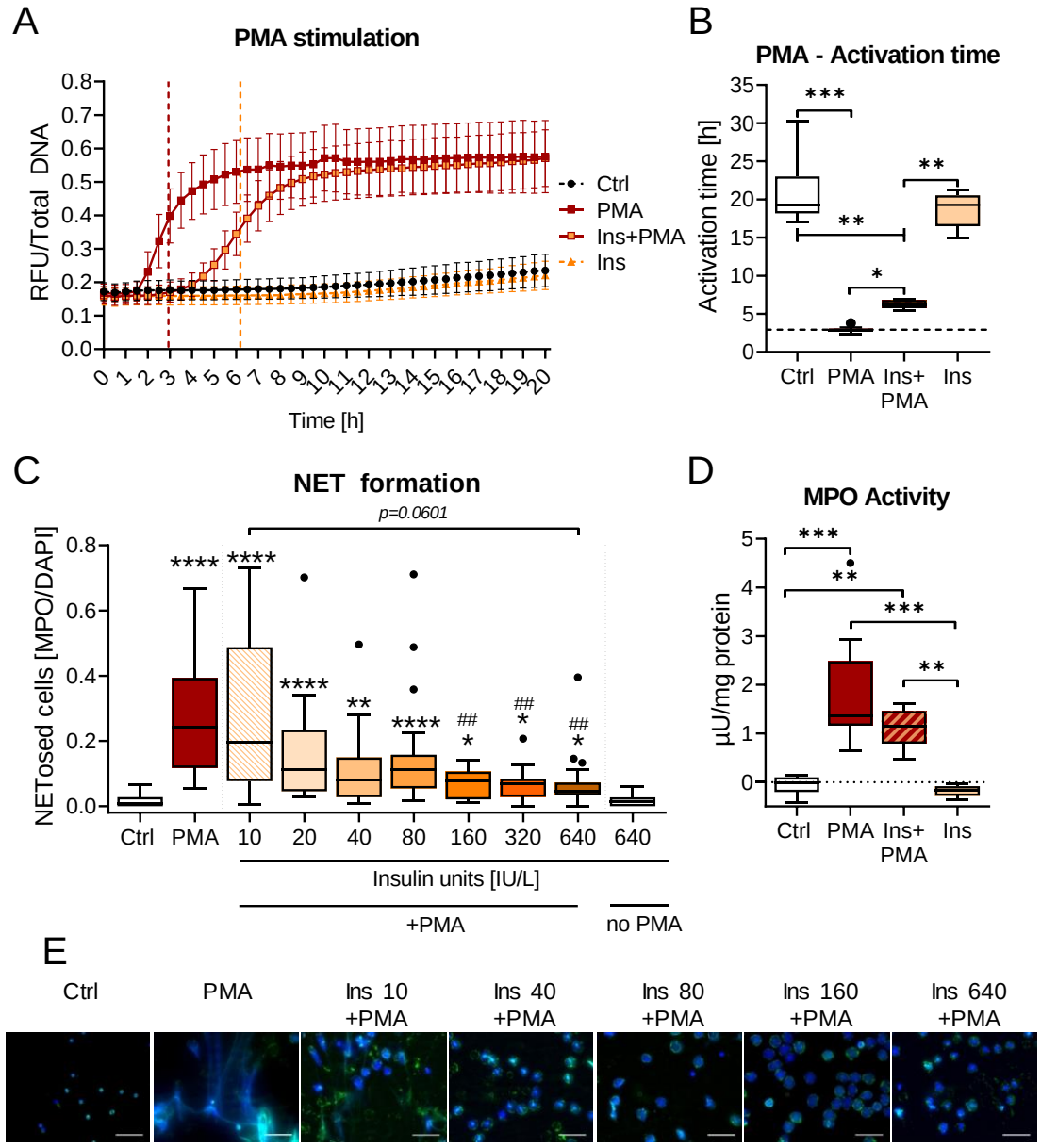

Figure 13: Delayed PMA-induced NET release of neutrophils by the addition of insulin was vonfirmed. **(A)** Time course of DNA release. Vertical lines indicate the calculated activation time (red=PMA, orange=Ins+PMA). **(B)** Activation time of NET formation with overnight measurement of DNA release; N=4, n=4 **(C)** Analysis of NET formation by immunofluorescence analysis; N=4, n=5. **(D)** Analysis of MPO activity after 1 h of stimulation; N=4-6, n=2. **(E)** Representative images of immunofluorescence staining of insulin dilution series. Numbers after Ins indicate the concentration of insulin in IU/L. The scale bar is 50 µm. *p<0.05, **p<0.01, ***p<0.001, ****p<0.0001, ##p<0.01. An asterisk above the boxes indicates significance compared with the control, and # indicates significance compared with the PMA-stimulated cells determined by the Kruskal-Wallis test.

Incubation of neutrophils with PMA and insulin overnight produced a clear shift in the DNA release curve to a later time point compared with PMA alone (Figure 13A). This shift can be seen in a delay in the activation time (time of half-maximal

stimulation) from 2.93±0.32 h (PMA alone) to 6.19±0.52 h (PMA and insulin; Figure 13B). There was a concentration-dependent reduction in NET formation (Figure 13C); it was significantly reduced beginning at 160 IU/L of insulin.

The images (Figure 13E) show large extracellular structures visible only after treatment with PMA alone and treatment with PMA and low insulin concentrations (up to 40 IU/L). With higher insulin concentrations, the typical lobulated nuclear structures of neutrophils cannot be observed anymore, and there is no release of DNA outside of the cells. This indicates activation of the cells but without full NET release. Insulin alone did not affect NET formation even at the highest tested concentration (Figure 13C). The MPO activity was slightly but non-significantly reduced with PMA+insulin compared to PMA alone (Figure 13D), while insulin alone did not induce MPO activity.

For further analysis of the reduced NET formation by insulin, ROS was measured and signaling pathways were analyzed.

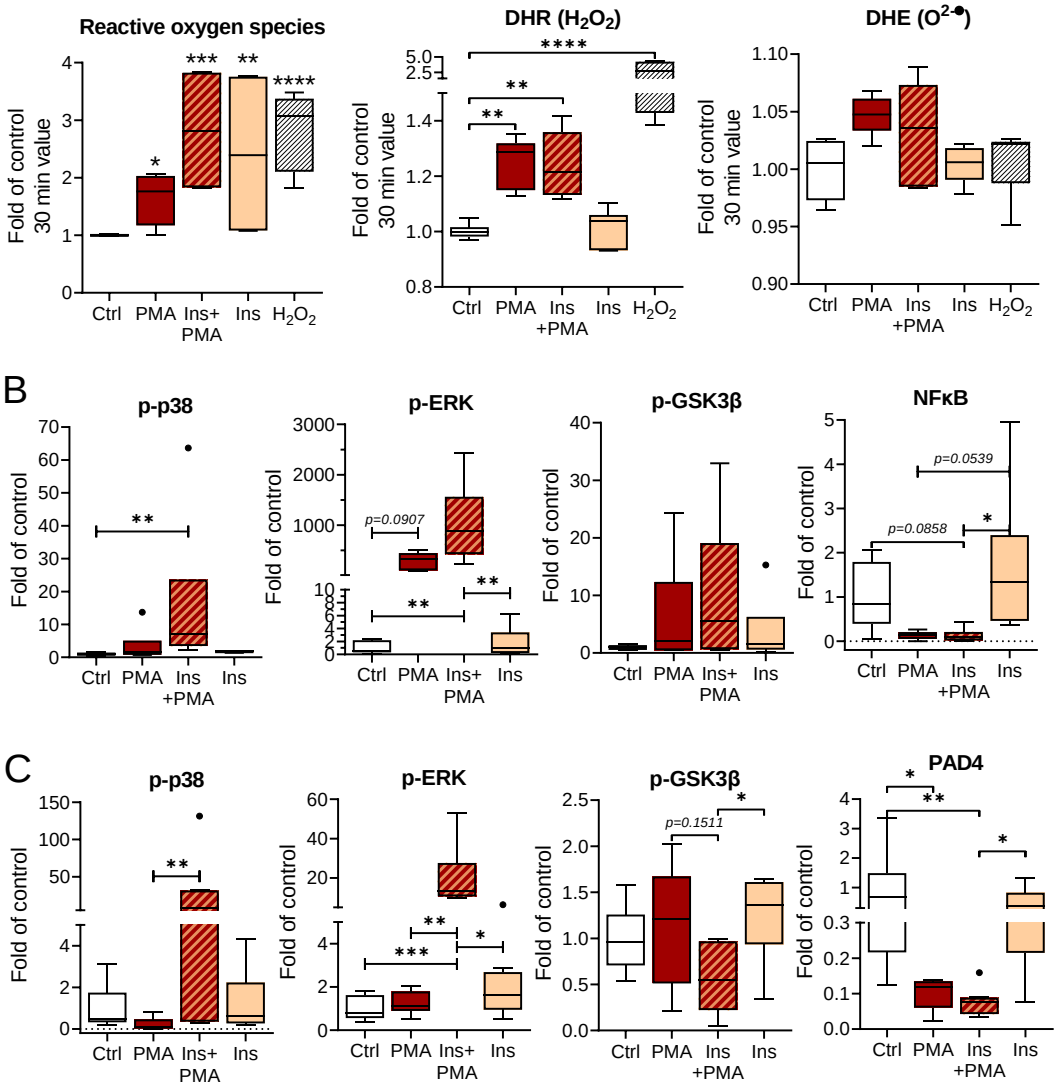

Figure 14: Cellular activation occurs by insulin and PMA treatment. **(A)** Measurement of different kinds of reactive oxygen species. Determination of general reactive oxygen species by DCFH-DA; N=3, n=3. **(B)** Analysis of intracellular signaling proteins after 1 h of stimulation; N=4, n=1-2 **(C)** Analysis of intracellular signaling proteins after 2 h of stimulation; N=4, n=2. DHR: dihydrorhodamine; DHE: dihydroethidium. *p<0.05, **p<0.01, ***p<0.001, ****p<0.0001 determined by the Kruskal-Wallis test.

All tested conditions significantly induced ROS compared with the control (Figure 14A, left). Insulin alone also generated ROS. PMA+Ins showed a higher level of ROS than PMA alone, but this difference was not significant. More specifically, PMA alone induced H_2O_2, but insulin alone did not (Figure 14A, middle). None of the stimulants triggered superoxide radical production (Figure 14A, right). PMA alone induced MAPK activation at 1 h (Figure 14B), but this activation was not persistent (Figure 14C). In contrast, PMA+Ins increased p-ERK and p-p38 levels

for more than 2 h. The level of p-GSK3β was slightly higher after 1-h treatment with PMA±Ins and dropped with PMA+Ins at 2 h. Nuclear factor kappa B (NF-κB; Figure 14B, right) and PAD4 (Figure 14C, right), both crucial proteins in NET activation and inflammation induction, were reduced by PMA treatment but not differentially affected by additional insulin. Insulin alone showed no effect compared with the unstimulated cells.

PMA is a robust but artificial inducer of NET formation. Thus, the effect of insulin was next analyzed in the presence of the natural inducers LPS and H_2O_2.

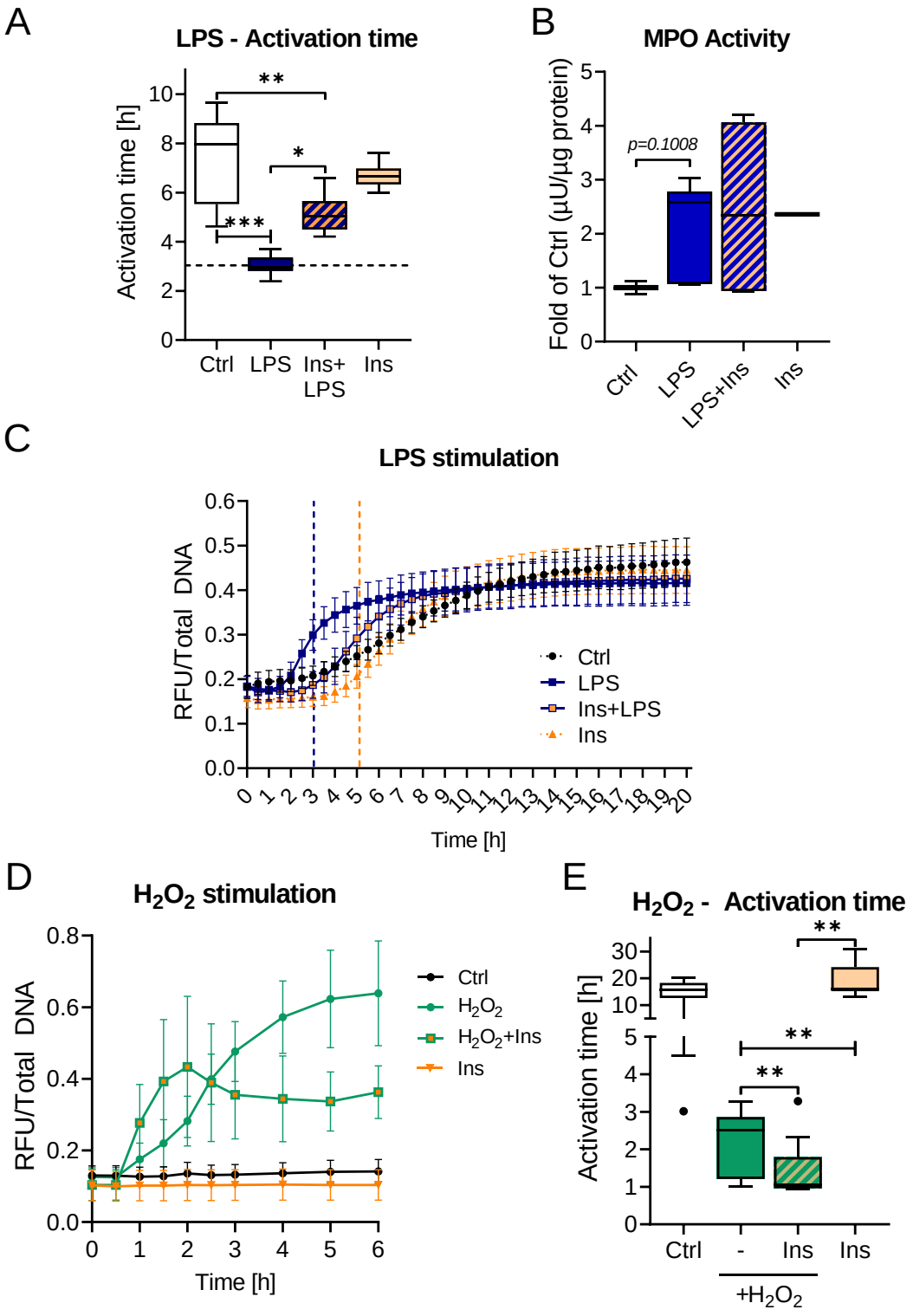

Figure 15: Insulin delays NET release by LPS but not H_2O_2. **(A)** Activation time of NET release determined by the Sytox Green Assay; N=4, n=4. **(B)** MPO activity of neutrophils after 1 h of stimulation; N=3, n=2. **(C)** Time course of DNA release overnight based on the Sytox Green Assay; N=4, n=4. **(D)** Time course of the Sytox Green Assay of H_2O_2 stimulation of neutrophils; N=3, n=3. **(E)** Activation time of NET release determined by the Sytox Green Assay with H_2O_2 stimulation; N=5, n≥3. *p<0.05, **p<0.01, ***p<0.001 determined by the Kruskal-Wallis test.

The addition of insulin to LPS-stimulated neutrophils also delayed NET release (Figure 15A), similarly to the delay seen with PMA stimulation (Figure 12). In the time course of the Sytox Green Assay, there was a shift in the activation curve between LPS stimulation alone (blue) and LPS+Ins stimulation (blue/orange) (Figure 15C). MPO activity was not affected by the addition of insulin, but LPS induced MPO activity (Figure 15B). In contrast, activation of NET release by H_2O_2 was accelerated by adding insulin (Figure 15E), but the time course analysis showed a clear drop in fluorescence after 2 h of stimulation, indicating cell death.

3.2 Isolated NETs are highly toxic to SCP-1 cells and activate monocytic cells

3.2.1 NETs are toxic to SCP-1 cells

Because increased NET formation was found in diabetic patients and insulin strongly regulated NET formation, it was investigated whether NETs influence cells involved in fracture healing. SCP-1 cells (resembling MSCs) and THP-1 cells (mimicking monocytes) were incubated with NETs. For this experiment, neutrophils were stimulated with PMA and NETs isolated from the supernatant by centrifugation. Quantification was based on DNA concentration measurements.

SCP-1 cells were incubated with various NET concentrations (0.0625 to 1 ng/µL), and viability was assessed by mitochondrial activity, total protein determination, and cell death measurements (Figure 16).

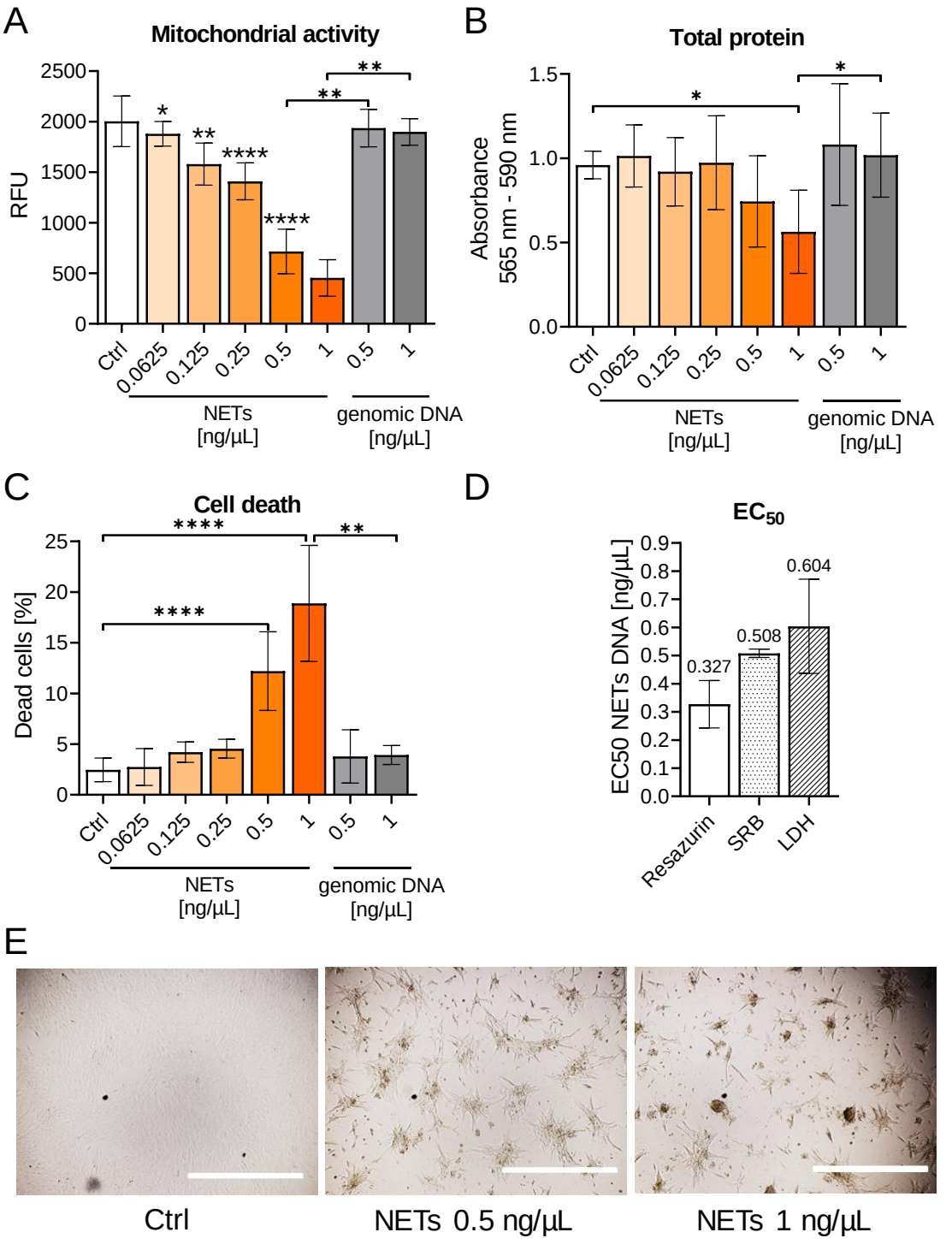

Figure 16: Isolated NETs are toxic to SCP-1 cells. SCP-1 cells were incubated with a dilution series of isolated NETs for 48 h. **(A)** Mitochondrial activity determined by resazurin conversion. **(B)** Total protein content determined by SRB staining. **(C)** Cell death determined by LDH release measurement normalized to lysed cells as a positive control. **(D)** EC_{50} of NETs based on different measurements; the number above each bar is the mean (individual graphs are presented in Supplementary Figure 6). **(E)** Representative microscopy images of SCP-1 cells after 48-h treatment. The scale bar is 1000 µm. N=3, n=3. *p<0.05, **p<0.01, ****p<0.0001 determined by the Kruskal-Wallis test. Data are shown as mean ± standard deviation.

The addition of NETs significantly reduced mitochondrial activity, beginning from 0.0625 ng/µL (Figure 16A). Higher NET concentrations further decreased mitochondrial activity. At 0.5 ng/µL, mitochondrial activity was reduced by more than half. The total protein content (Figure 16B) was reduced significantly at 1 ng/µL NETs, and cell death measured by LDH release was significantly induced by 0.5 ng/µL NETs (Figure 16C). Genomic DNA provided at 0.5 or 1 ng/µL did not affect the cells (Figure 16A-C). The EC_{50} was 0.327 ng/µL for resazurin, 0.508 ng/µL for SRB, and 0.604 ng/µL for LDH (Figure 16D). Figure 16E clearly shows the morphological changes of SCP-1 cells treated with NETs. At 0.5 ng/µL, the cells no longer formed a dense cell layer, but rather showed aggregation at specific spots. At 1 ng/µL, only a few cells were left attached. The curves used to calculate the EC_{50} of each measure are presented in Supplementary Figure 6.

Isolated NETs from high glucose treated neutrophils showed no difference to NETs isolated from normal glucose conditions (Supplementary Figure 7).

3.2.2 Determination of the toxic component of isolated NETs

To determine the toxic component of the isolated NETs, different NET pre-treatments were tested, and the viability of the SCP-1 cells was evaluated. All treatments had been tested for toxicity to the cells (Supplementary Figure 3), and non-toxic concentrations were used. PMSF was excluded from experiments because it was toxic at low concentrations (Supplementary Figure 3).

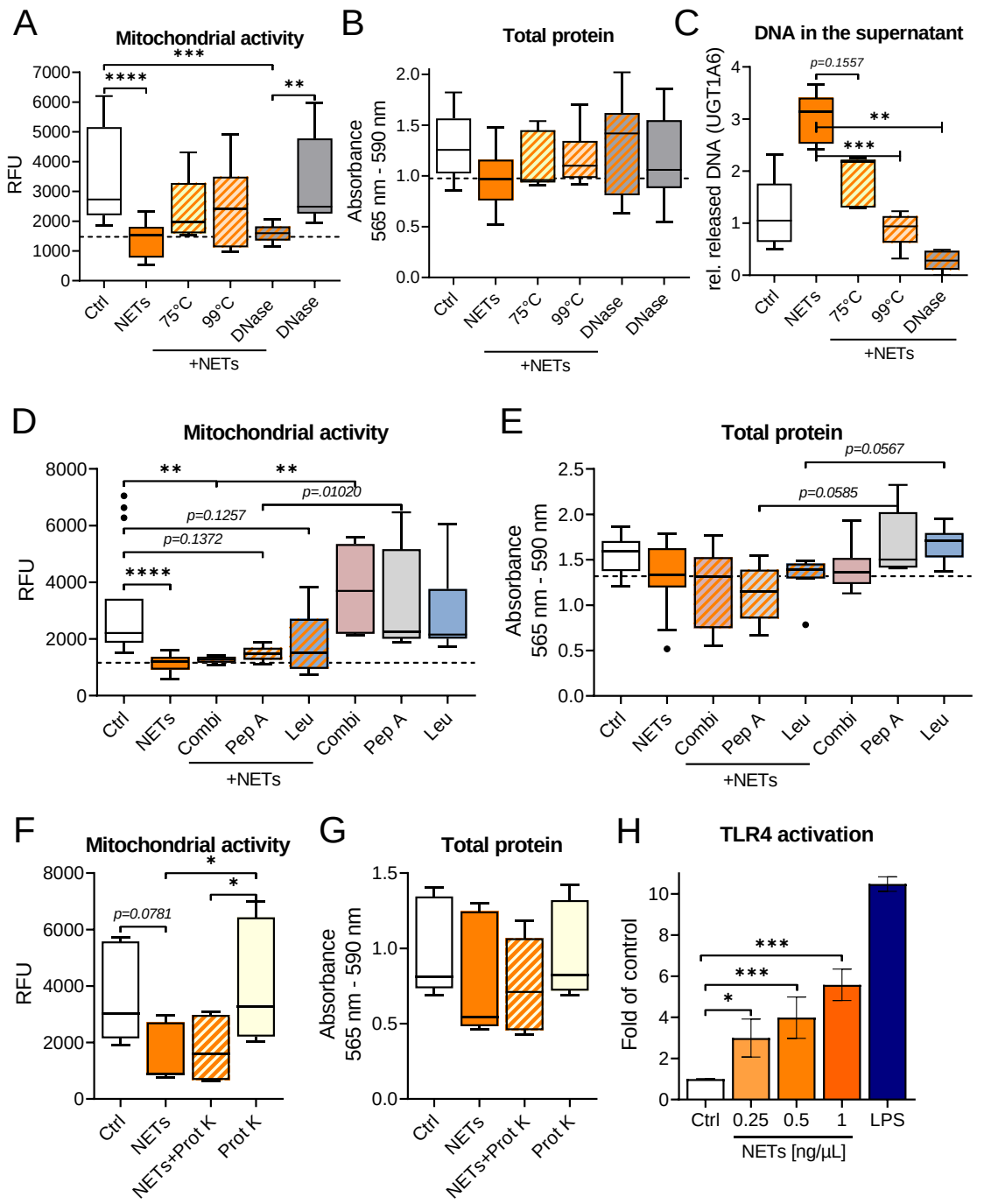

Figure 17: Toxicity of NETs is only effectively reduced by heat treatment. **(A)**, **(B)**, **(C)** Test of DNase and heat treatment to reduce the toxicity of NETs. Cells were co-incubated with 0.5 ng/µL NETs and 200 U/mL DNase, or NETs were pre-treated with heat (99°C 10 min, 75°C 20 min) before addition to the cells. **(A)** Mitochondrial activity determined by resazurin conversion. **(B)** Total protein content determined by SRB staining. **(C)** Determination of DNA content in the supernatant of treated SCP-1 cells by UGT1A6 PCR. **(D)**, **(E)** Evaluating the effect of protease inhibitors on NET toxicity. Co-incubation of SCP-1 cells with 0.5 ng/µL NETs and 1 µg/mL pepstatin A (Pep A) or 5 µg/mL leupeptin (Leu) or a combination of both (Combi). **(D)** Mitochondrial activity determined by resazurin conversion. **(E)** Total protein content determined by SRB staining. **(F)**, **(G)** Evaluating the effect of proteinase K on NET toxicity; 0.5 µg/mL proteinase K was co-incubated with SCP-1 cells and 0.5 ng/µL NETs for 48 h. **(H)** Analysis of

TLR4 activation in the HEK-Blue reporter cell line. LPS served as a positive control. Data are shown as the mean ± standard error of the mean. N=3, n=3. *p<0.05, **p<0.01, ***p<0.001, ****p<0.0001 determined by the Kruskal-Wallis test.

The DNA of the NETs was reduced significantly by treatment at 99°C and with DNase treatment and slightly reduced by treatment at 75°C (Figure 17C). Pre-treatment of NETs with a high temperature (75 or 99°C) reduced the negative effect of NETs on mitochondrial activity in SCP-1 cells. In contrast, DNase showed no effect on mitochondrial activity compared with NETs alone (Figure 17A). NETs slightly reduced the total protein content, and heat or DNase treatment increased the protein content. However, the effects on total protein were not significant in any of the conditions (Figure 17B).

Protease inhibitors (Leu, Pep A, or a combination of both) did not reduce the negative effect of NETs on mitochondrial activity or total protein content in SCP-1 cells (Figure 17A+B). Proteinase K as a general protein degrader did not change NET toxicity (Figure 17F+G).

To find out more about the mechanism NETs induced in SCP-1 cells, a TLR4 HEK-Blue reporter cell line was incubated with different NET concentrations (Figure 17H). NETs showed concentration-dependent activation of TLR4 in the reporter cell line: 1 ng/µL NETs induced TLR4 at half the level of the positive control (LPS), while lower NET concentrations (0.25 and 0.5 ng/µL) still significantly induced TLR4.

A reduction in toxicity could only be achieved with harsh methods like very high temperatures. Removal of NETs could be another option to reduce toxicity. For this, SCP-1 cells were incubated with NETs for 48 h, washed, and then incubated for another 48 h without NETs. Viability was evaluated, and the DNA content in the supernatant and around the cells was determined.

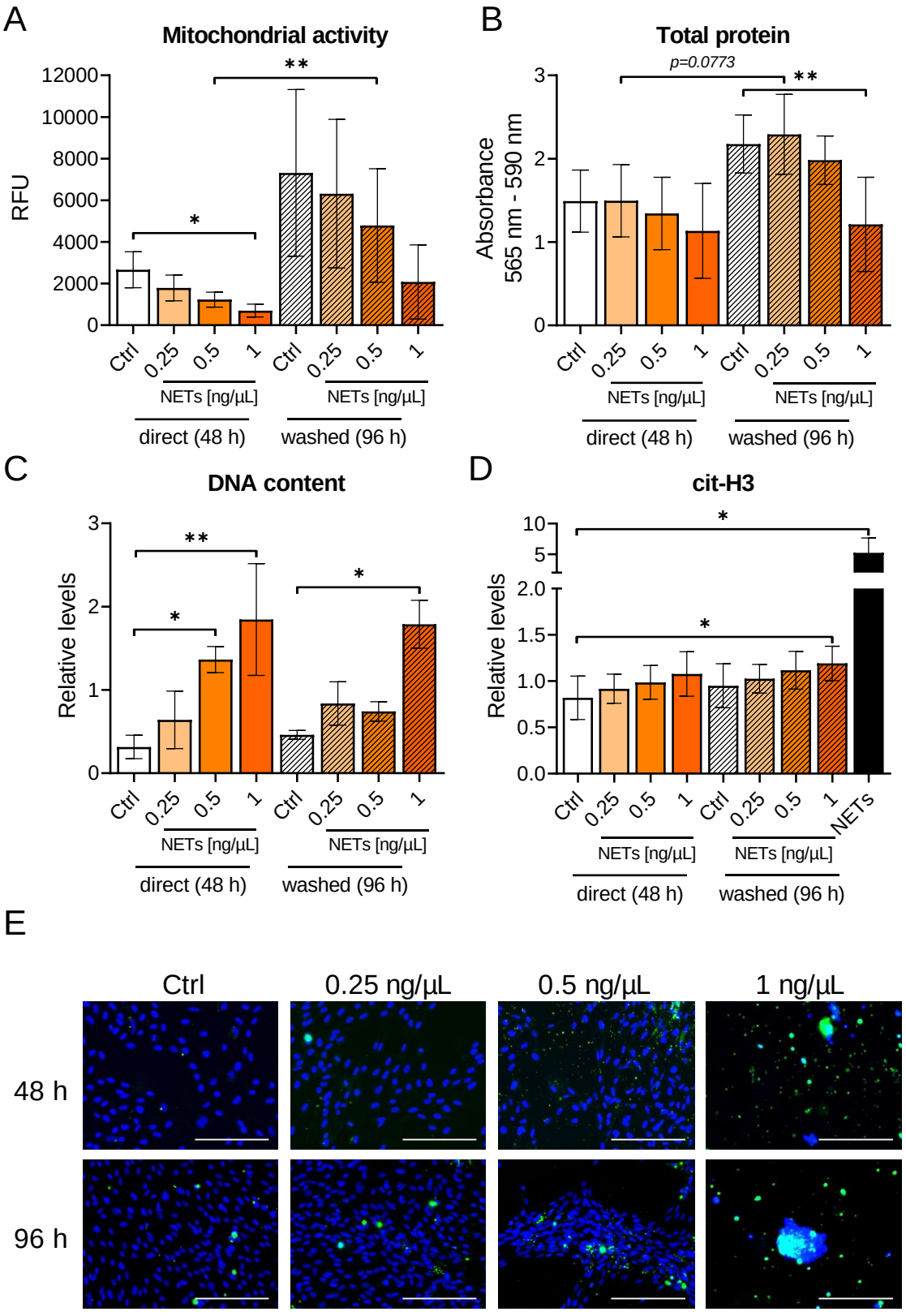

Figure 18: SCP-1 cells do not recover from the toxic effects of NETs in a short period of time. SCP-1 cells were incubated for 48 h with NETs, washed, and then incubated for another 48 h without NETs. **(A)** Mitochondrial activity after 48 and 96 h determined by resazurin conversion. **(B)** Total protein determined by SRB staining. **(C)** DNA content measured by Sytox Green staining

(D) cit-H3 levels in the supernatant of treated SCP-1 cells determined by dot blot. **(E)** Representative images of Sytox Green (green) and Hoechst 33342 (blue) staining. The scale bar is 200 µm. N=3, n=3. *p<0.05, **p<0.01 determined by the Kruskal-Wallis test.

Mitochondrial activity increased from 48 to 96 h in all conditions (Figure 18A). However, the mitochondrial activity in the NET-treated cells was still lower than in the control cells. A significant increase in mitochondrial activity could be observed only in the 0.5 ng/µL group. An elevated total protein content could also be seen from 48 to 96 h, but the 1 ng/µL group still showed a significantly lower total protein content compared with the control group (Figure 18B). The DNA content in the supernatant was significantly higher in both the 0.5 and 1 ng/µL groups compared with the control at 48 h. This effect persisted for 1 ng/µL at 96 h but not for 0.5 ng/µL (Figure 18C). In addition, a high amount of dying cells could also support the increase in DNA concentration.

In the supernatant of NET-treated SCP-1 cells, cit-H3 gradually increased as the NET concentration increased. Pure isolated NETs showed a very high cit-H3 content. However, this difference was only significant for the 1 ng/µL group at 96 h compared with the control group at 48 h (Figure 18D). The Sytox Green staining revealed that at 1 ng/µL, only a few cells were left attached. For the other concentrations, there were small green spots distributed over the cellular layer (Figure 18E, upper panel). These small green spots were reduced at 96 h (Figure 18E, lower panel).

3.2.1 Effect on THP-1 cells

Monocytes are the second cell type that arrive in the fracture gap. Here, the effect of isolated NETs on the activation of THP-1 cells, a monocytic cell line, was analyzed. Activation of THP-1 cells to an inflammatory state has been shown to negatively influence osteogenic migration and differentiation (Zhang *et al.*, 2017).

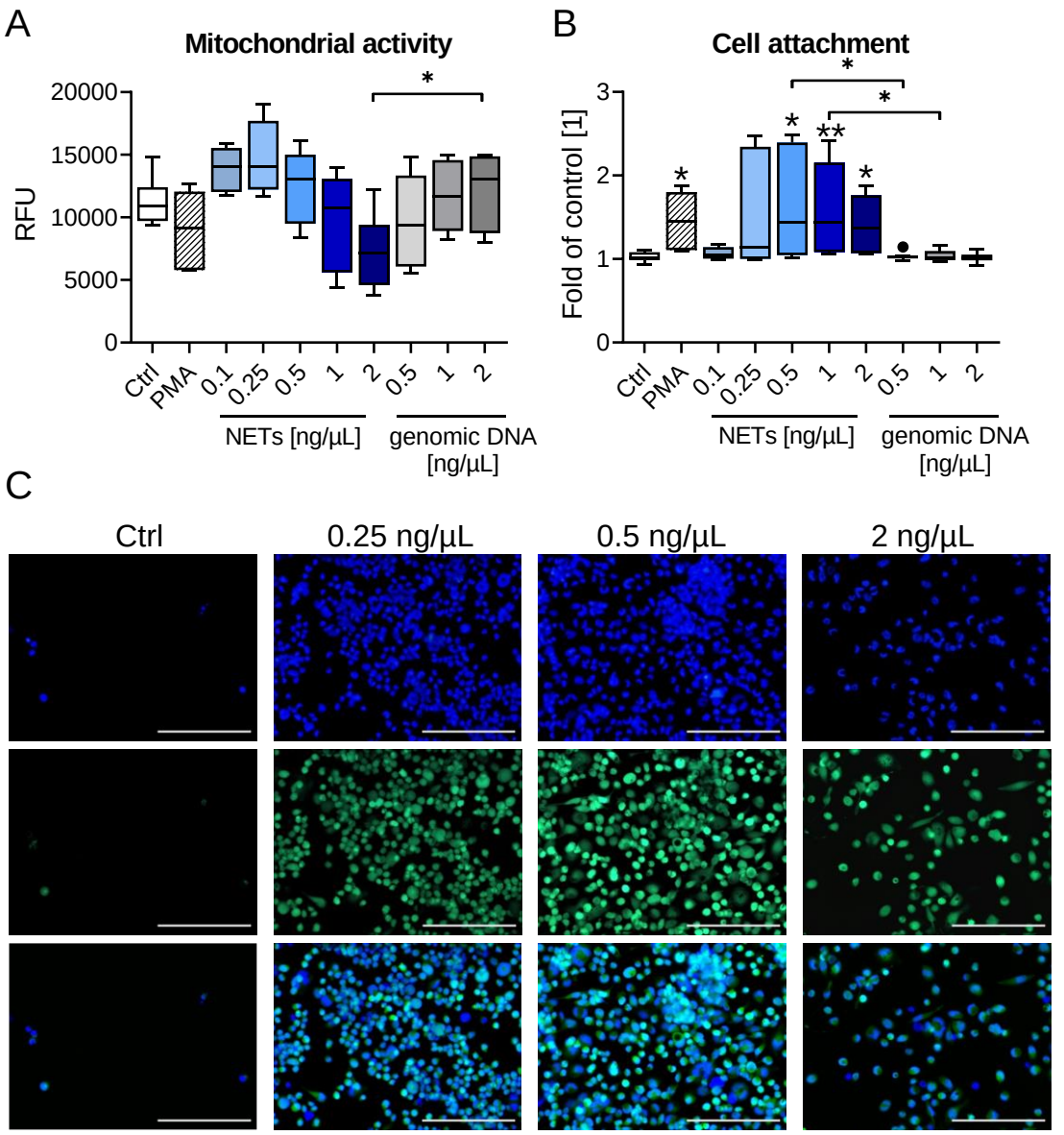

Figure 19: THP-1 cells are activated by NETs. THP-1 cells were incubated with different NET concentrations for 48 h. **(A)** Mitochondrial activity determined by resazurin conversion. **(B)** Cell attachment determined by Hoechst 33342 staining. **(C)** Live staining of THP-1 cells. The upper row shows nuclear staining by Hoechst 33342, the middle row shows live staining by Calcein AM, and the lower row shows overlay images. The scale bar is 200 µm. N=3, n=3. *p<0.05, **p<0.01 determined by the Kruskal-Wallis test. An asterisk above a box indicates significance compared with the control.

The mitochondrial activity of THP-1 cells was only slightly affected by the addition of NETs (Figure 19A). Low NET concentrations (0.1 or 0.25 ng/µL) slightly increased the mitochondrial activity, whereas higher concentrations (1-2 ng/µL) reduced it. THP-1 cell attachment was measured to indicate cell activation (Figure 19B). PMA and NET concentrations from 0.5 to 2 ng/µL significantly induced cellular attachment. The addition of genomic DNA did not induce cellular

attachment. Cell attachment was also confirmed by microscopy (Figure 19C). Almost no cells were attached to the plate in the control condition (left panel). NET concentrations of 0.25 and 0.5 ng/µL (middle panels) induced cellular attachment, whereas with 2 ng/µL, fewer cells attached compared with the lower NET concentrations (right panels).

To test whether THP-1 cells can reduce the toxicity of NETs on SCP-1 cells, THP-1 cells were incubated with 0.5 ng/µL NETs as described previously, and the supernatant was collected. SCP-1 cells were treated for 48 h with these THP-1-conditioned NETs, and mitochondrial activity and the total protein content were analyzed as readouts of viability.

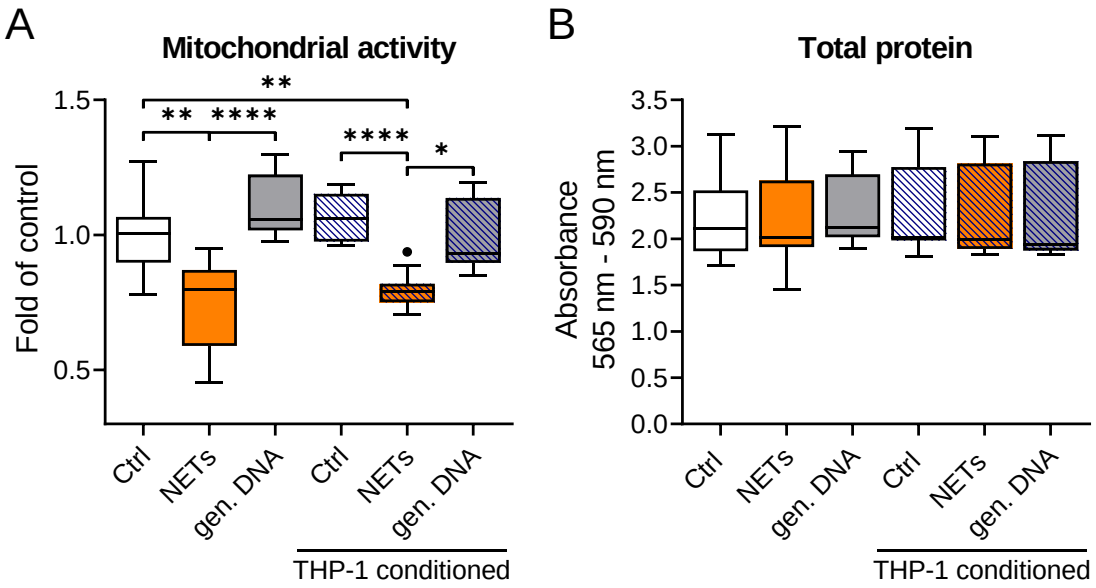

Figure 20: THP-1 cell pre-treatment does not reduce the toxicity of NETs to SCP-1 cells. SCP-1 cells were treated for 48 h with THP-1-conditioned NETs. **(A)** Mitochondrial activity determined by resazurin conversion. **(B)** Total protein content determined by SRB staining. N=3, n=3. *p<0.05, **p<0.01, ****p<0.0001 determined by the Kruskal-Wallis test.

Mitochondrial activity was significantly reduced with either NETs only or THP-1-conditioned NETs (Figure 20A) compared with the basal and the THP-1-conditioned control. Treatment with genomic DNA or THP-1-conditioned genomic DNA did not affect the mitochondrial activity of SCP-1 cells. The total protein content was unaffected by the treatments (Figure 20B). THP-1 cells could not reduce the negative effect of NETs on SCP-1 cells.

3.2.1 Effect of NETs on the migration of SCP-1 cells

Migration is an essential part of successful fracture healing. Thus, the migration of SCP-1 cells in the presence of NETs was analyzed.

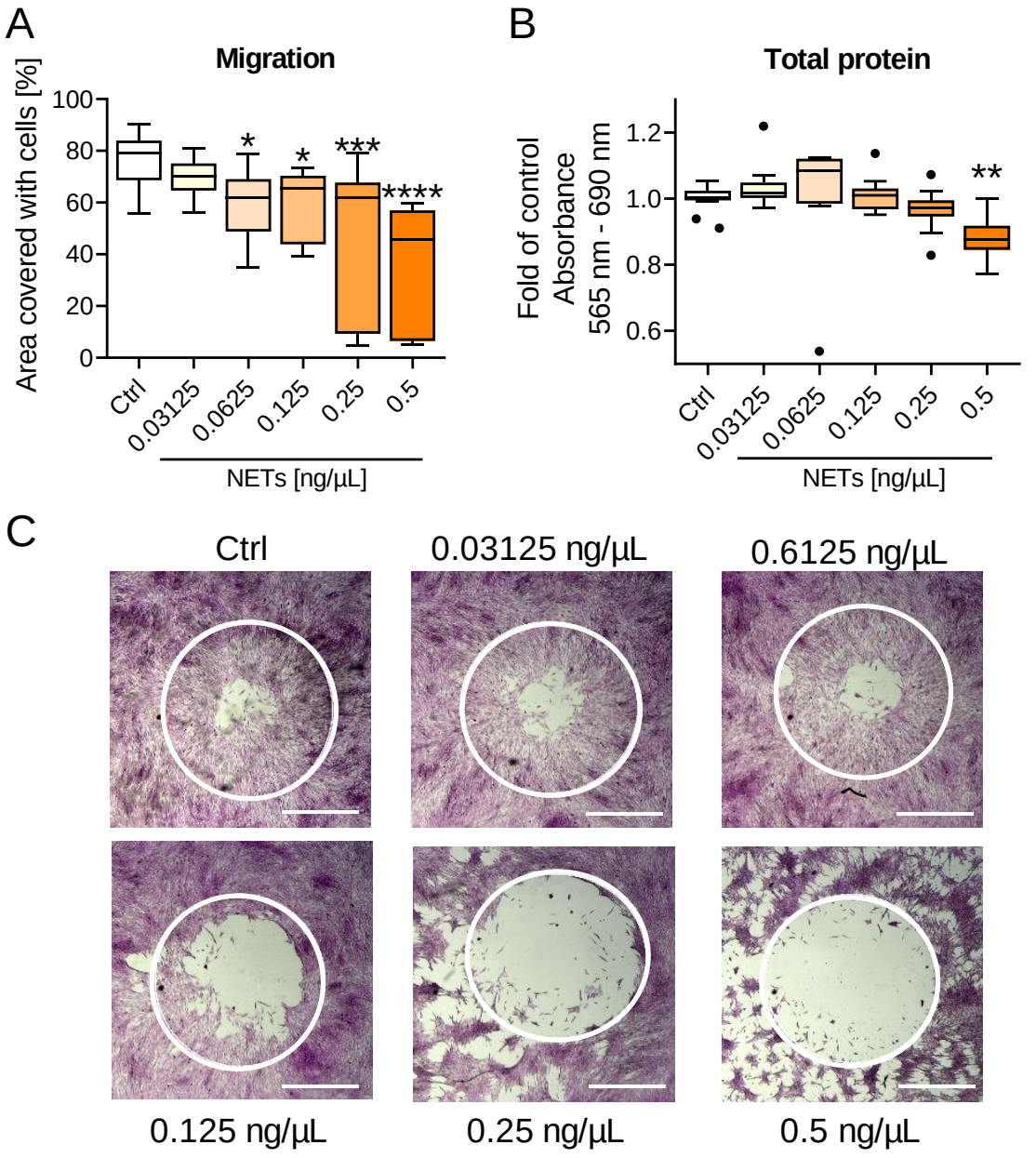

Figure 21: NETs reduce migration of SCP-1 cells. Migration of SCP-1 cells was analyzed by using the Oris cell migration assay after 45 h. **(A)** Migration of cells analyzed by using the initially free area covered with cells. **(B)** Total protein content determined by SRB staining. **(C)** Representative images of the migration assay stained with SRB after 45 h. White circles indicate the original free area. The scale bar is 1000 µm. N=3, n=4. *p<0.05, **p<0.01, ***p<0.001, ****p<0.0001 compared with the control, determined by the Kruskal-Wallis test.

Migration was significantly reduced already at 0.0625 ng/µL NETs (Figure 21A). Increasing the NET concentration further decreased the migration of SCP-1 cells, whereas the total protein content was only significantly reduced at 0.5 ng/µL NETs (Figure 21B). The reduced migration could also be directly observed in the microscopy images (Figure 21C), with an increase in the free area as the NET concentration increased compared with the control.

3.2.2 Effect of NETs on differentiation of SCP-1 cells

When MSCs arrive in the fracture gap, they need to differentiate into osteogenic cells to form new bone matrix. Differentiation of SCP-1 cells was investigated after a single exposure to NETs at the beginning of the differentiation period. This setup resembles an inflammatory reaction at the beginning of fracture healing with or without NET formation.

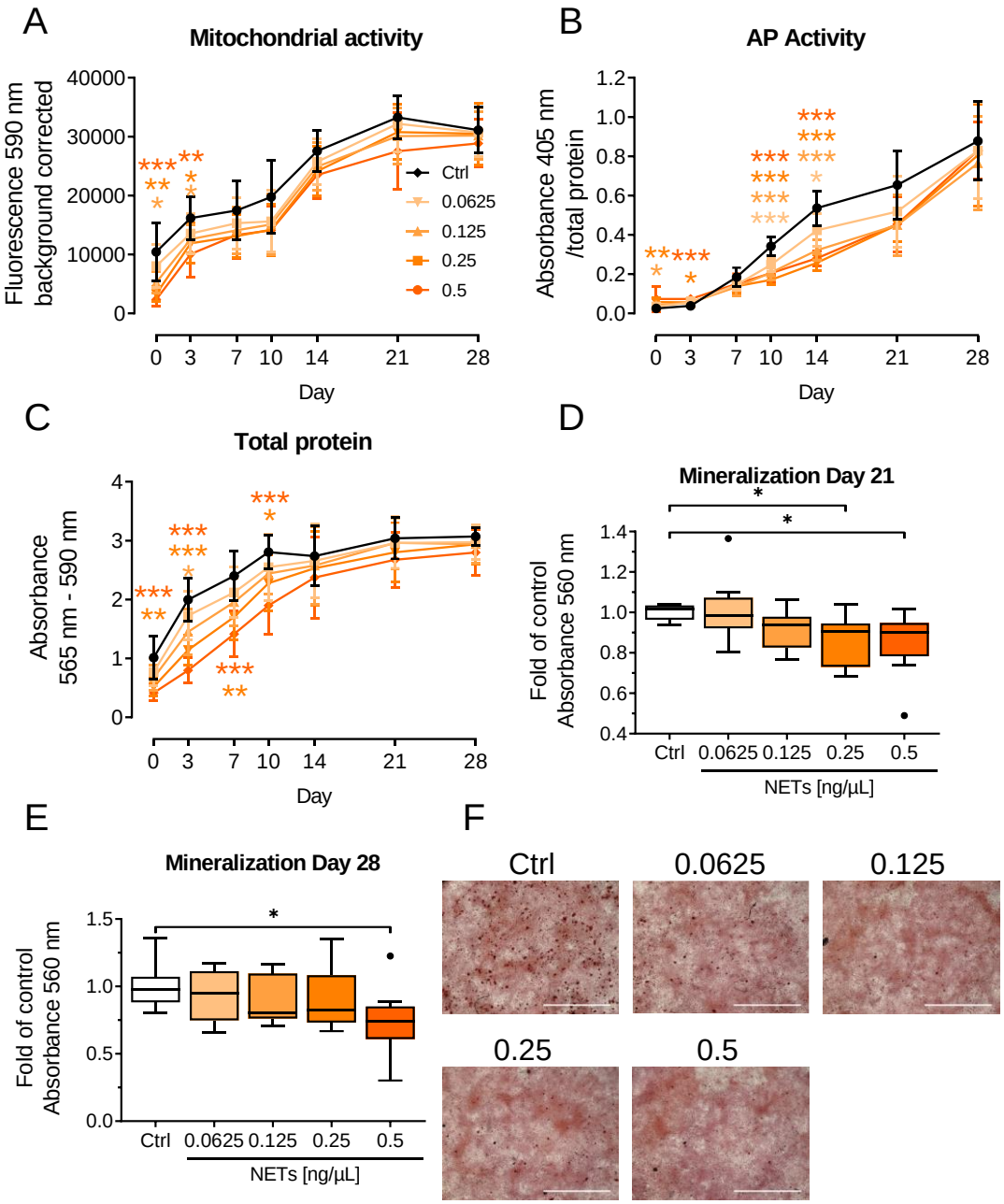

Figure 22: Differentiation of SCP-1 cells is reduced under the influence of NETs. SCP-1 cells were incubated with a dilution series of isolated NETs for 48 h in growth medium. Then, differentiation was started by the addition of differentiation medium (day 0). Cells were differentiated for 28 days. **(A)** Mitochondrial activity determined by resazurin conversion. **(B)** AP activity measurement **(C)** Total protein content determined by SRB staining. **(D)** Mineralization determined by Alizarin Red staining on day 21. **(E)** Mineralization determined by Alizarin Red staining on day 28. **(F)** Representative microscopy images of Alizarin Red staining on day 28. The number above each image indicates the NET concentration in ng/µL. The scale bar is 2000 µm. N=3, n=3. *p<0.05, **p<0.01, ***p<0.001 determined by the Kruskal-Wallis test. The colors indicate significance compared with the control. Data are shown as the mean ± standard deviation.

NETs significantly reduced mitochondrial activity until day 3 (Figure 22A). After that, mitochondrial activity was still slightly lower, but the effect was no longer

significant. The total protein content was negatively affected until day 10 at the higher NET concentrations (0.25 and 0.5 ng/µL). From day 14, there was not a significant difference for any condition (Figure 22C). The AP activity was strongly affected by incubation with NETs. On days 10 and 14, all NET concentrations significantly reduced the total protein-normalized AP activity; on day 21, the difference was no longer significant. On day 28, the AP activity of NET-treated SCP-1 cells reached the level of control cells (Figure 22B). Mineralization was significantly reduced at day 21 at the higher NET concentrations (0.25 and 0.5 ng/µL, Figure 22D) and still at the highest NET concentration at day 28 (Figure 22E). The representative images of Alizarin Red staining at day 28 (Figure 22F) show the beginning of small matrix spots in control cells, which are absent at 0.5 ng/µL and reduced at the lower NET concentrations.

Overall, recovery of the cells could be seen starting from day 14. On day 28, AP activity in NET-treated cells reached the levels of control cells. This substantial and lasting effect of isolated NETs on MSCs raised more questions about possible factors that influence NET formation rates in humans. PAD4 is an essential protein for NET formation, and *PADI4* SNPs are relevant for the formation of NETs and the pathogenicity of diseases like RA (Harris *et al.*, 2008).

3.3 Clinical outlook

The three SNPs of *PADI4* have a high co-incidence (nearly 1) and result in three amino acid changes in the final protein. Because PAD4 is an essential protein in NET formation, the effect of this altered protein on NET formation was investigated in neutrophils from healthy volunteers.

3.3.1 *PADI4* polymorphisms influence NET formation and PAD4 protein levels

The *PADI4* variant of each healthy volunteer was determined by ARMS-PCR. For each group, neutrophils from at least seven donors were isolated, and NET formation and activation of cells were analyzed at baseline and in response to PMA and CI stimulation. Table 12 shows the characteristics of the two study groups.

Table 12: Characteristics of the study cohort.

Group	Donors	Mean age [years]	Gender (F/M)	p-Value age/gender
Major	8	35.25	3/5	0.890
Minor	7	34.43	2/5	0.737

Activation of neutrophils was analyzed by using the Sytox Green Assay to measure later activation (NET release) and by using bio-impedance measurement to measure early activation. Together with bio-impedance measurement, live-microscopy images were evaluated for NET formation as described previously (Linnemann *et al.*, 2020).

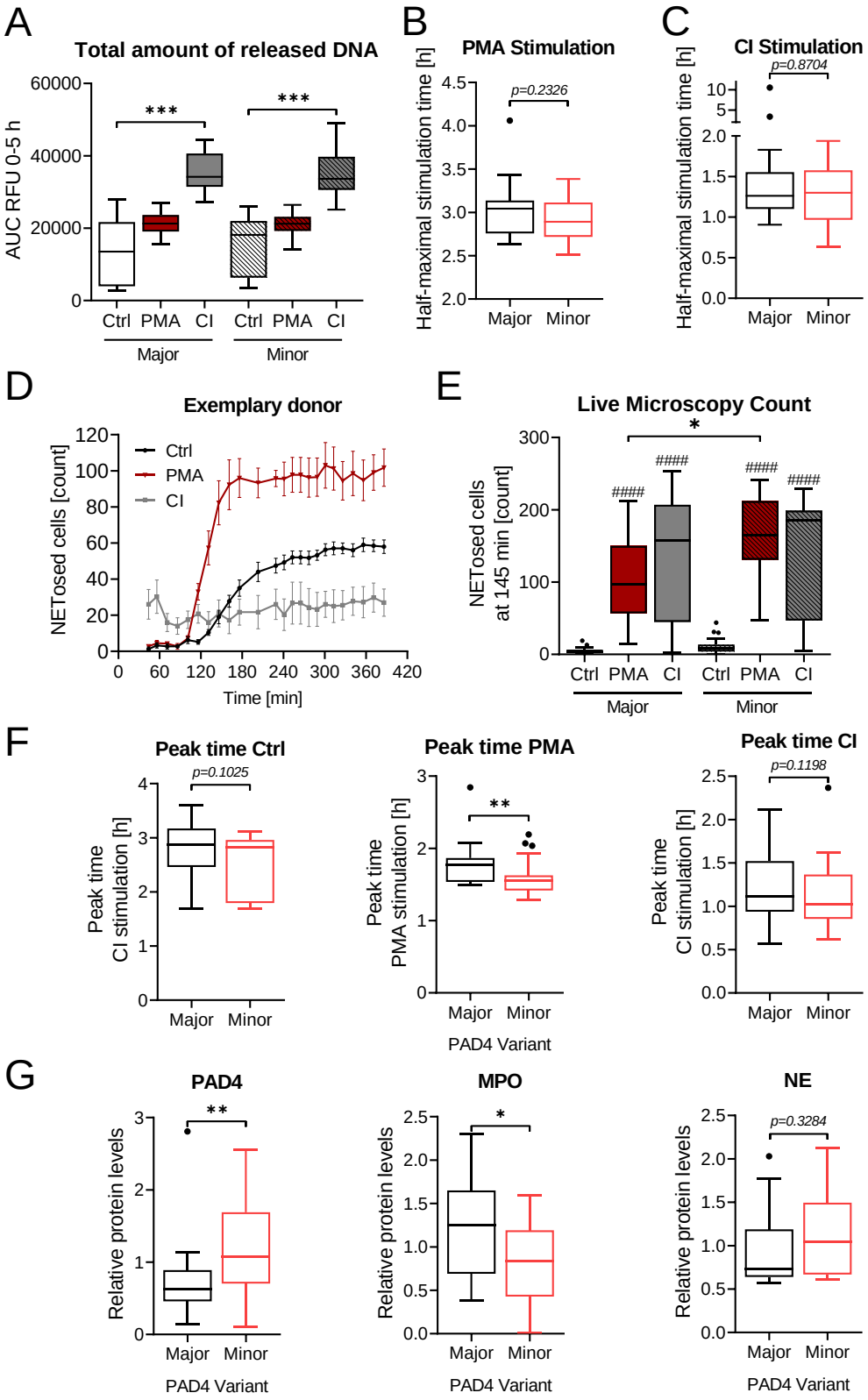

Figure 23: *PADI4* SNPs influence NET release. **(A)**, **(B)**, **(C)** Analysis of NET release by the Sytox Green Assay. **(A)** Total amount of DNA release determined by calculating the AUC from 0-5 h. **(B)** Half-maximal stimulation time of PMA stimulation. **(C)** Half-maximal stimulation time of CI stimulation; N≥7, n=3. **(D)**, **(E)** Analysis of NET release by live microscopy imaging. **(D)**

Representative time course of the count of NETosed cells of one donor. **(E)** Counts of NETosed cells at 145 min; N≥7, n=4 **(F)** Peak time of bio-impedance measurement for the three different stimulants; N≥7, n=4 **(G)** PAD4, MPO, and NE protein levels determined by western blot/dot blot; N≥7, n=3. *p<0.05, **p<0.01, ***p<0.001 determined by the Kruskal-Wallis test (multiple comparisons) or the Mann-Whitney U test (single comparison).

The total amount of released DNA, as determined by the Sytox Green Assay, was not different between the major and the minor groups (Figure 23A). The activation time of NET release by PMA or CI stimulation did not differ between the major and the minor groups (Figure 23B+C). Figure 23D shows a representative time course of the live-microscopy analysis of NET release. Evaluation at 145 min revealed a significantly higher amount of NETosed cells in the minor group than in the major group (Figure 23E). With CI, no difference could be seen. Measurement of the early activation by bio-impedance revealed a slightly faster but non-significant activation in the minor group in control cells or with CI stimulation (Figure 23F). With PMA, neutrophil activation happened significantly earlier in the minor group than in the major group (Figure 23F).

To find out more about possible underlying reasons, the levels of important proteins were determined. PAD4 levels were significantly higher in the minor group, whereas MPO levels were significantly lower in the minor group (Figure 23G). NE levels were not affected by the PAD4 variant.

3.3.2 Patients with a chronic wound patients release fewer NETs than patients with an acute wound

To check the clinical relevance of NET formation, neutrophils were isolated from patients with acute wounds (<30 days), sub-chronic wounds (30-90 days), and chronic wounds (>90 days). NET release was analyzed from unstimulated and stimulated (PMA, CI) neutrophils by using the Sytox Green Assay. The patient characteristics can be found in Table 13.

Table 13: Characteristics of patients with acute, sub-chronic, and chronic wounds.

	Acute	Sub-chronic	Chronic	Overall p-value
Sample number	10	6	6	-
Wound duration [days]	14±9.6	66.6±27.0	357.3±316.6	<0.0001
Age [years]	56.9±12.8	59.6±20.2	52.3±14.2	0.8689
BMI [kg/m^2]	25.9±3.7	26.5±4.3	28.1±7.0	0.8355
Female [%]	16.67	28.57	44.44	>0.9999
Smoker [%]	87.5	60	50	>0.9999
Diabetes [%]	8.3	20	16.7	>0.9999
Infection of wound [%]	50	80	66.7	>0.9999

BMI: body mass index

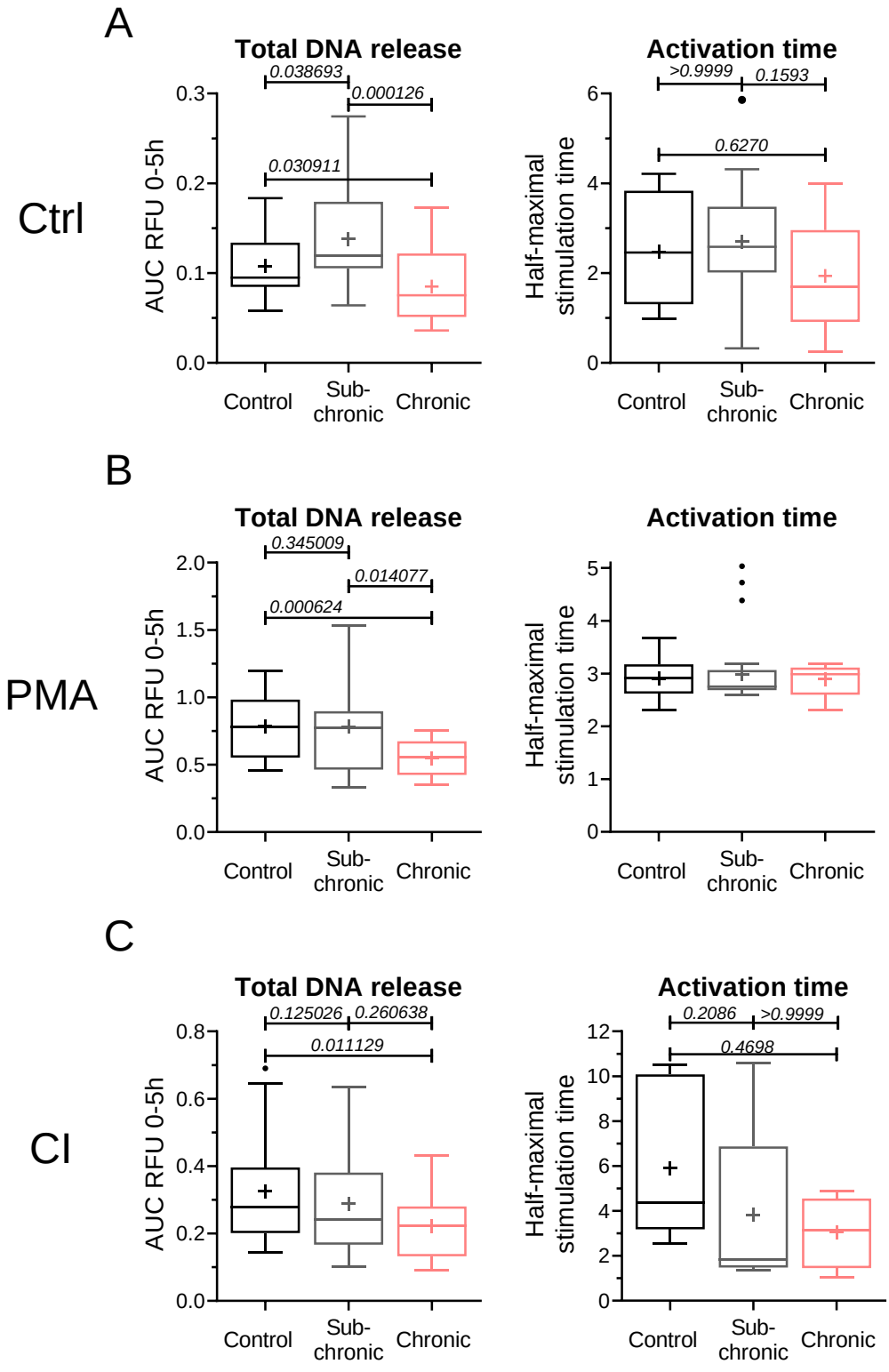

Figure 24: Patients with chronic wounds release fewer NETs than patients with acute wounds. **(A)**, **(B)**, **(C)** Analysis of DNA release by the Sytox Green Assay with different stimulants. Total DNA release was determined by calculating the AUC for 0-5 h. The activation time is presented as the half-maximal stimulation time for **(A)** Control, **(B)** PMA, and **(C)** CI. N≥7, n=3. The italic numbers in the graphs indicate p-values determined by the Kruskal-Wallis test.

Unstimulated neutrophils from patients with sub-chronic wounds showed a significantly higher NET release than control neutrophils or neutrophils from patients with chronic wounds (Figure 24A, left). After PMA stimulation, the neutrophils of patients with sub-chronic wounds were not different from the neutrophils of control patients (Figure 24B, left).

The neutrophils of patients with chronic wounds released a significantly lower amount of NETs than the neutrophils of control patients and patients with sub-chronic wounds without stimulation and after PMA stimulation (Figure 24B, left). With CI stimulation, the neutrophils of patients with chronic wounds released significantly fewer NETs than the neutrophils of control patients, but no significant difference was observed compared with the neutrophils of patients with sub-chronic wounds (Figure 24C, left). For PMA and CI stimulation, no differences could be seen in the activation time between the neutrophils from the different groups (Figure 24B+C, right).

Regarding clinical applications, SCP-1 cell supernatant induced a substantial reduction in PMA-induced NET release (Supplementary Figure 8).

4. Discussion

Various clinical complications often characterize advanced T2DM. One of them is delayed healing of fractures and wounds, resulting in an increased complication rate. Fractures occur in nearly every person at least once in their lifetime. Diabetes is one of the main risk factors for the development of delayed fracture healing or even a non-union (Picke *et al.*, 2019). Although many advances have been made, the reasons for this are still not well understood. Besides angio- and neuropathies, T2DM patients have an overactive immune system resulting in a constant inflammatory state. The immune system plays a pivotal role in the induction of fracture healing (Schmidt-Bleek *et al.*, 2012); thus, it is very likely that a disturbed immune system play a role in the delayed fracture healing of T2DM patients.

4.1 NET formation in diabetic patients

In the trauma patient cohort analyzed here, the neutrophils of DM patients released more NETs when exposed to all stimuli, especially the NOX-dependent ones (PMA, H_2O_2). Unstimulated neutrophils from T2DM patients also released more NETs than neutrophils from control patients; however, this difference was not significant because the total NET release in unstimulated neutrophils was low. In many cases, the formation of NETs contributes to disease pathogenicity (Mitsios *et al.*, 2016), particularly in the development of type 1 diabetes (Sodré *et al.*, 2021). T2DM patients have been shown to release more NETs without stimulation (Wang *et al.*, 2018). Still, in certain cases, isolated T2DM neutrophils no longer react to stimuli, and NET release is less than from healthy control neutrophils, suggesting neutrophil exhaustion (Carestia *et al.*, 2016). In the present investigation, this was different; neutrophils from DM patients released more or the same amount of NETs in response to all tested stimuli compared to control patients.

One reason for the increased NET release could be the increased PAD4 levels observed in T2DM patients. PAD4 is an essential protein in NET formation, being activated by ROS-dependent and ROS-independent stimuli (Thiam *et al.*, 2020). The rate of cit-H3 did not differ between controls and T2DM patients in response

to CI stimulation, suggesting a different role for PAD4. PAD4 overexpression could generate a kind of NET release in osteogenic U2OS cells, although osteosarcoma cells usually do not release NETs (Leshner *et al.*, 2012). An increase in cit-H3 could not be observed in the present study, but NET release was also not increased with CI stimulation. However, in the limited number of patients, it was not investigated whether the increased NET release in DM patients after PMA stimulation was due to increased cit-H3 levels.

There are several factors responsible for increased NET formation in T2DM patients. An inflammatory phenotype (Ehnert *et al.*, 2015b), increased ROS (Bartlett *et al.*, 2020), and increased activation of MAPKs (Wang *et al.*, 2019) are all prerequisites for NET formation. There were no hints in the present study for neutrophil exhaustion (reduced NET formation in response to stimuli), as had been seen in another study (Cichon *et al.*, 2021). One possible reason could be the medication T2DM patients receive in standard care in Germany. For example, metformin, one of the leading oral drugs to treat T2DM patients in Germany (Landgraf *et al.*, 2019), has been shown to reduce NET formation (Carestia *et al.*, 2016, Menegazzo *et al.*, 2018). Moreover, it has been demonstrated that metformin can partially suppress the release of pro-inflammatory cytokines in freshly diagnosed diabetics (Lee *et al.*, 2013). Thus, it is conceivable that this may contribute to the reversion of increased NET formation observed in T2DM patients under metformin treatment (Carestia *et al.*, 2016).

4.2 HG effect on NET formation

In the present study, neutrophils from T2DM patients showed higher NET release after stimulation with PMA. To find out more about the underlying mechanisms, the neutrophils from healthy volunteers were incubated in diabetic conditions. *In vitro*, HG was tested for the ability to induce NETs in neutrophils from healthy volunteers, a phenomenon that had been shown in a previous study (Menegazzo *et al.*, 2015). In contrast, in the present study, a standard HG concentration (25 mM; Häussling *et al.*, 2021) did not induce NET formation in healthy neutrophils. Likewise, in two other studies, glucose alone did not affect NET formation (Cichon *et al.*, 2021, Joshi *et al.*, 2013). HG changes the osmolarity of

the cell culture medium, similarly to mannitol, which has been shown to inhibit PMA-induced NET formation (Menegazzo *et al.*, 2015) and to act as a ROS scavenger (Larsen *et al.*, 2002). A change in osmolarity might also prevent NET formation by HG. However, 24-h pre-stimulation of neutrophils with HG increased NET formation, but the response was reduced when combined with stimuli such as LPS and IL-6 (Joshi *et al.*, 2013). Notably, no such effect could be observed in the present study. This could be due to the shorter pre-stimulation time with the diabetic conditions (a maximum of 6 h compared with 24 h), which was chosen due to increased cell death of neutrophils after 5-6 h.

In another *in vitro* study, HG-induced NET formation in a concentration-dependent manner by a ROS-dependent mechanism (Wang *et al.*, 2018). However, ROS formation induced by HG could not be observed in this study. The missing ROS induction may have blocked NET formation, as shown previously (Kirchner *et al.*, 2012).

ROS quenching by autologous plasma may further prevent HG-induced NET release. All experiments were conducted with 2% autologous plasma to increase the survival rate and to reduce basal activation of neutrophils. Indeed, the present findings are in line with experiments showing that autologous plasma inhibits ROS production in PBMCs (Veloso *et al.*, 2008). In another study, serum albumin also reduced NET formation (Zheng *et al.*, 2021). Similarly, neutrophils exposed to 2% human serum did not show NET release induced by high glucose (Joshi *et al.*, 2013), although in another study from the same group, HG induced significant NET release with 2% human serum (Joshi *et al.*, 2016). Nevertheless, the present study did not totally remove plasma to better mimic the *in vivo* situation.

Taken together, these results indicate that other conditions (*e.g.*, elevated cytokine levels) but not HG are possibly responsible for higher NET formation in T2DM patients.

4.3 Insulin effect on NET formation

Insulin is the second factor with a substantial role in diabetes. At the beginning of T2DM, insulin levels increase together with glucose as a compensatory mechanism. Later, when the pancreas can no longer produce such high amounts

of insulin, insulin levels decrease, and insulin needs to be replaced by external application.

Insulin not only regulates blood sugar levels but is also a potent regulator of the innate immune response (Sunahara *et al.*, 2012). Up to now, the effect of insulin on NET release had not been investigated. Given that HG did not directly affect the formation of NETs with or without additional stimuli, insulin was further examined as the second player in T2DM. Insulin in combination with HG delayed PMA-induced NET formation.

A more detailed analysis of the effect of insulin on NET formation revealed a dose-dependent suppression of NET formation, which was not entirely blocked but delayed by some hours. This effect was also seen when neutrophils were exposed to LPS. Interestingly, co-incubation of CI plus insulin did not affect NET formation. CI uses a ROS-independent pathway to activate NET release, whereas PMA or LPS rely on ROS production for NET formation (de Bont *et al.*, 2018). Consequently, the interference of insulin with ROS would only delay the effects of the ROS-dependent stimuli PMA and LPS. An influence on ROS pathways is supported by the observed accelerated NET formation with H_2O_2 plus additional insulin. However, microscopy images indicated that necrosis occurred due to very high levels of ROS production rather than NET formation.

Basal insulin application induced high levels of general ROS, but not specifically H_2O_2 or $O^{2-\bullet}$. One hypothesis is that an imbalance in the types of ROS prevents NET formation. MPO could be a decisive factor here. The MPO activity was slightly reduced by insulin application, a fact that had been established in a mouse model (Stegenga *et al.*, 2008) and in isolated neutrophils (Oldenborg, 1999). MPO catalyzes the reaction of H_2O_2 to HOCl (Winterbourn and Kettle, 2012) and is necessary for NET formation (Kenny *et al.*, 2017, Metzler *et al.*, 2011). The specific types of ROS produced by MPO may be necessary for NET formation. Thus, reduced activity could diminish NET formation, similarly to what had been observed in neutrophils from patients with reduced MPO activity (Metzler *et al.*, 2011).

In more detail, analyses of signaling pathways revealed that insulin plus PMA overactivated MAPKs. While activation of ERK and p-38 is essential for NET formation by PMA (de Bont *et al.*, 2018, Hakkim *et al.*, 2011), in this study it did not induce NET formation. A similar effect of insulin has been observed in macrophages: Its application induced MAPKs and inflammatory cytokines but prevented activation of PKC (Tessaro *et al.*, 2017), which is the target of PMA-induced NETosis. Therefore, insulin may initially inhibit PMA- or LPS-induced PKC activation in neutrophils and delay NET formation. However, PKC inhibition also inhibits NET formation by CI (Neeli and Radic, 2013) which was not seen with insulin.

Besides the already described factors, PAD4 plays an essential role in NET formation (Tatsiy and McDonald, 2018). PAD4 levels were not affected by insulin treatment of neutrophils, but insulin induced high ROS, a phenomenon that could inhibit PAD4 activity (Damgaard *et al.*, 2017). Thus, the increased ROS induction by insulin addition could inhibit PAD4 activity. While the inhibition of PAD4 activity is sufficient to prevent NET formation (Lewis *et al.*, 2015), PAD4 activity was not directly investigated in this study.

Clinically, insulin application has been used successfully to improve the survival of critically ill patients even if they did not have diabetes (van den Berghe *et al.*, 2001). In diabetics, insulin application reduces circulating plasminogen activator-inhibitor 1 and tissue factor to decrease the risk for thrombosis development (Aljada *et al.*, 2002). Released NETs interact with both plasminogen activator inhibitor 1 and tissue factor, leading to an increased risk for thrombosis (Stakos *et al.*, 2015, von Brühl *et al.*, 2012). Insulin could thus modify the initial release of NETs and prevent the consequences of formed NETs by reducing interactors.

The strong insulin effect further suggests that pre-diabetic patients who already have increased insulin levels and insulin resistance are affected. Because approximately 50% of all patients in German hospitals have diabetes or are prediabetic, this finding might be highly relevant in clinical settings (Kufeldt *et al.*, 2018).

4.4 Toxic effect of NETs

Once NETs are released, they exert different effects on surrounding cells and tissues. The main components of NETs are antimicrobial proteins, DNA, histones, and other neutrophil-specific proteins like MPO or NE (Petretto *et al.*, 2019). PMA-induced NETs were notably toxic to SCP-1 cells. In melanoma cells, DNA was the toxic component of NETs leading to cell death (Schedel *et al.*, 2020). DNase effectively reduced the toxicity of NETs in this specific cell type, but in SCP-1 cells, DNase just slightly reduced the toxicity of NETs. Furthermore, SCP-1 cells were much more sensitive to NETs than melanoma cells (Schedel *et al.*, 2020). Recovery was prolonged after removal of NETs or during differentiation of SCP-1 cells. This finding suggests that NETs may have a persistent negative effect on tissue, as previously shown in SLE (Hakkim *et al.*, 2010).

DNase is often postulated as the first-line treatment against NET-induced tissue damage. However, some studies have shown that the DNA itself is not the toxic compound of released NETs (Haritha *et al.*, 2019, Kajioka *et al.*, 2021, Martins-Cardoso *et al.*, 2020). Moreover, NETs without protein components did not activate macrophages (Lazzaretto and Fadeel, 2019). Thus, DNase application was found not to be sufficient to prevent NETs-induced endothelial and epithelial cell death (Saffarzadeh *et al.*, 2012). Only inhibition of PAD4 or NE prevented endothelial tissue damage (Kolaczkowska *et al.*, 2015). Furthermore, histones and NE were necessary to induce an inflammatory response from macrophages (Haritha *et al.*, 2019). This supports the present results where only heat treatment efficiently prevented NET toxicity to SCP-1 cells.

The activation of TLR4 by isolated NETs in the HEK reporter cell line represents strong evidence that histones are a major reactive component of NETs. In previous studies, histones could activate TLR2 and TLR4 in platelets (Semeraro *et al.*, 2011), and NETs could activate TLR4, but not TLR2 or TLR9 (Tsourouktsoglou *et al.*, 2020). In the latter study, histones were the major contributor to TLR4 activation whereas DNA just supported endolysosomal receptor translocation. Histone-induced activation of TLR4 led to IL-8 release in epithelial cells (Kawano *et al.*, 2014), which could further induce attraction and

activation of neutrophils (Bernhard *et al.*, 2021), thus enhancing inflammation. Additionally, histones are toxic to several kinds of cells like human umbilical vein endothelial cells (HUVECs) (Mizuta *et al.*, 2020), HeLa cells (Knopf *et al.*, 2019), and retinal epithelial cells (Kawano *et al.*, 2014). Histones as a toxic component would allow for the usage of anti-histone antibodies as a possible effective treatment to prevent NET cell toxicity (Deng *et al.*, 2020).

Clearance of NETs by macrophages is also thought to be essential to reduce NET toxicity (Nakazawa *et al.*, 2016). However, the toxicity of NETs to SCP-1 cells could not be achieved after THP-1 cell incubation, although NETs did activate THP-1 cells. Researchers have reported general activation of THP-1 cells by NETs into a pro-inflammatory phenotype (Hu *et al.*, 2019). This action is dependent on the stimulus: activation and clearance of NETs by macrophages could either beneficial for healing (Munir *et al.*, 2020) or contribute to further progression of inflammation (An *et al.*, 2019). However, after longer exposure, NETs could induce apoptosis in macrophages and dendritic cells (DCs) (Donis-Maturano *et al.*, 2015), thus reducing the potential for clearance. Diabetes changes the environmental conditions (cytokines, glucose, insulin) and the composition of NETs (Soongsathitanon *et al.*, 2019). The combination of the fracture gap conditions (low pH, low oxygen) with the diabetic conditions could hamper the clearance potential of macrophages and increase tissue damage. This may contribute to a negative effect of NETs in diabetics, especially in fracture healing.

4.5 Effect of NETs on the functionality of SCP-1 cells

For proper fracture healing, not only survival and proliferation of MSCs but also migration and differentiation are essential. Factors in the fracture gap are responsible for attracting MSCs (Ishikawa *et al.*, 2014), which later need to differentiate into chondrocytes or osteoblasts to form the bone matrix. While neutrophils had been shown to inhibit matrix formation of MSCs (Bastian *et al.*, 2018a), the effect of NETs on MSCs had not yet been evaluated until this study.

Migration of SCP-1 cells in the presence of NETs was already inhibited at low concentrations, without toxicity to the cells. Normally, MSC migration is induced

by a variety of factors (mostly cytokines and growth factors) (Fu *et al.*, 2019). In general, factors released from neutrophils can induce migration of MSCs (Zhang *et al.*, 2020) —for example, into the fracture hematoma (Hoff *et al.*, 2016) —but the present study revealed that NETs are not favorable for MSC migration. The negative effect on migration occurred at lower NET concentrations than the negative effect on cell number, suggesting that the reduced migration is not only an effect of reduced viability. In diabetic conditions, there is less MSC migration and markedly reduced induction of migration by secreted factors of PBMCs (Linnemann *et al.*, 2021). A similar phenomenon could account for NETs: NET formation is increased in diabetic conditions, and the released NETs further reduce MSC migration.

For the subsequent differentiation of MSCs, the inflammatory environment of the fracture gap is essential (Herrmann *et al.*, 2019). NET formation could have a strong influence here, as shown by the activation of THP-1 cells. Neutrophils and monocytes are strong regulators of the inflammatory status in the fracture gap, and macrophages massively modify the MSC migration and differentiation (Champagne *et al.*, 2002, Chen *et al.*, 2012, Ekstrom *et al.*, 2013, Nicolaidou *et al.*, 2012). Thus, altered activation of macrophages by NETs could contribute to the altered behavior of MSCs. However, it is not clear whether this would be negative or beneficial for healing. A wound healing study in mice showed that NETs properly cleared by macrophages in combination with applied MSCs improve healing (Munir *et al.*, 2020). However, depending on the activation status of macrophages, they could also inhibit migration and osteogenic differentiation of MSCs (Chen *et al.*, 2012, Zhang *et al.*, 2017). NET-induced polarization of macrophages could thus have a strong influence on the differentiation of MSCs.

Nevertheless, MSCs could also be directly affected in their differentiation by released NETs. In this study, NETs activated TLR4. TLR4-mediated MSC activation leads to profound cytokine release (He *et al.*, 2016). While low-level TLR4 activation is beneficial for osteogenic differentiation of MSCs (Muthukuru and Darveau, 2014), strong activation of TLR signaling leads to reduced osteogenic differentiation (Zhu *et al.*, 2019). First, the direct effect of NETs on osteogenic differentiation of MSCs was investigated here. Of note, researchers

had shown that neutrophils inhibit osteogenic differentiation of MSCs, but they had not investigated NETs (Bastian *et al.*, 2018a).

In this study, only the effect of NETs on MSCs was investigated, although MSCs can also affect NET formation. The immunosuppressive effects of MSCs are well accepted. Studies on NET formation in the presence of MSCs have shown a reduction in NET formation that prevented tissue damage (Jiang *et al.*, 2016), and reduced MSC-mediated neutrophil activation can also dampen LPS-induced sepsis (Ahn *et al.*, 2020). However, MSCs can also have the reverse effect on neutrophils. In the tumor microenvironment, MSCs release IL-8, thus inducing the attraction of neutrophils (Grégoire *et al.*, 2015). Furthermore, MSCs prevent neutrophils from undergoing apoptosis (Grégoire *et al.*, 2015). The effect of MSCs is dependent on their activation status and microenvironment. TLR4-activated MSCs have a more beneficial effect on bacterial clearance and neutrophil-mediated resolution of inflammation than non-activated MSCs (Brandau et al., 2014). A similar effect has been observed in a mouse wound healing model where only TLR4-activated MSCs showed a strong positive effect on healing (Munir *et al.*, 2020). In the present study, isolated NETs activated TLR4. These bidirectional interactions were not considered here and must be seen as a limitation.

4.6 The influence of *PADI4* and its SNPs on NET formation

NET formation seems to be highly relevant for the functionality of MSCs, and several diseases are associated with overshooting NET formation (Mitsios *et al.*, 2016). Hence, regulation of NET formation has a very high therapeutic potential. A key regulator of NET formation is PAD4 (Thiam *et al.*, 2020). *PADI4* SNPs are predictive for the risk of development of RA (Harris et al., 2008). In the current study, a minor haplotype of *PADI4* (positions 163, 245, 335) was associated with higher PAD4 protein levels and increased NET formation after stimulation in healthy volunteers. The increased NET formation could be correlated directly to increased PAD4 levels. These results fit previous data, where the minor haplotype stabilized PAD4 protein and directly affected its activity (Horikoshi *et al.*, 2011).

Researchers have shown that PAD4 overexpression can induce the release of NET-like structures even in osteogenic cells (Leshner *et al.*, 2012), which normally do not form NETs, underlining the strong effect of PAD4 on NET formation. PAD4 overexpression led to a strong increase in cit-H3 levels, providing evidence for a strong increase in PAD4 activity. PAD4 activity is highly dependent on calcium (Leshner *et al.*, 2012), a fact that could be very relevant in the setting of fracture hematoma, where calcium levels can be up to 10 times higher than normal (Walters *et al.*, 2018). While high calcium levels are relevant for matrix formation in bone healing, they could also activate PAD4. Neutrophils exposed to high calcium levels have been shown to release ROS via PAD4 activation (Zhou *et al.*, 2018), possibly further promoting NET formation.

The effects of *PADI4* SNPs and their associated effects on protein levels means there is likely clinical relevance. In combination with other prerequisites for increased NET formation like diabetes, RA, or another chronic inflammatory disease, the variant could strongly influence healing abilities in the case of trauma. There are several instances for which PAD4 inhibition is beneficial for healing (Kaur *et al.*, 2020, Wong *et al.*, 2015). PAD4 is also a key player for the development of sepsis in several mouse models (Liang *et al.*, 2018, Zhao *et al.*, 2020). However, PAD4 inhibition could be detrimental when the immune defense against pathogens is critical, like gastrointestinal infection with *Citrobacter rodentium* (Saha *et al.*, 2019) or in the defense against necrotizing fasciitis (Li *et al.*, 2010). PAD4 does not seem to be the main player in all cases. For example, in a skeletal muscle ischemia-reperfusion model, TLR7/8/9 inhibition was more effective than PAD4 inhibition in preventing tissue damage by NETs (Edwards *et al.*, 2020).

PAD4 itself can be a self-antigen, contributing to immunity in chronic inflammatory diseases. In RA, anti-PAD4 antibodies have been associated with increased disease activity (Harris *et al.*, 2008). The authors identified three *PADI4* SNPs in the antibody-binding region that possibly alter the immunogenicity of PAD4 (Harris *et al.*, 2008). Furthermore, PAD4 can induce auto-immunity through the citrullination of other proteins (Damgaard *et al.*, 2014, Suzuki *et al.*, 2003). Increased PAD4 levels by the minor variant and/or T2DM could thus influence

inflammation on three levels: NET formation, modification of other proteins, and autoimmunity of PAD4 itself.

In the pathogenesis of T2DM, the role of PAD4 is still not clear. For type 1 diabetes, PAD4 seems to play role in the development of autoimmunity against the beta-cells of the pancreas (Sodré *et al.*, 2021). If this is also true for later stages of type 2 diabetes is not clear. In fact, T2DM patients have elevated NET markers in the blood (Miyoshi *et al.*, 2016) and increased PAD4 levels as shown in this study. Increased PAD4 levels due to the minor variant could further contribute to the progression of T2DM.

4.7 Clinical relevance of NET formation and PAD4

Neutrophils from patients with chronic wounds released fewer NETs than neutrophils from patients with acute wounds. In contrast, neutrophils from patients with sub-chronic wounds released more NETs than those from patients with acute wounds without additional stimulation. After stimulation, the neutrophils from patients with chronic wounds released fewer NETs than the neutrophils from patients with acute or sub-chronic wounds. These data are contrary to studies from mice where higher local NET release was associated with delayed wound healing (Fadini *et al.*, 2016, Heuer *et al.*, 2021). These results suggest that lower NET release from circulating neutrophils may be associated with higher release at local sites. However, NET formation directly at wound sites was not investigated in the present study.

The reduced NET formation of peripheral neutrophils from patients with chronic wounds after additional stimulation could actually be a sign of neutrophil exhaustion, leading to a reduced defense against pathogens and delayed healing. Such an effect could be observed in a sepsis mouse model, where destruction of NETs by DNase worsened sepsis and was only effective in preventing tissue damage when combined with antibiotic therapy (Czaikoski *et al.*, 2016). Dysregulation of NET release may lead to delayed healing by impairing clearance of invading pathogens and/or tissue damage by excessive NETs.

Another factor that could influence the ability of neutrophils to form NETs could be the micronutrient status of patients. Malnutrition and vitamin D deficiency are

also highly relevant aspects in trauma patients (Ihle *et al.*, 2017, Wintermeyer *et al.*, 2016). Vitamin D3 and omega poly-unsaturated fatty acid supplementation inhibited PMA-induced NET formation in neutrophils from diabetic patients with purulent necrotizing injuries on the lower limbs (Basyreva *et al.*, 2021). Further, aged individuals showed impaired NET formation and subsequent bacterial clearance (Hazeldine *et al.*, 2014). This could be a relevant for aged individuals, another high-risk group for the development of complications after trauma (Beshay *et al.*, 2020).

In the context of bone, PAD4 inhibition or DNase treatment prevented aseptic implant loosening in a mouse model, and NETs have been found in human fibrotic samples of aseptic loosened implants (Kuyl *et al.*, 2021). Thus, increased PAD4 levels as found in diabetic patients could increase the risk for implant loosening after hip or knee arthroplasty.

To prevent the negative effects of NETs on tissue, the Food and Drug Administration–approved drug chloroquine has shown promising effects in skeletal muscle, even more than PAD4 inhibition (Edwards *et al.*, 2020). Chloroquine has also shown promise in reducing the severity of pancreatitis (Murthy *et al.*, 2019).

4.8 Conclusion and outlook

DM patients show higher NET formation and higher PAD4 levels, both of which are associated with delayed healing, tissue damage, and complications. *In vitro*, HG could not induce NET formation, but insulin inhibited it, revealing a strong regulatory ability. NETs showed a detrimental effect on MSCs and activated monocytes. Both cell types strongly influence fracture healing. A combination of the *PADI4* minor variant and a secondary disease like diabetes could enhance NET release and contribute to complications or delayed healing. Thus, determining the *PADI4* variant or the PAD4 levels may be a predictive factor for the development of complications. A correlation of the PAD4 minor variant with clinical data would be helpful to validate the *in vitro* data presented in this study. A direct investigation of fracture hematoma from T2DM patients could follow to

directly prove locally increased NET formation. Alternatively, fracture hematoma from a diabetic mouse model (like *db/db*) could be investigated.

A local intervention at the fracture site with DNase, PAD4 or NE inhibitors, or chloroquine could promote healing. However, interventions must be carefully applied because the fight against infections can be severely hampered when NET formation is inhibited. For all the possible interventions, especially in fracture healing, greater understanding of the role of NETs is still needed to reestablish the balance between the infection-fighting potential of NET formation and the possible detrimental effects on tissue integrity.

5. Abstract

Diabetes is a global disease with a strongly increasing prevalence and incidence. In Germany, about 9 million people are living with diabetes, most of them with type 2. Type 2 diabetes impairs vascularization, nerve signal transfer, and kidney function. Additionally, type 2 diabetic patients have impaired healing abilities: Wounds and fractures need more time to heal, and complications occur more often. After a fracture, the immune system is rapidly activated in the fracture gap. The induced inflammatory process is essential for fracture healing, starting with the arrival of neutrophils. Neutrophils have strong phagocytic abilities and can release large amounts of cytokines, thus inducing strong inflammation. They can also release their DNA as a defense mechanism, which then organizes in large net-like structures covered with antimicrobial proteins and proteases—so-called neutrophil extracellular traps (NETs). One of the main proteins involved in NET formation is peptidyl arginine deiminase type IV (PAD4), which is responsible for the induction of chromatin decondensation. NETs have been shown to impair wound healing in diabetic mice and are released after trauma. The negative effect on wound healing could be improved by PAD4 knockout or DNase treatment. In this study, the possible role of NETs in diabetic fracture healing was investigated.

To investigate NET release in diabetic conditions, neutrophils were isolated from patients or healthy volunteers, and NET release was measured by using the Sytox Green Assay. Neutrophils from healthy volunteer were stimulated with controlled diabetic conditions *in vitro* (high glucose, high insulin). Reaction to different stimulants (phorbol 12-myristate 13-acetate [PMA], calcium ionophore A23187 [CI], lipopolysaccharide [LPS], H_2O_2) was investigated in diabetic conditions. Variants of *PADI4* and their effect on NET release were analyzed. Intracellular processes were analyzed by western blot, and reactive oxygen species (ROS) and myeloperoxidase (MPO) activity were measured. Isolated NETs from stimulated neutrophils were added to a mesenchymal stem cell (MSC) line (SCP-1 cells), and viability (mitochondrial activity, total protein, lactate dehydrogenase release) and functional parameters (migration, osteogenic

differentiation) were analyzed. The reaction of monocytes to isolated NETs was analyzed by measuring activation and viability.

Neutrophils from diabetic patients released more NETs at baseline and after stimulation with PMA or H_2O_2 but not CI. They had increased PAD4 levels, but the MPO and citrullinated histone H3 levels were not altered. Neutrophils from healthy volunteers did not show NET release in response to high glucose or high glucose with insulin. Combination of diabetic conditions with CI did not alter NET release, but high insulin delayed NET release in response to PMA or LPS by 2-3 h (+3.26 h with PMA, +2.09 h with LPS). Insulin induced high levels of ROS with and without PMA whereas high glucose did not induce ROS. Further, insulin with PMA significantly induced two mitogen-activated proteins kinases, with increased phosphor-extracellular signal-regulated kinase and phospo-p38, but slightly reduced MPO activity. In a *PADI4* minor variant haplotype, NET formation was significantly accelerated, and PAD4 levels increased. Isolated NETs were very toxic to SCP-1 cells, and migration was already reduced at non-toxic concentrations of NETs. Single-dose exposure of NETs at the beginning of osteogenic differentiation significantly reduced alkaline phosphatase activity and matrix formation. Recovery from NET exposure regarding viability could be achieved between days 10 and 14 of differentiation. NETs activated Toll-like receptor 4. Monocytes were activated at lower NET doses, and their viability was decreased with higher NET concentrations.

In conclusion, NET formation in diabetic patients was increased, but not because of high glucose. Insulin had a strong regulatory function on NET formation, possibly deregulating NET formation. A minor *PADI4* haplotype could increase the deregulation in type 2 diabetic patients. The increased NET formation could then have a strong negative effect on MSCs and contribute to delayed fracture healing in type 2 diabetic patients.

6. Zusammenfassung

Diabetes ist eine Stoffwechselerkrankung mit stark steigender Prävalenz in Deutschland. Typ 2 Diabetes geht mit erhöhtem Blutzucker und Insulinresistenz einher was verschiedene Nebenerkrankungen zur Folge hat. Neben Nieren- und Nervenschäden führt Typ 2 Diabetes zu einem erhöhten Risiko für kardiovaskuläre Erkrankungen und Problemen bei der Wund- und Frakturheilung. Knochen brauchen länger, um zu heilen und es kommt öfter zu Komplikationen. Zusätzlich ist das Frakturrisiko erhöht. Nach einer Fraktur wandern Immunzellen in den Frakturspalt ein und erzeugen eine Entzündung. Dieser Entzündungsprozess ist essenziell für die Frakturheilung. Neutrophile sind die ersten Zellen, die in den Frakturspalt einwandern. Sie tragen durch die Freisetzung von Zytokinen zur Entzündung bei und phagozytieren Zellschrott. Zusätzlich können Neutrophile ihre DNA als weiteren Abwehrmechanismus freisetzen. Diese freigesetzte DNA bildet große Strukturen, so genannte *neutrophil extracellular traps* (NETs), die mit Proteinen und Histonen besetzt ist. Eines der wichtigsten Proteine für die Bildung von NETs ist PAD4, welches durch die Citrullinierung von Histonen zur Dekondensation von Chromatin führt und dessen Freisetzung ermöglicht. Erhöhte NETs Freisetzung wurde mit verschlechterter Wundheilung in Mäusen assoziiert. Dies konnte durch einen Knockout von PAD4 oder die Zugabe von DNase verhindert werden. Daher soll in dieser Studie die Rolle von NETs in der Frakturheilung von Diabetikern untersucht werden.

Zur Untersuchung der Freisetzung von NETs in diabetischen Bedingungen wurden Neutrophile von Diabetikern isoliert oder Neutrophile von gesunden Freiwilligen kontrollierten diabetischen Bedingungen *in vitro* ausgesetzt (viel Glukose, viel Insulin). Die Freisetzung von NETs wurde mittels Sytox Green Assay und Immunfluoreszenzfärbung nach Stimulation (PMA, Calcium Ionophor (CI), LPS, H_2O_2) bestimmt. PAD4 Varianten wurden bestimmt und deren Effekt auf die NETs Freisetzung in Neutrophilen analysiert. Intrazelluläre Prozesse wurden mittels Western Blot untersucht. Reaktive Sauerstoff Spezies (ROS) und die Myeloperoxidase Aktivität wurden bestimmt. Für die Analyse des Effekts von

NETs auf Zellen der Frakturheilung, wurden NETs von stimulierten Neutrophilen mittels Zentrifugation isoliert. NETs wurden zu einer mesenchymalen Stammzelllinie (SCP-1 Zellen) gegeben und die Viabilität (mitochondriale Aktivität, totaler Proteingehalt, LDH Freisetzung) und funktionale Parameter (Migration, osteogene Differenzierung) gemessen. Bei Monozyten (THP-1 Zellen) wurde der Einfluss von isolierten NETs auf die Aktivierung und die Viabilität bestimmt.

Neutrophile von Typ 2 Diabetikern bildeten signifikant mehr NETs nach Stimulation mit PMA oder H_2O_2 aber nicht CI. Sie zeigten erhöhte PAD4 Level, aber cit-H3 oder MPO waren nach Stimulation nicht verändert. Viel Glukose und/oder viel Insulin induzierten keine NETs Freisetzung in Neutrophilen von gesunden Freiwilligen. In Kombination mit einem zweiten Stimulus zeigte sich keine Veränderung mit CI, aber mit PMA und LPS verzögerte viel Insulin die NETs Freisetzung signifikant um 2-3 h (3,26 h mit PMA, 2,09 h mit LPS). Insulin induzierte hohe ROS Level mit und ohne zusätzliches PMA wogegen viel Glukose kein ROS induzierte. Zusätzlich induzierte Insulin mit PMA die MAPKinasen p-ERK und p-p38, gleichzeitig war die MPO Aktivität leicht reduziert. Neutrophile mit einer Minorvariante von PAD4 zeigten erhöhte NET Freisetzung und erhöhte PAD4 Level. Isolierte NETs wirkten toxisch auf SCP-1 Zellen und reduzierten die Migration signifikant schon in nicht-toxischen Konzentrationen. Nach einer einmaligen NETs Exposition zeigten SCP-1 Zellen eine deutlich reduzierte AP Aktivität und verringerte Mineralisierung. Die Wiederherstellung der Viabilität im Vergleich zur Kontrolle konnte erst an Tag 10-14 erreicht werden. Monozyten zeigten eine Aktivierung mit niedrigen NETs Konzentrationen und eine verringerte Viabilität mit höheren Konzentrationen. Es konnte gezeigt werden, dass NETs TLR4 aktivieren.

Zusammenfassend konnte eine erhöhte NETs Freisetzung bei Typ 2 Diabetikern gezeigt werden, die aber nicht durch viel Glukose verursacht wurde. Insulin hatte eine stark regulierende Funktion auf die NETs Freisetzung. In Kombination mit einer PAD4 Minorvariante könnte eine starke Dysregulation zu verstärkter NETs Freisetzung führen. Der stark negative Effekt auf mesenchymale Stammzellen könnte dann zu einer verzögerten Frakturheilung in Typ 2 Diabetikern beitragen.

7. References

Abaricia, J. O., Shah, A. H., Musselman, R. M. & Olivares-Navarrete, R. 2020. Hydrophilic titanium surfaces reduce neutrophil inflammatory response and NETosis. *Biomaterials Science,* 8**,** 2289-2299.

Ackerman, J. E., Geary, M. B., Orner, C. A., Bawany, F. & Loiselle, A. E. 2017. Obesity/Type II diabetes alters macrophage polarization resulting in a fibrotic tendon healing response. *PLoS One,* 12**,** e0181127.

Agarwal, S., Loder, S. J., Cholok, D., Li, J., Bian, G., Yalavarthi, S., Li, S., Carson, W. F., Hwang, C., Marini, S., Pagani, C., Edwards, N., Delano, M. J., Standiford, T. J., Knight, J. S., Kunkel, S. L., Mishina, Y., Ward, P. A. & Levi, B. 2019. Disruption of Neutrophil Extracellular Traps (NETs) Links Mechanical Strain to Post-traumatic Inflammation. *Frontiers in Immunology,* 10.

Ahn, S. Y., Maeng, Y. S., Kim, Y. R., Choe, Y. H., Hwang, H. S. & Hyun, Y. M. 2020. In vivo monitoring of dynamic interaction between neutrophil and human umbilical cord blood-derived mesenchymal stem cell in mouse liver during sepsis. *Stem Cell Research & Therapy,* 11**,** 44.

Al-Khafaji, A. B., Tohme, S., Yazdani, H. O., Miller, D., Huang, H. & Tsung, A. 2016. Superoxide induces Neutrophil Extracellular Trap Formation in a TLR-4 and NOX-dependent mechanism. *Molecular Medicine,* 22**,** 621-631.

Alexandraki, K. I., Piperi, C., Ziakas, P. D., Apostolopoulos, N. V., Makrilakis, K., Syriou, V., Diamanti-Kandarakis, E., Kaltsas, G. & Kalofoutis, A. 2008. Cytokine secretion in long-standing diabetes mellitus type 1 and 2: associations with low-grade systemic inflammation. *Journal of Clinical Immunology,* 28**,** 314-21.

Aljada, A., Ghanim, H., Mohanty, P., Kapur, N. & Dandona, P. 2002. Insulin Inhibits the Pro-Inflammatory Transcription Factor Early Growth Response Gene-1 (Egr)-1 Expression in Mononuclear Cells (MNC) and Reduces Plasma Tissue Factor (TF) and Plasminogen Activator Inhibitor-1 (PAI-1) Concentrations. *The Journal of Clinical Endocrinology & Metabolism,* 87**,** 1419-1422.

Altrichter, J., Zedler, S., Kraft, R., Faist, E., Mitzner, S. R., Sauer, M., Windolf, J., Scholz, M. & Lögters, T. 2010. Neutrophil-derived circulating free DNA (cf-DNA/NETs), a potential prognostic marker for mortality in patients with severe burn injury. *European Journal of Trauma and Emergency Surgery,* 36**,** 551-7.

Amulic, B., Cazalet, C., Hayes, G. L., Metzler, K. D. & Zychlinsky, A. 2012. Neutrophil function: from mechanisms to disease. *Annual Review of Immunology,* 30**,** 459-89.

Amulic, B., Knackstedt, S. L., Abu Abed, U., Deigendesch, N., Harbort, C. J., Caffrey, B. E., Brinkmann, V., Heppner, F. L., Hinds, P. W. & Zychlinsky, A. 2017. Cell-Cycle Proteins Control Production of Neutrophil Extracellular Traps. *Developmental Cell,* 43**,** 449-462.e5.

An, Z., Li, J., Yu, J., Wang, X., Gao, H., Zhang, W., Wei, Z., Zhang, J., Zhang, Y., Zhao, J. & Liang, X. 2019. Neutrophil extracellular traps induced by IL-8

aggravate atherosclerosis via activation NF-κB signaling in macrophages. *Cell cycle (Georgetown, Tex.),* 18**,** 2928-2938.

Arampatzioglou, A., Papazoglou, D., Konstantinidis, T., Chrysanthopoulou, A., Mitsios, A., Angelidou, I., Maroulakou, I., Ritis, K. & Skendros, P. 2018. Clarithromycin Enhances the Antibacterial Activity and Wound Healing Capacity in Type 2 Diabetes Mellitus by Increasing LL-37 Load on Neutrophil Extracellular Traps. *Frontiers in Immunology,* 9**,** 2064.

Arita, K., Hashimoto, H., Shimizu, T., Nakashima, K., Yamada, M. & Sato, M. 2004. Structural basis for Ca(2+)-induced activation of human PAD4. *Nature Structural and Molecular Biology,* 11**,** 777-83.

Armstrong, D. G., Swerdlow, M. A., Armstrong, A. A., Conte, M. S., Padula, W. V. & Bus, S. A. 2020. Five year mortality and direct costs of care for people with diabetic foot complications are comparable to cancer. *Journal of Foot and Ankle Research,* 13**,** 16.

Aspera-Werz, R. H., Chen, T., Ehnert, S., Zhu, S., Fröhlich, T. & Nussler, A. K. 2019. Cigarette Smoke Induces the Risk of Metabolic Bone Diseases: Transforming Growth Factor Beta Signaling Impairment via Dysfunctional Primary Cilia Affects Migration, Proliferation, and Differentiation of Human Mesenchymal Stem Cells. *International Journal of Molecular Sciences,* 20**,** 2915.

Baltzis, D., Eleftheriadou, I. & Veves, A. 2014. Pathogenesis and Treatment of Impaired Wound Healing in Diabetes Mellitus: New Insights. *Advances in Therapy,* 31**,** 817-836.

Bang, S.-Y., Han, T.-U., Choi, C.-B., Sung, Y.-K., Bae, S.-C. & Kang, C. 2010. Peptidyl arginine deiminase type IV (PADI4) haplotypes interact with shared epitope regardless of anti-cyclic citrullinated peptide antibody or erosive joint status in rheumatoid arthritis: a case control study. *Arthritis Research & Therapy,* 12**,** R115.

Bartlett, D. B., Slentz, C. A., Willis, L. H., Hoselton, A., Huebner, J. L., Kraus, V. B., Moss, J., Muehlbauer, M. J., Spielmann, G., Muoio, D. M., Koves, T. R., Wu, H., Huffman, K. M., Lord, J. M. & Kraus, W. E. 2020. Rejuvenation of Neutrophil Functions in Association With Reduced Diabetes Risk Following Ten Weeks of Low-Volume High Intensity Interval Walking in Older Adults With Prediabetes - A Pilot Study. *Frontiers in Immunology,* 11**,** 729.

Bastian, O. W., Croes, M., Alblas, J., Koenderman, L., Leenen, L. P. H. & Blokhuis, T. J. 2018a. Neutrophils Inhibit Synthesis of Mineralized Extracellular Matrix by Human Bone Marrow-Derived Stromal Cells In Vitro. *Frontiers in Immunology,* 9**,** 945.

Bastian, O. W., Koenderman, L., Alblas, J., Leenen, L. P. & Blokhuis, T. J. 2016. Neutrophils contribute to fracture healing by synthesizing fibronectin+ extracellular matrix rapidly after injury. *Clinical Immunology,* 164**,** 78-84.

Bastian, O. W., Mrozek, M. H., Raaben, M., Leenen, L. P. H., Koenderman, L. & Blokhuis, T. J. 2018b. Serum from the Human Fracture Hematoma Contains a Potent Inducer of Neutrophil Chemotaxis. *Inflammation,* 41**,** 1084-1092.

Basyreva, L. Y., Vakhrusheva, T. V., Letkeman, Z. V., Maximov, D. I., Fedorova, E. A., Panasenko, O. M., Ostrovsky, E. M. & Gusev, S. A. 2021. Effect of

Vitamin D3 in combination with Omega-3 Polyunsaturated Fatty Acids on NETosis in Type 2 Diabetes Mellitus Patients. *Oxidative Medicine and Cellular Longevity,* 2021**,** 8089696.

Behnen, M., Leschczyk, C., Moller, S., Batel, T., Klinger, M., Solbach, W. & Laskay, T. 2014. Immobilized immune complexes induce neutrophil extracellular trap release by human neutrophil granulocytes via FcgammaRIIIB and Mac-1. *Journal of Immunology* 193**,** 1954-65.

Bernhard, S., Hug, S., Stratmann, A. E. P., Erber, M., Vidoni, L., Knapp, C. L., Thomaß, B. D., Fauler, M., Nilsson, B., Nilsson Ekdahl, K., Föhr, K., Braun, C. K., Wohlgemuth, L., Huber-Lang, M. & Messerer, D. a. C. 2021. Interleukin 8 Elicits Rapid Physiological Changes in Neutrophils That Are Altered by Inflammatory Conditions. *Journal of Innate Immunity,* 13**,** 225-241.

Beshay, M., Mertzlufft, F., Kottkamp, H. W., Reymond, M., Schmid, R. A., Branscheid, D. & Vordemvenne, T. 2020. Analysis of risk factors in thoracic trauma patients with a comparison of a modern trauma centre: a mono-centre study. *World Journal of Emergency Surgery,* 15**,** 45.

Bocker, W., Yin, Z., Drosse, I., Haasters, F., Rossmann, O., Wierer, M., Popov, C., Locher, M., Mutschler, W., Docheva, D. & Schieker, M. 2008. Introducing a single-cell-derived human mesenchymal stem cell line expressing hTERT after lentiviral gene transfer. *Journal of Cellular and Molecular Medicine,* 12**,** 1347-59.

Bosetti, M., Boccafoschi, F., Leigheb, M. & Cannas, M. F. 2007. Effect of different growth factors on human osteoblasts activities: a possible application in bone regeneration for tissue engineering. *Biomolecular Engineering,* 24**,** 613-8.

Braian, C., Hogea, V. & Stendahl, O. 2013. Mycobacterium tuberculosis- induced neutrophil extracellular traps activate human macrophages. *Journal of Innate Immunity,* 5**,** 591-602.

Briant, K., Koay, Y.-H., Otsuka, Y. & Swanton, E. 2015. ERAD of proteins containing aberrant transmembrane domains requires ubiquitylation of cytoplasmic lysine residues. *Journal of Cell Science,* 128**,** 4112-4125.

Brighton, C. T. 1984. The biology of fracture repair. *Instructional Course Lectures,* 33**,** 60-82.

Brinkmann, V., Reichard, U., Goosmann, C., Fauler, B., Uhlemann, Y., Weiss, D. S., Weinrauch, Y. & Zychlinsky, A. 2004. Neutrophil extracellular traps kill bacteria. *Science,* 303**,** 1532-5.

Brinkmann, V. & Zychlinsky, A. 2007. Beneficial suicide: why neutrophils die to make NETs. *Nature Reviews Microbiology,* 5**,** 577-582.

Bruschi, M., Petretto, A., Santucci, L., Vaglio, A., Pratesi, F., Migliorini, P., Bertelli, R., Lavarello, C., Bartolucci, M., Candiano, G., Prunotto, M. & Ghiggeri, G. M. 2019. Neutrophil Extracellular Traps protein composition is specific for patients with Lupus nephritis and includes methyl-oxidized alphaenolase (methionine sulfoxide 93). *Scientific Reports,* 9**,** 7934.

Bryk, A. H., Prior, S. M., Plens, K., Konieczynska, M., Hohendorff, J., Malecki, M. T., Butenas, S. & Undas, A. 2019. Predictors of neutrophil extracellular traps markers in type 2 diabetes mellitus: associations with a

prothrombotic state and hypofibrinolysis. *Cardiovascular Diabetology,* 18**,** 49.

Calori, G. M., Albisetti, W., Agus, A., Iori, S. & Tagliabue, L. 2007. Risk factors contributing to fracture non-unions. *Injury,* 38 Suppl 2**,** S11-8.

Carestia, A., Frechtel, G., Cerrone, G., Linari, M. A., Gonzalez, C. D., Casais, P. & Schattner, M. 2016. NETosis before and after Hyperglycemic Control in Type 2 Diabetes Mellitus Patients. *PLoS One,* 11**,** e0168647.

Carmona-Rivera, C., Carlucci, P. M., Goel, R. R., James, E., Brooks, S. R., Rims, C., Hoffmann, V., Fox, D. A., Buckner, J. H. & Kaplan, M. J. 2020. Neutrophil extracellular traps mediate articular cartilage damage and enhance cartilage component immunogenicity in rheumatoid arthritis. *JCI Insight,* 5**,** e139388.

Carnevale, V., Romagnoli, E., D'erasmo, L. & D'erasmo, E. 2014. Bone damage in type 2 diabetes mellitus. *Nutrition, Metabolism & Cardiovascular Diseases,* 24**,** 1151-1157.

Castillo, R. C., Bosse, M. J., Mackenzie, E. J., Patterson, B. M. & Group, L. S. 2005. Impact of smoking on fracture healing and risk of complications in limb-threatening open tibia fractures. *Journal of Orthopaedic Trauma,* 19**,** 151-157.

Champagne, C. M., Takebe, J., Offenbacher, S. & Cooper, L. F. 2002. Macrophage cell lines produce osteoinductive signals that include bone morphogenetic protein-2. *Bone,* 30**,** 26-31.

Chan, J. K., Glass, G. E., Ersek, A., Freidin, A., Williams, G. A., Gowers, K., Espirito Santo, A. I., Jeffery, R., Otto, W. R., Poulsom, R., Feldmann, M., Rankin, S. M., Horwood, N. J. & Nanchahal, J. 2015. Low-dose TNF augments fracture healing in normal and osteoporotic bone by up-regulating the innate immune response. *EMBO Molecular Medicine,* 7**,** 547-561.

Chen, C., Chen, Q., Nie, B., Zhang, H., Zhai, H., Zhao, L., Xia, P., Lu, Y. & Wang, N. 2020. Trends in Bone Mineral Density, Osteoporosis, and Osteopenia Among U.S. Adults With Prediabetes, 2005-2014. *Diabetes Care,* 43**,** 1008-1015.

Chen, C., Uludağ, H., Wang, Z., Rezansoff, A. & Jiang, H. 2012. Macrophages Inhibit Migration, Metabolic Activity and Osteogenic Differentiation of Human Mesenchymal Stem Cells in vitro. *Cells Tissues Organs,* 195**,** 473-483.

Chen, G. Y. & Nuñez, G. 2010. Sterile inflammation: sensing and reacting to damage. *Nature Reviews Immunology,* 10**,** 826-837.

Chrysanthopoulou, A., Mitroulis, I., Apostolidou, E., Arelaki, S., Mikroulis, D., Konstantinidis, T., Sivridis, E., Koffa, M., Giatromanolaki, A., Boumpas, D. T., Ritis, K. & Kambas, K. 2014. Neutrophil extracellular traps promote differentiation and function of fibroblasts. *Journal of Pathology,* 233**,** 294-307.

Cichon, I., Ortmann, W. & Kolaczkowska, E. 2021. Metabolic Pathways Involved in Formation of Spontaneous and Lipopolysaccharide-Induced Neutrophil Extracellular Traps (NETs) Differ in Obesity and Systemic Inflammation. *International Journal of Molecular Sciences,* 22**,** 7718.

Consortium, G. P., Auton, A., Brooks, L. D., Durbin, R. M., Garrison, E. P., Kang, H. M., Korbel, J. O., Marchini, J. L., Mccarthy, S., Mcvean, G. A. & Abecasis, G. R. 2015. A global reference for human genetic variation. *Nature,* 526**,** 68-74.

Costa, N. A., Gut, A. L., Azevedo, P. S., Polegato, B. F., Magalhaes, E. S., Ishikawa, L. L. W., Bruder, R. C. S., Silva, E. a. D., Goncalves, R. B., Tanni, S. E., Rogero, M. M., Norde, M. M., Cunha, N. B., Zornoff, L. a. M., De Paiva, S. a. R. & Minicucci, M. F. 2018. Peptidylarginine deiminase 4 concentration, but not PADI4 polymorphisms, is associated with ICU mortality in septic shock patients. *Journal of Cell and Molecular Medicine,* 22**,** 4732-4737.

Crane, J. L. & Cao, X. 2014. Bone marrow mesenchymal stem cells and TGF-β signaling in bone remodeling. *The Journal of Clinical Investigation,* 124**,** 466-472.

Czaikoski, P. G., Mota, J. M. S. C., Nascimento, D. C., Sônego, F., Castanheira, F. V. E. S., Melo, P. H., Scortegagna, G. T., Silva, R. L., Barroso-Sousa, R., Souto, F. O., Pazin-Filho, A., Figueiredo, F., Alves-Filho, J. C. & Cunha, F. Q. 2016. Neutrophil Extracellular Traps Induce Organ Damage during Experimental and Clinical Sepsis. *PLoS One,* 11**,** e0148142.

Damgaard, D., Bjørn, M. E., Jensen, P. Ø. & Nielsen, C. H. 2017. Reactive oxygen species inhibit catalytic activity of peptidylarginine deiminase. *Journal of Enzyme Inhibition and Medicinal Chemistry,* 32**,** 1203-1208.

Damgaard, D., Senolt, L., Nielsen, M. F., Pruijn, G. J. & Nielsen, C. H. 2014. Demonstration of extracellular peptidylarginine deiminase (PAD) activity in synovial fluid of patients with rheumatoid arthritis using a novel assay for citrullination of fibrinogen. *Arthritis Research and Therapy,* 16**,** 498.

De Bont, C. M., Koopman, W. J. H., Boelens, W. C. & Pruijn, G. J. M. 2018. Stimulus-dependent chromatin dynamics, citrullination, calcium signalling and ROS production during NET formation. *Biochimica Biophysica Acta Molecular Cell Research,* 1865**,** 1621-1629.

De Buhr, N. & Von Kockritz-Blickwede, M. 2016. How Neutrophil Extracellular Traps Become Visible. *Journal of Immunology Research,* 2016**,** 4604713.

Debels, H., Galea, L., Han, X. L., Palmer, J., Van Rooijen, N., Morrison, W. & Abberton, K. 2013. Macrophages play a key role in angiogenesis and adipogenesis in a mouse tissue engineering model. *Tissue Engineering Part A,* 19**,** 2615-25.

Dede, A. D., Tournis, S., Dontas, I. & Trovas, G. 2014. Type 2 diabetes mellitus and fracture risk. *Metabolism,* 63**,** 1480-90.

Deng, Q., Pan, B., Alam, H. B., Liang, Y., Wu, Z., Liu, B., Mor-Vaknin, N., Duan, X., Williams, A. M., Tian, Y., Zhang, J. & Li, Y. 2020. Citrullinated Histone H3 as a Therapeutic Target for Endotoxic Shock in Mice. *Frontiers in Immunology,* 10.

Denning, N.-L., Aziz, M., Gurien, S. D. & Wang, P. 2019. DAMPs and NETs in Sepsis. *Frontiers in Immunology,* 10.

Donis-Maturano, L., Sánchez-Torres, L. E., Cerbulo-Vázquez, A., Chacón-Salinas, R., García-Romo, G. S., Orozco-Uribe, M. C., Yam-Puc, J. C., González-Jiménez, M. A., Paredes-Vivas, Y. L., Calderón-Amador, J., Estrada-Parra, S., Estrada-García, I. & Flores-Romo, L. 2015. Prolonged

exposure to neutrophil extracellular traps can induce mitochondrial damage in macrophages and dendritic cells. *Springerplus,* 4**,** 161.

Douda, D. N., Khan, M. A., Grasemann, H. & Palaniyar, N. 2015. SK3 channel and mitochondrial ROS mediate NADPH oxidase-independent NETosis induced by calcium influx. *proceedings of the national academy of sciences of the united states of america,* 112**,** 2817-22.

Dyer, M. R., Chen, Q., Haldeman, S., Yazdani, H., Hoffman, R., Loughran, P., Tsung, A., Zuckerbraun, B. S., Simmons, R. L. & Neal, M. D. 2018. Deep vein thrombosis in mice is regulated by platelet HMGB1 through release of neutrophil-extracellular traps and DNA. *Scientific Reports,* 8**,** 2068.

Edwards, N. J., Hwang, C., Marini, S., Pagani, C. A., Spreadborough, P. J., Rowe, C. J., Yu, P., Mei, A., Visser, N., Li, S., Hespe, G. E., Huber, A. K., Strong, A. L., Shelef, M. A., Knight, J. S., Davis, T. A. & Levi, B. 2020. The role of neutrophil extracellular traps and TLR signaling in skeletal muscle ischemia reperfusion injury. *FASEB Journal,* 34**,** 15753-15770.

Ehnert, S., Baur, J., Schmitt, A., Neumaier, M., Lucke, M., Dooley, S., Vester, H., Wildemann, B., Stockle, U. & Nussler, A. K. 2010. TGF-beta1 as possible link between loss of bone mineral density and chronic inflammation. *PLoS One,* 5**,** e14073.

Ehnert, S., Falldorf, K., Fentz, A. K., Ziegler, P., Schroter, S., Freude, T., Ochs, B. G., Stacke, C., Ronniger, M., Sachtleben, J. & Nussler, A. K. 2015a. Primary human osteoblasts with reduced alkaline phosphatase and matrix mineralization baseline capacity are responsive to extremely low frequency pulsed electromagnetic field exposure - Clinical implication possible. *Bone Reports,* 3**,** 48-56.

Ehnert, S., Fentz, A. K., Schreiner, A., Birk, J., Wilbrand, B., Ziegler, P., Reumann, M. K., Wang, H., Falldorf, K. & Nussler, A. K. 2017. Extremely low frequency pulsed electromagnetic fields cause antioxidative defense mechanisms in human osteoblasts via induction of *O2(-) and H2O2. *Scientific Reports,* 7**,** 14544.

Ehnert, S., Freude, T., Ihle, C., Mayer, L., Braun, B., Graeser, J., Flesch, I., Stockle, U., Nussler, A. K. & Pscherer, S. 2015b. Factors circulating in the blood of type 2 diabetes mellitus patients affect osteoblast maturation - description of a novel in vitro model. *Experimental Cell Research,* 332**,** 247-58.

Ehnert, S., Linnemann, C., Braun, B., Botsch, J., Leibiger, K., Hemmann, P. & Nussler, A. K. 2019. One-Step ARMS-PCR for the Detection of SNPs-Using the Example of the PADI4 Gene. *Methods and Protocols,* 2.

Ehnert, S., Zhao, J., Pscherer, S., Freude, T., Dooley, S., Kolk, A., Stockle, U., Nussler, A. K. & Hube, R. 2012. Transforming growth factor beta1 inhibits bone morphogenic protein (BMP)-2 and BMP-7 signaling via upregulation of Ski-related novel protein N (SnoN): possible mechanism for the failure of BMP therapy? *BMC Medicine,* 10**,** 101.

Einhorn, T. A. & Gerstenfeld, L. C. 2015. Fracture healing: mechanisms and interventions. *Nature Reviews Rheumatology,* 11**,** 45-54.

Ekstrom, K., Omar, O., Graneli, C., Wang, X., Vazirisani, F. & Thomsen, P. 2013. Monocyte exosomes stimulate the osteogenic gene expression of mesenchymal stem cells. *PLoS One,* 8**,** e75227.

Fadini, G. P., Albiero, M., De Kreutzenberg, S. V., Boscaro, E., Cappellari, R., Marescotti, M., Poncina, N., Agostini, C. & Avogaro, A. 2013. Diabetes Impairs Stem Cell and Proangiogenic Cell Mobilization in Humans. *Diabetes Care,* 36**,** 943-949.

Fadini, G. P., Menegazzo, L., Rigato, M., Scattolini, V., Poncina, N., Bruttocao, A., Ciciliot, S., Mammano, F., Ciubotaru, C. D., Brocco, E., Marescotti, M. C., Cappellari, R., Arrigoni, G., Millioni, R., Vigili De Kreutzenberg, S., Albiero, M. & Avogaro, A. 2016. NETosis Delays Diabetic Wound Healing in Mice and Humans. *Diabetes,* 65**,** 1061-71.

Farrera, C. & Fadeel, B. 2013. Macrophage clearance of neutrophil extracellular traps is a silent process. *Journal of Immunology,* 191**,** 2647-56.

Federation, I. D. 2019. *IDF Diabetes Atlas, 9th edn.,* Brussels, International Diabetes Federation.

Ferraro, F., Lymperi, S., Mendez-Ferrer, S., Saez, B., Spencer, J. A., Yeap, B. Y., Masselli, E., Graiani, G., Prezioso, L., Rizzini, E. L., Mangoni, M., Rizzoli, V., Sykes, S. M., Lin, C. P., Frenette, P. S., Quaini, F. & Scadden, D. T. 2011. Diabetes impairs hematopoietic stem cell mobilization by altering niche function. *Science Translational Medicine,* 3**,** 104ra101.

Förster, Y., Schmidt, J. R., Wissenbach, D. K., Pfeiffer, S. E. M., Baumann, S., Hofbauer, L. C., Von Bergen, M., Kalkhof, S. & Rammelt, S. 2016. Microdialysis Sampling from Wound Fluids Enables Quantitative Assessment of Cytokines, Proteins, and Metabolites Reveals Bone Defect-Specific Molecular Profiles. *PLoS One,* 11**,** e0159580.

Freude, T., Braun, K. F., Haug, A., Pscherer, S., Stockle, U., Nussler, A. K. & Ehnert, S. 2012. Hyperinsulinemia reduces osteoblast activity in vitro via upregulation of TGF-beta. *Journal of Molecular Medicine (Berlin),* 90**,** 1257-66.

Fu, X., Liu, G., Halim, A., Ju, Y., Luo, Q. & Song, G. 2019. Mesenchymal Stem Cell Migration and Tissue Repair. *Cells,* 8**,** 784.

Goldmann, O. & Medina, E. 2012. The expanding world of extracellular traps: not only neutrophils but much more. *Frontiers Immunology,* 3**,** 420.

Goswami, J., Macarthur, T., Bailey, K., Spears, G., Kozar, R. A., Auton, M., Dong, J. F., Key, N. S., Heller, S., Loomis, E., Hall, N. W., Johnstone, A. L. & Park, M. S. 2021. Neutrophil Extracellular Trap Formation and Syndecan-1 Shedding Are Increased After Trauma. *Shock,* 56**,** 433-439.

Grégoire, M., Guilloton, F., Pangault, C., Mourcin, F., Sok, P., Latour, M., Amé-Thomas, P., Flecher, E., Fest, T. & Tarte, K. 2015. Neutrophils trigger a NF-κB dependent polarization of tumor-supportive stromal cells in germinal center B-cell lymphomas. *Oncotarget,* 6**,** 16471-16487.

Greiner, G. G., Emmert-Fees, K. M. F., Becker, J., Rathmann, W., Thorand, B., Peters, A., Quante, A. S., Schwettmann, L. & Laxy, M. 2020. Toward targeted prevention: risk factors for prediabetes defined by impaired fasting glucose, impaired glucose tolerance and increased HbA1c in the population-based KORA study from Germany. *Acta Diabetologica,* 57**,** 1481-1491.

Grøgaard, B., Gerdin, B. & Reikerås, O. 1990. The polymorphonuclear leukocyte: has it a role in fracture healing? *Archives of Orthopaedic and Trauma Surgery,* 109**,** 268-271.

Grundnes, O. & Reikerås, O. 1993. The importance of the hematoma for fracture healing in rats. *Acta Orthopaedica Scandinavia,* 64**,** 340-342.

Hacker, S., Mittermayr, R., Nickl, S., Haider, T., Lebherz-Eichinger, D., Beer, L., Mitterbauer, A., Leiss, H., Zimmermann, M., Schweiger, T., Keibl, C., Hofbauer, H., Gabriel, C., Pavone-Gyöngyösi, M., Redl, H., Tschachler, E., Mildner, M. & Ankersmit, H. J. 2016. Paracrine Factors from Irradiated Peripheral Blood Mononuclear Cells Improve Skin Regeneration and Angiogenesis in a Porcine Burn Model. *Scientific Reports,* 6**,** 25168.

Hakkim, A., Fuchs, T. A., Martinez, N. E., Hess, S., Prinz, H., Zychlinsky, A. & Waldmann, H. 2011. Activation of the Raf-MEK-ERK pathway is required for neutrophil extracellular trap formation. *Nature Chemical Biology,* 7**,** 75-7.

Hakkim, A., Fürnrohr, B. G., Amann, K., Laube, B., Abed, U. A., Brinkmann, V., Herrmann, M., Voll, R. E. & Zychlinsky, A. 2010. Impairment of neutrophil extracellular trap degradation is associated with lupus nephritis. *proceedings of the national academy of sciences of the united states of america,* 107**,** 9813-9818.

Hamann, C., Kirschner, S., Günther, K.-P. & Hofbauer, L. C. 2012. Bone, sweet bone—osteoporotic fractures in diabetes mellitus. *Nature Reviews Endocrinology,* 8**,** 297-305.

Haritha, V. H., Seena, P., Shaji, B. V., Nithin, T. U., Hazeena, V. N. & Anie, Y. 2019. Monocyte clearance of apoptotic neutrophils is unhindered in the presence of NETosis, but proteins of NET trigger ETosis in monocytes. *Immunology Letters,* 207**,** 36-45.

Harris, M. L., Darrah, E., Lam, G. K., Bartlett, S. J., Giles, J. T., Grant, A. V., Gao, P., Scott, W. W., Jr., El-Gabalawy, H., Casciola-Rosen, L., Barnes, K. C., Bathon, J. M. & Rosen, A. 2008. Association of autoimmunity to peptidyl arginine deiminase type 4 with genotype and disease severity in rheumatoid arthritis. *Arthritis & Rheumatology,* 58**,** 1958-1967.

Hazeldine, J., Dinsdale, R. J., Harrison, P. & Lord, J. M. 2019. Traumatic Injury and Exposure to Mitochondrial-Derived Damage Associated Molecular Patterns Suppresses Neutrophil Extracellular Trap Formation. *Frontiers Immunology,* 10**,** 685.

Hazeldine, J., Harris, P., Chapple, I. L., Grant, M., Greenwood, H., Livesey, A., Sapey, E. & Lord, J. M. 2014. Impaired neutrophil extracellular trap formation: a novel defect in the innate immune system of aged individuals. *Aging Cell,* 13**,** 690-698.

He, X., Wang, H., Jin, T., Xu, Y., Mei, L. & Yang, J. 2016. TLR4 Activation Promotes Bone Marrow MSC Proliferation and Osteogenic Differentiation via Wnt3a and Wnt5a Signaling. *PLoS One,* 11**,** e0149876.

Heidemann, C., Kuhnert, R., Born, S. & Scheidt-Nave, C. 2017. 12-Monats-Prävalenz des bekannten Diabetes mellitus in Deutschland. Robert Koch-Institut, Epidemiologie und Gesundheitsberichterstattung.

Heijink, I. H., Pouwels, S. D., Leijendekker, C., De Bruin, H. G., Zijlstra, G. J., Van Der Vaart, H., Ten Hacken, N. H., Van Oosterhout, A. J., Nawijn, M. C. & Van Der Toorn, M. 2015. Cigarette smoke-induced damage-associated molecular pattern release from necrotic neutrophils triggers

proinflammatory mediator release. *The American Journal of Respiratory Cell and Molecular Biology,* 52**,** 554-62.

Hemmers, S., Teijaro, J. R., Arandjelovic, S. & Mowen, K. A. 2011. PAD4-mediated neutrophil extracellular trap formation is not required for immunity against influenza infection. *PLoS One,* 6**,** e22043.

Hernandez, R. K., Do, T. P., Critchlow, C. W., Dent, R. E. & Jick, S. S. 2012. Patient-related risk factors for fracture-healing complications in the United Kingdom General Practice Research Database. *Acta Orthop,* 83**,** 653-60.

Herrmann, M., Stanić, B., Hildebrand, M., Alini, M. & Verrier, S. 2019. In vitro simulation of the early proinflammatory phase in fracture healing reveals strong immunomodulatory effects of CD146-positive mesenchymal stromal cells. *Journal of Tissue Engineering and Regenerative Medicine,* 13**,** 1466-1481.

Heuer, A., Stiel, C., Elrod, J., Königs, I., Vincent, D., Schlegel, P., Trochimiuk, M., Appl, B., Reinshagen, K., Raluy, L. P. & Boettcher, M. 2021. Therapeutic Targeting of Neutrophil Extracellular Traps Improves Primary and Secondary Intention Wound Healing in Mice. *Frontiers in Immunology,* 12**,** 614347.

Hirota, T., Levy, J. H. & Iba, T. 2020. The influence of hyperglycemia on neutrophil extracellular trap formation and endothelial glycocalyx damage in a mouse model of type 2 diabetes. *Microcirculation,* 27**,** e12617.

Hoff, P., Gaber, T., Strehl, C., Schmidt-Bleek, K., Lang, A., Huscher, D., Burmester, G. R., Schmidmaier, G., Perka, C., Duda, G. N. & Buttgereit, F. 2016. Immunological characterization of the early human fracture hematoma. *Immunology Research,* 64**,** 1195-1206.

Hoppe, B., Häupl, T., Gruber, R., Kiesewetter, H., Burmester, G. R., Salama, A. & Dörner, T. 2006. Detailed analysis of the variability of peptidylarginine deiminase type 4 in German patients with rheumatoid arthritis: a case-control study. *Arthritis Research & Therapy,* 8**,** R34-R34.

Horikoshi, N., Tachiwana, H., Saito, K., Osakabe, A., Sato, M., Yamada, M., Akashi, S., Nishimura, Y., Kagawa, W. & Kurumizaka, H. 2011. Structural and biochemical analyses of the human PAD4 variant encoded by a functional haplotype gene. *Acta Crystallographica. Section D, Biological Crystallography,* 67**,** 112-118.

Hu, Q., Shi, H., Zeng, T., Liu, H., Su, Y., Cheng, X., Ye, J., Yin, Y., Liu, M., Zheng, H., Wu, X., Chi, H., Zhou, Z., Jia, J., Sun, Y., Teng, J. & Yang, C. 2019. Increased neutrophil extracellular traps activate NLRP3 and inflammatory macrophages in adult-onset Still's disease. *Arthritis Research & Therapy,* 21**,** 9.

Ihle, C., Freude, T., Bahrs, C., Zehendner, E., Braunsberger, J., Biesalski, H. K., Lambert, C., Stockle, U., Wintermeyer, E., Grunwald, J., Grunwald, L., Ochs, G., Flesch, I. & Nussler, A. 2017. Malnutrition - An underestimated factor in the inpatient treatment of traumatology and orthopedic patients: A prospective evaluation of 1055 patients. *Injury,* 48**,** 628-636.

Ishikawa, M., Ito, H., Kitaori, T., Murata, K., Shibuya, H., Furu, M., Yoshitomi, H., Fujii, T., Yamamoto, K. & Matsuda, S. 2014. MCP/CCR2 signaling is essential for recruitment of mesenchymal progenitor cells during the early phase of fracture healing. *PLoS One,* 9**,** e104954.

Jiang, D., Muschhammer, J., Qi, Y., Kugler, A., De Vries, J. C., Saffarzadeh, M., Sindrilaru, A., Beken, S. V., Wlaschek, M., Kluth, M. A., Ganss, C., Frank, N. Y., Frank, M. H., Preissner, K. T. & Scharffetter-Kochanek, K. 2016. Suppression of Neutrophil-Mediated Tissue Damage-A Novel Skill of Mesenchymal Stem Cells. *Stem Cells,* 34**,** 2393-406.

Jin, L., Liu, Y., Jing, C., Wang, R., Wang, Q. & Wang, H. 2020. Neutrophil extracellular traps (NETs)-mediated killing of carbapenem-resistant hypervirulent Klebsiella pneumoniae (CR-hvKP) are impaired in patients with diabetes mellitus. *Virulence,* 11**,** 1122-1130.

Joshi, M. B., Baipadithaya, G., Balakrishnan, A., Hegde, M., Vohra, M., Ahamed, R., Nagri, S. K., Ramachandra, L. & Satyamoorthy, K. 2016. Elevated homocysteine levels in type 2 diabetes induce constitutive neutrophil extracellular traps. *Scientific Reports,* 6**,** 36362.

Joshi, M. B., Lad, A., Bharath Prasad, A. S., Balakrishnan, A., Ramachandra, L. & Satyamoorthy, K. 2013. High glucose modulates IL-6 mediated immune homeostasis through impeding neutrophil extracellular trap formation. *FEBS Letters,* 587**,** 2241-2246.

Julier, Z., Park, A. J., Briquez, P. S. & Martino, M. M. 2017. Promoting tissue regeneration by modulating the immune system. *Acta Biomaterialia,* 53**,** 13-28.

Kahm, K., Laxy, M., Schneider, U., Rogowski, W. H., Lhachimi, S. K. & Holle, R. 2018. Health Care Costs Associated With Incident Complications in Patients With Type 2 Diabetes in Germany. *Diabetes Care,* 41**,** 971-978.

Kajioka, H., Kagawa, S., Ito, A., Yoshimoto, M., Sakamoto, S., Kikuchi, S., Kuroda, S., Yoshida, R., Umeda, Y., Noma, K., Tazawa, H. & Fujiwara, T. 2021. Targeting neutrophil extracellular traps with thrombomodulin prevents pancreatic cancer metastasis. *Cancer Letters,* 497**,** 1-13.

Kaufman, T., Magosevich, D., Moreno, M. C., Guzman, M. A., D'atri, L. P., Carestia, A., Fandiño, M. E., Fondevila, C. & Schattner, M. 2017. Nucleosomes and neutrophil extracellular traps in septic and burn patients. *Clinical Immunology,* 183**,** 254-262.

Kaur, T., Dumoga, S., Koul, V. & Singh, N. 2020. Modulating neutrophil extracellular traps for wound healing. *Biomater Sci,* 8**,** 3212-3223.

Kawano, H., Ito, T., Yamada, S., Hashiguchi, T., Maruyama, I., Hisatomi, T., Nakamura, M. & Sakamoto, T. 2014. Toxic effects of extracellular histones and their neutralization by vitreous in retinal detachment. *Laboratory Investigation,* 94**,** 569-585.

Kenny, E. F., Herzig, A., Kruger, R., Muth, A., Mondal, S., Thompson, P. R., Brinkmann, V., Bernuth, H. V. & Zychlinsky, A. 2017. Diverse stimuli engage different neutrophil extracellular trap pathways. *Elife,* 6**,** e24437.

Khandpur, R., Carmona-Rivera, C., Vivekanandan-Giri, A., Gizinski, A., Yalavarthi, S., Knight, J. S., Friday, S., Li, S., Patel, R. M., Subramanian, V., Thompson, P., Chen, P., Fox, D. A., Pennathur, S. & Kaplan, M. J. 2013. NETs are a source of citrullinated autoantigens and stimulate inflammatory responses in rheumatoid arthritis. *Science Translational Medicine,* 5**,** 178ra40.

Kirchner, T., Möller, S., Klinger, M., Solbach, W., Laskay, T. & Behnen, M. 2012. The Impact of Various Reactive Oxygen Species on the Formation of Neutrophil Extracellular Traps. *Mediators of Inflammation,* 2012**,** 849136.

Knight, M. N. & Hankenson, K. D. 2013. Mesenchymal Stem Cells in Bone Regeneration. *Advances in wound care,* 2**,** 306-316.

Knopf, J., Leppkes, M., Schett, G., Herrmann, M. & Muñoz, L. E. 2019. Aggregated NETs Sequester and Detoxify Extracellular Histones. *Frontiers in Immunology,* 10.

Kolaczkowska, E., Jenne, C. N., Surewaard, B. G., Thanabalasuriar, A., Lee, W. Y., Sanz, M. J., Mowen, K., Opdenakker, G. & Kubes, P. 2015. Molecular mechanisms of NET formation and degradation revealed by intravital imaging in the liver vasculature. *Nat Commun,* 6**,** 6673.

Kolar, P., Gaber, T., Perka, C., Duda, G. N. & Buttgereit, F. 2011. Human early fracture hematoma is characterized by inflammation and hypoxia. *Clinical Orthopaedics and Related Research,* 469**,** 3118-3126.

Konnecke, I., Serra, A., El Khassawna, T., Schlundt, C., Schell, H., Hauser, A., Ellinghaus, A., Volk, H. D., Radbruch, A., Duda, G. N. & Schmidt-Bleek, K. 2014. T and B cells participate in bone repair by infiltrating the fracture callus in a two-wave fashion. *Bone,* 64**,** 155-65.

Kovtun, A., Bergdolt, S., Wiegner, R., Radermacher, P., Huber-Lang, M. & Ignatius, A. 2016. The crucial role of neutrophil granulocytes in bone fracture healing. *European Cells and Materials,* 32**,** 152-162.

Kröger, K., Berg, C., Santosa, F., Malyar, N. & Reinecke, H. 2017. Lower Limb Amputation in Germany. *Deutsches Ärzteblatt International,* 114**,** 130-136.

Kufeldt, J., Kovarova, M., Adolph, M., Staiger, H., Bamberg, M., Häring, H. U., Fritsche, A. & Peter, A. 2018. Prevalence and Distribution of Diabetes Mellitus in a Maximum Care Hospital: Urgent Need for HbA1c-Screening. *Experimental and Clinical Endocrinology & Diabetes,* 126**,** 123-129.

Kuyl, E. V., Shu, F., Sosa, B. R., Lopez, J. D., Qin, D., Pannellini, T., Ivashkiv, L. B., Greenblatt, M. B., Bostrom, M. P. G. & Yang, X. 2021. Inhibition of PAD4 mediated neutrophil extracellular traps prevents fibrotic osseointegration failure in a tibial implant murine model : an animal study. *The Bone & Joint Journal,* 103-B**,** 135-144.

Laggner, M., Copic, D., Nemec, L., Vorstandlechner, V., Gugerell, A., Gruber, F., Peterbauer, A., Ankersmit, H. J. & Mildner, M. 2020. Therapeutic potential of lipids obtained from γ-irradiated PBMCs in dendritic cell-mediated skin inflammation. *EBioMedicine,* 55**,** 102774.

Landgraf, R., Aberle, J., Birkenfeld, A. L., Gallwitz, B., Kellerer, M., Klein, H., Müller-Wieland, D., Nauck, M. A., Reuter, H.-M. & Siegel, E. 2019. Therapie des Typ-2-Diabetes. *Diabetologie und Stoffwechsel,* 14**,** S167-S187.

Larsen, M., Webb, G., Kennington, S., Kelleher, N., Sheppard, J., Kuo, J. & Unsworth-White, J. 2002. Mannitol in cardioplegia as an oxygen free radical scavenger measured by malondialdehyde. *Perfusion,* 17**,** 51-55.

Lazzaretto, B. & Fadeel, B. 2019. Intra- and Extracellular Degradation of Neutrophil Extracellular Traps by Macrophages and Dendritic Cells. *Journal of Immunology,* 203**,** 2276-2290.

Lee, H.-M., Kim, J.-J., Kim, H. J., Shong, M., Ku, B. J. & Jo, E.-K. 2013. Upregulated NLRP3 Inflammasome Activation in Patients With Type 2 Diabetes. *Diabetes,* 62**,** 194.

Lefrancais, E., Mallavia, B., Zhuo, H., Calfee, C. S. & Looney, M. R. 2018. Maladaptive role of neutrophil extracellular traps in pathogen-induced lung injury. *JCI Insight,* 3**,** e98178.

Leshner, M., Wang, S., Lewis, C., Zheng, H., Chen, X. A., Santy, L. & Wang, Y. 2012. PAD4 mediated histone hypercitrullination induces heterochromatin decondensation and chromatin unfolding to form neutrophil extracellular trap-like structures. *Frontiers in Immunology,* 3**,** 307.

Lewis, H. D., Liddle, J., Coote, J. E., Atkinson, S. J., Barker, M. D., Bax, B. D., Bicker, K. L., Bingham, R. P., Campbell, M., Chen, Y. H., Chung, C. W., Craggs, P. D., Davis, R. P., Eberhard, D., Joberty, G., Lind, K. E., Locke, K., Maller, C., Martinod, K., Patten, C., Polyakova, O., Rise, C. E., Rudiger, M., Sheppard, R. J., Slade, D. J., Thomas, P., Thorpe, J., Yao, G., Drewes, G., Wagner, D. D., Thompson, P. R., Prinjha, R. K. & Wilson, D. M. 2015. Inhibition of PAD4 activity is sufficient to disrupt mouse and human NET formation. *Nature Chemical Biology,* 11**,** 189-91.

Li, H., Itagaki, K., Sandler, N., Gallo, D., Galenkamp, A., Kaczmarek, E., Livingston, D. H., Zeng, Y., Lee, Y. T., Tang, I. T., Isal, B., Otterbein, L. & Hauser, C. J. 2015. Mitochondrial damage-associated molecular patterns from fractures suppress pulmonary immune responses via formyl peptide receptors 1 and 2. *Journal of Trauma and Acute Care Surgery,* 78**,** 272-279; discussion 279-281.

Li, H., Liu, J., Yao, J., Zhong, J., Guo, L. & Sun, T. 2016. Fracture initiates systemic inflammatory response syndrome through recruiting polymorphonuclear leucocytes. *Immunologic Research,* 64**,** 1053-1059.

Li, P., Li, M., Lindberg, M. R., Kennett, M. J., Xiong, N. & Wang, Y. 2010. PAD4 is essential for antibacterial innate immunity mediated by neutrophil extracellular traps. *journal of experimental medicine,* 207**,** 1853-1862.

Liang, Y., Pan, B., Alam, H. B., Deng, Q., Wang, Y., Chen, E., Liu, B., Tian, Y., Williams, A. M., Duan, X., Wang, Y., Zhang, J. & Li, Y. 2018. Inhibition of peptidylarginine deiminase alleviates LPS-induced pulmonary dysfunction and improves survival in a mouse model of lethal endotoxemia. *European Journal of Pharmacology,* 833**,** 432-440.

Lichte, P., Kobbe, P., Almahmoud, K., Pfeifer, R., Andruszkow, H., Hildebrand, F., Lefering, R., Pape, H.-C. & Trauma Register, D. G. U. 2015. Post-traumatic thrombo-embolic complications in polytrauma patients. *International Orthopaedics,* 39**,** 947-954.

Linnemann, C., Savini, L., Rollmann, M. F., Histing, T., Nussler, A. K. & Ehnert, S. 2021. Altered Secretome of Diabetic Monocytes Could Negatively Influence Fracture Healing-An In Vitro Study. *International Journal of Molecular Sciences,* 22**,** 9212.

Linnemann, C., Venturelli, S., Konrad, F., Nussler, A. K. & Ehnert, S. 2020. Bio-impedance measurement allows displaying the early stages of neutrophil extracellular traps. *EXCLI journal,* 19**,** 1481-1495.

Liton, P. B., Lin, Y., Luna, C., Li, G., Gonzalez, P. & Epstein, D. L. 2008. Cultured Porcine Trabecular Meshwork Cells Display Altered Lysosomal Function

When Subjected to Chronic Oxidative Stress. *Investigative Ophthalmology & Visual Science,* 49**,** 3961-3969.

Liu, D., Yang, P., Gao, M., Yu, T., Shi, Y., Zhang, M., Yao, M., Liu, Y. & Zhang, X. 2019a. NLRP3 activation induced by neutrophil extracellular traps sustains inflammatory response in the diabetic wound. *Clinical Science,* 133**,** 565-582.

Liu, L., Mao, Y., Xu, B., Zhang, X., Fang, C., Ma, Y., Men, K., Qi, X., Yi, T., Wei, Y. & Wei, X. 2019b. Induction of neutrophil extracellular traps during tissue injury: Involvement of STING and Toll-like receptor 9 pathways. *Cell Proliferation,* 52**,** e12579.

Liu, L., Zhang, W., Su, Y., Chen, Y., Cao, X. & Wu, J. 2021. The impact of neutrophil extracellular traps on deep venous thrombosis in patients with traumatic fractures. *Clinica Chimica Acta,* 519**,** 231-238.

Loi, F., Córdova, L. A., Pajarinen, J., Lin, T.-H., Yao, Z. & Goodman, S. B. 2016. Inflammation, fracture and bone repair. *Bone,* 86**,** 119-130.

Lood, C., Blanco, L. P., Purmalek, M. M., Carmona-Rivera, C., De Ravin, S. S., Smith, C. K., Malech, H. L., Ledbetter, J. A., Elkon, K. B. & Kaplan, M. J. 2016. Neutrophil extracellular traps enriched in oxidized mitochondrial DNA are interferogenic and contribute to lupus-like disease. *Nature Medicine,* 22**,** 146-53.

Lowry, O. H., Rosebrough, N. J., Farr, A. L. & Randall, R. J. 1951. Protein measurement with the Folin phenol reagent. *Journal of Biological Chemistry,* 193**,** 265-275.

Lu, C., Rollins, M., Hou, H., Swartz, H. M., Hopf, H., Miclau, T. & Marcucio, R. S. 2008. Tibial fracture decreases oxygen levels at the site of injury. *Iowa Orthopedic Journal,* 28**,** 14-21.

Majewski, P., Majchrzak-Gorecka, M., Grygier, B., Skrzeczynska-Moncznik, J., Osiecka, O. & Cichy, J. 2016. Inhibitors of Serine Proteases in Regulating the Production and Function of Neutrophil Extracellular Traps. *Frontiers in Immunology,* 7.

Mantovani, A., Cassatella, M. A., Costantini, C. & Jaillon, S. 2011. Neutrophils in the activation and regulation of innate and adaptive immunity. *Nature Reviews Immunology,* 11**,** 519-531.

Margraf, S., Lögters, T., Reipen, J., Altrichter, J., Scholz, M. & Windolf, J. 2008. Neutrophil-derived circulating free DNA (cf-DNA/NETs): a potential prognostic marker for posttraumatic development of inflammatory second hit and sepsis. *Shock,* 30**,** 352-358.

Martinod, K., Demers, M., Fuchs, T. A., Wong, S. L., Brill, A., Gallant, M., Hu, J., Wang, Y. & Wagner, D. D. 2013. Neutrophil histone modification by peptidylarginine deiminase 4 is critical for deep vein thrombosis in mice. *proceedings of the national academy of sciences of the united states of america,* 110**,** 8674-8679.

Martins-Cardoso, K., Almeida, V. H., Bagri, K. M., Rossi, M. I., Mermelstein, C. S., König, S. & Monteiro, R. Q. 2020. Neutrophil Extracellular Traps (NETs) Promote Pro-Metastatic Phenotype in Human Breast Cancer Cells through Epithelial–Mesenchymal Transition. *Cancers,* 12.

Maruyama, M., Rhee, C., Utsunomiya, T., Zhang, N., Ueno, M., Yao, Z. & Goodman, S. B. 2020. Modulation of the Inflammatory Response and Bone Healing. *Frontiers in Endocrinology,* 11.

Massarenti, L., Enevold, C., Damgaard, D., Ødum, N., Nielsen, C. H. & Jacobsen, S. 2019. Peptidylarginine deiminase-4 gene polymorphisms are associated with systemic lupus erythematosus and lupus nephritis. *Scandinavian Journal of Rheumatology,* 48**,** 133-140.

Mastronardi, F. G., Wood, D. D., Mei, J., Raijmakers, R., Tseveleki, V., Dosch, H.-M., Probert, L., Casaccia-Bonnefil, P. & Moscarello, M. A. 2006. Increased Citrullination of Histone H3 in Multiple Sclerosis Brain and Animal Models of Demyelination: A Role for Tumor Necrosis Factor-Induced Peptidylarginine Deiminase 4 Translocation. *The Journal of Neuroscience,* 26**,** 11387.

Mcilroy, D. J., Jarnicki, A. G., Au, G. G., Lott, N., Smith, D. W., Hansbro, P. M. & Balogh, Z. J. 2014. Mitochondrial DNA neutrophil extracellular traps are formed after trauma and subsequent surgery. *J Crit Care,* 29**,** 1133.e1-5.

Menegazzo, L., Ciciliot, S., Poncina, N., Mazzucato, M., Persano, M., Bonora, B., Albiero, M., Vigili De Kreutzenberg, S., Avogaro, A. & Fadini, G. P. 2015. NETosis is induced by high glucose and associated with type 2 diabetes. *Acta Diabetol,* 52**,** 497-503.

Menegazzo, L., Scattolini, V., Cappellari, R., Bonora, B. M., Albiero, M., Bortolozzi, M., Romanato, F., Ceolotto, G., Vigili De Kreutzeberg, S., Avogaro, A. & Fadini, G. P. 2018. The antidiabetic drug metformin blunts NETosis in vitro and reduces circulating NETosis biomarkers in vivo. *Acta Diabetologica,* 55**,** 593-601.

Mergaert, A. M., Bawadekar, M., Nguyen, T. Q., Massarenti, L., Holmes, C. L., Rebernick, R., Schrodi, S. J. & Shelef, M. A. 2019. Reduced Anti-Histone Antibodies and Increased Risk of Rheumatoid Arthritis Associated with a Single Nucleotide Polymorphism in PADI4 in North Americans. *International Journal of Molecular Sciences,* 20**,** 3093.

Metzler, K. D., Fuchs, T. A., Nauseef, W. M., Reumaux, D., Roesler, J., Schulze, I., Wahn, V., Papayannopoulos, V. & Zychlinsky, A. 2011. Myeloperoxidase is required for neutrophil extracellular trap formation: implications for innate immunity. *Blood,* 117**,** 953-959.

Metzler, K. D., Goosmann, C., Lubojemska, A., Zychlinsky, A. & Papayannopoulos, V. 2014. A myeloperoxidase-containing complex regulates neutrophil elastase release and actin dynamics during NETosis. *Cell Reports,* 8**,** 883-896.

Middleton, E. A., He, X. Y., Denorme, F., Campbell, R. A., Ng, D., Salvatore, S. P., Mostyka, M., Baxter-Stoltzfus, A., Borczuk, A. C., Loda, M., Cody, M. J., Manne, B. K., Portier, I., Harris, E. S., Petrey, A. C., Beswick, E. J., Caulin, A. F., Iovino, A., Abegglen, L. M., Weyrich, A. S., Rondina, M. T., Egeblad, M., Schiffman, J. D. & Yost, C. C. 2020. Neutrophil extracellular traps contribute to immunothrombosis in COVID-19 acute respiratory distress syndrome. *Blood,* 136**,** 1169-1179.

Mitsios, A., Arampatzioglou, A., Arelaki, S., Mitroulis, I. & Ritis, K. 2016. NETopathies? Unraveling the Dark Side of Old Diseases through Neutrophils. *Frontiers in Immunology,* 7**,** 678.

Miyoshi, A., Yamada, M., Shida, H., Nakazawa, D., Kusunoki, Y., Nakamura, A., Miyoshi, H., Tomaru, U., Atsumi, T. & Ishizu, A. 2016. Circulating Neutrophil Extracellular Trap Levels in Well-Controlled Type 2 Diabetes and Pathway Involved in Their Formation Induced by High-Dose Glucose. *Pathobiology,* 83**,** 243-51.

Mizuno, K., Mineo, K., Tachibana, T., Sumi, M., Matsubara, T. & Hirohata, K. 1990. The osteogenetic potential of fracture haematoma. Subperiosteal and intramuscular transplantation of the haematoma. *The Journal of Bone & Joint Surgery. British Version,* 72**,** 822-829.

Mizuta, Y., Akahoshi, T., Guo, J., Zhang, S., Narahara, S., Kawano, T., Murata, M., Tokuda, K., Eto, M., Hashizume, M. & Yamaura, K. 2020. Exosomes from adipose tissue-derived mesenchymal stem cells ameliorate histone-induced acute lung injury by activating the PI3K/Akt pathway in endothelial cells. *Stem Cell Research & Therapy,* 11**,** 508.

Mondal, S. & Thompson, P. R. 2019. Protein Arginine Deiminases (PADs): Biochemistry and Chemical Biology of Protein Citrullination. *Accounts of Chemical Research,* 52**,** 818-832.

Munir, S., Basu, A., Maity, P., Krug, L., Haas, P., Jiang, D., Strauss, G., Wlaschek, M., Geiger, H., Singh, K. & Scharffetter-Kochanek, K. 2020. TLR4-dependent shaping of the wound site by MSCs accelerates wound healing. *EMBO reports,* 21**,** e48777.

Murthy, P., Singhi, A. D., Ross, M. A., Loughran, P., Paragomi, P., Papachristou, G. I., Whitcomb, D. C., Zureikat, A. H., Lotze, M. T., Zeh Iii, H. J. & Boone, B. A. 2019. Enhanced Neutrophil Extracellular Trap Formation in Acute Pancreatitis Contributes to Disease Severity and Is Reduced by Chloroquine. *Frontiers in Immunology,* 10**,** 28.

Muthukuru, M. & Darveau, R. P. 2014. TLR signaling that induces weak inflammatory response and SHIP1 enhances osteogenic functions. *Bone Res,* 2**,** 14031.

Nakazawa, D., Shida, H., Kusunoki, Y., Miyoshi, A., Nishio, S., Tomaru, U., Atsumi, T. & Ishizu, A. 2016. The responses of macrophages in interaction with neutrophils that undergo NETosis. *Journal of Autoimmunity,* 67**,** 19-28.

Namboori, P. K. K., Vineeth, K. V., Rohith, V., Hassan, I., Sekhar, L., Sekhar, A. & Nidheesh, M. 2011. The ApoE gene of Alzheimer's disease (AD). *Functional & Integrative Genomics,* 11**,** 519-522.

Naranbhai, V., Fairfax, B. P., Makino, S., Humburg, P., Wong, D., Ng, E., Hill, A. V. & Knight, J. C. 2015. Genomic modulators of gene expression in human neutrophils. *Nature Communications,* 6**,** 7545.

Neeli, I. & Radic, M. 2013. Opposition between PKC isoforms regulates histone deimination and neutrophil extracellular chromatin release. *Frontiers in Immunology,* 4**,** 38.

Neubert, E., Meyer, D., Rocca, F., Gunay, G., Kwaczala-Tessmann, A., Grandke, J., Senger-Sander, S., Geisler, C., Egner, A., Schon, M. P., Erpenbeck, L. & Kruss, S. 2018. Chromatin swelling drives neutrophil extracellular trap release. *Nature Communications,* 9**,** 3767.

Nicolaidou, V., Wong, M. M., Redpath, A. N., Ersek, A., Baban, D. F., Williams, L. M., Cope, A. P. & Horwood, N. J. 2012. Monocytes induce STAT3

activation in human mesenchymal stem cells to promote osteoblast formation. *PLoS One,* 7**,** e39871.

Nikolaou, V. S., Efstathopoulos, N., Kontakis, G., Kanakaris, N. K. & Giannoudis, P. V. 2009. The influence of osteoporosis in femoral fracture healing time. *Injury,* 40**,** 663-8.

Oikawa, A., Siragusa, M., Quaini, F., Mangialardi, G., Katare, R. G., Caporali, A., Van Buul, J. D., Van Alphen, F. P., Graiani, G., Spinetti, G., Kraenkel, N., Prezioso, L., Emanueli, C. & Madeddu, P. 2010. Diabetes mellitus induces bone marrow microangiopathy. *Arteriosclerosis, Thrombosis, and Vascular Biology,* 30**,** 498-508.

Oldenborg, P. A. 1999. Effects of insulin on N-formyl-methionyl-leucyl-phenylalanine (fMet-Leu-Phe)-stimulated production of reactive oxygen metabolites from normal human neutrophils. *Inflamm Res,* 48**,** 404-11.

Otawara, M., Roushan, M., Wang, X., Ellett, F., Yu, Y. M. & Irimia, D. 2018. Microfluidic Assay Measures Increased Neutrophil Extracellular Traps Circulating in Blood after Burn Injuries. *Scientific Reports,* 8**,** 16983.

Paffrath, T., Wafaisade, A., Lefering, R., Simanski, C., Bouillon, B., Spanholtz, T., Wutzler, S. & Maegele, M. 2010. Venous thromboembolism after severe trauma: incidence, risk factors and outcome. *Injury,* 41**,** 97-101.

Papayannopoulos, V., Metzler, K. D., Hakkim, A. & Zychlinsky, A. 2010. Neutrophil elastase and myeloperoxidase regulate the formation of neutrophil extracellular traps. *Journal of Cell Biology,* 191**,** 677-691.

Parackova, Z., Zentsova, I., Vrabcova, P., Klocperk, A., Sumnik, Z., Pruhova, S., Petruzelkova, L., Hasler, R. & Sediva, A. 2020. Neutrophil Extracellular Trap Induced Dendritic Cell Activation Leads to Th1 Polarization in Type 1 Diabetes. *Frontiers in Immunology,* 11**,** 661.

Petretto, A., Bruschi, M., Pratesi, F., Croia, C., Candiano, G., Ghiggeri, G. & Migliorini, P. 2019. Neutrophil extracellular traps (NET) induced by different stimuli: A comparative proteomic analysis. *PLoS One,* 14**,** e0218946.

Pfeiffenberger, M., Bartsch, J., Hoff, P., Ponomarev, I., Barnewitz, D., Thöne-Reineke, C., Buttgereit, F., Gaber, T. & Lang, A. 2019. Hypoxia and mesenchymal stromal cells as key drivers of initial fracture healing in an equine in vitro fracture hematoma model. *PLoS One,* 14**,** e0214276.

Picke, A. K., Campbell, G., Napoli, N., Hofbauer, L. C. & Rauner, M. 2019. Update on the impact of type 2 diabetes mellitus on bone metabolism and material properties. *Endocrrine Connections,* 8**,** R55-R70.

Pieterse, E., Hofstra, J., Berden, J., Herrmann, M., Dieker, J. & Van Der Vlag, J. 2015. Acetylated histones contribute to the immunostimulatory potential of neutrophil extracellular traps in systemic lupus erythematosus. *Clinical and Experimental Immunology,* 179**,** 68-74.

Pieterse, E., Rother, N., Garsen, M., Hofstra, J. M., Satchell, S. C., Hoffmann, M., Loeven, M. A., Knaapen, H. K., Van Der Heijden, O. W. H., Berden, J. H. M., Hilbrands, L. B. & Van Der Vlag, J. 2017. Neutrophil Extracellular Traps Drive Endothelial-to-Mesenchymal Transition. *Arteriosclerosis, Thrombosis, and Vascular Biology,* 37**,** 1371-1379.

Pieterse, E., Rother, N., Yanginlar, C., Gerretsen, J., Boeltz, S., Munoz, L. E., Herrmann, M., Pickkers, P., Hilbrands, L. B. & Van Der Vlag, J. 2018.

Cleaved N-terminal histone tails distinguish between NADPH oxidase (NOX)-dependent and NOX-independent pathways of neutrophil extracellular trap formation. *Annals of Rheumatic Diseases,* 77**,** 1790-1798.

Pilsczek, F. H., Salina, D., Poon, K. K. H., Fahey, C., Yipp, B. G., Sibley, C. D., Robbins, S. M., Green, F. H. Y., Surette, M. G., Sugai, M., Bowden, M. G., Hussain, M., Zhang, K. & Kubes, P. 2010. A Novel Mechanism of Rapid Nuclear Neutrophil Extracellular Trap Formation in Response to Staphylococcus aureus. *The Journal of Immunology,* 185**,** 7413.

Pscherer, S., Freude, T., Forst, T., Nussler, A. K., Braun, K. F. & Ehnert, S. 2013. Anti-diabetic treatment regulates pro-fibrotic TGF-beta serum levels in type 2 diabetics. *Diabetology & Metabolic Syndrome,* 5**,** 48.

Pscherer, S., Kostev, K., Dippel, F. W. & Rathmann, W. 2016. Fracture risk in patients with type 2 diabetes under different antidiabetic treatment regimens: a retrospective database analysis in primary care. *Diabetes Metab Syndr Obes,* 9**,** 17-23.

Pscherer, S., Nussler, A., Bahrs, C., Reumann, M., Ihle, C., Stockle, U., Ehnert, S., Freude, T., Ochs, B. G., Flesch, I. & Ziegler, P. 2017a. [Retrospective Analysis of Diabetics with Regard to Treatment Duration and Costs]. *Zeitschrift für Orthopädie und Unfallchirurgie,* 155**,** 72-76.

Pscherer, S., Sandmann, G. H., Ehnert, S., Nussler, A. K., Stockle, U. & Freude, T. 2015. Delayed Fracture Healing in Diabetics with Distal Radius Fractures. *Acta Chir Orthop Traumatol Cech,* 82**,** 268-73.

Pscherer, S., Sandmann, G. H., Ehnert, S., Nussler, A. K., Stockle, U. & Freude, T. 2017b. Delayed Fracture Healing in Diabetics with Distal Radius Fractures. *Acta Chirurgiae Orthopaedicae et Traumatologiae Cechoslovaca,* 84**,** 24-29.

Ramasamy, S. K., Kusumbe, A. P., Wang, L. & Adams, R. H. 2014. Endothelial Notch activity promotes angiogenesis and osteogenesis in bone. *Nature,* 507**,** 376-380.

Randeria, S. N., Thomson, G. J. A., Nell, T. A., Roberts, T. & Pretorius, E. 2019. Inflammatory cytokines in type 2 diabetes mellitus as facilitators of hypercoagulation and abnormal clot formation. *Cardiovascular Diabetology,* 18**,** 72.

Rayner, B. S., Zhang, Y., Brown, B. E., Reyes, L., Cogger, V. C. & Hawkins, C. L. 2018. Role of hypochlorous acid (HOCl) and other inflammatory mediators in the induction of macrophage extracellular trap formation. *Free Radical Biology and Medicine,* 129**,** 25-34.

Rhee, S. Y. & Kim, Y. S. 2018. The Role of Advanced Glycation End Products in Diabetic Vascular Complications. *Diabetes Metab J,* 42**,** 188-195.

Rutkovskiy, A., Stensløkken, K.-O. & Vaage, I. J. 2016. Osteoblast Differentiation at a Glance. *Medical science monitor basic research,* 22**,** 95-106.

Saffarzadeh, M., Juenemann, C., Queisser, M. A., Lochnit, G., Barreto, G., Galuska, S. P., Lohmeyer, J. & Preissner, K. T. 2012. Neutrophil extracellular traps directly induce epithelial and endothelial cell death: a predominant role of histones. *PLoS One,* 7**,** e32366.

Saha, P., Yeoh, B. S., Xiao, X., Golonka, R. M., Singh, V., Wang, Y. & Vijay-Kumar, M. 2019. PAD4-dependent NETs generation are indispensable for

intestinal clearance of Citrobacter rodentium. *Mucosal Immunology,* 12**,** 761-771.

Sämann, A., Tajiyeva, O., Müller, N., Tschauner, T., Hoyer, H., Wolf, G. & Müller, U. A. 2008. Prevalence of the diabetic foot syndrome at the primary care level in Germany: a cross-sectional study. *Diabetic Medicine,* 25**,** 557-563.

Sarahrudi, K., Thomas, A., Mousavi, M., Kaiser, G., Köttstorfer, J., Kecht, M., Hajdu, S. & Aharinejad, S. 2011. Elevated transforming growth factor-beta 1 (TGF-β1) levels in human fracture healing. *Injury,* 42**,** 833-837.

Sassi, F., Buondonno, I., Luppi, C., Spertino, E., Stratta, E., Di Stefano, M., Ravazzoli, M., Isaia, G., Trento, M., Passera, P., Porta, M., Isaia, G. C. & D'amelio, P. 2018. Type 2 diabetes affects bone cells precursors and bone turnover. *BMC Endocrine Disorders,* 18**,** 55.

Schedel, F., Mayer-Hain, S., Pappelbaum, K. I., Metze, D., Stock, M., Goerge, T., Loser, K., Sunderkötter, C., Luger, T. A. & Weishaupt, C. 2020. Evidence and impact of neutrophil extracellular traps in malignant melanoma. *Pigment Cell & Melanoma Research,* 33**,** 63-73.

Schlundt, C., El Khassawna, T., Serra, A., Dienelt, A., Wendler, S., Schell, H., Van Rooijen, N., Radbruch, A., Lucius, R., Hartmann, S., Duda, G. N. & Schmidt-Bleek, K. 2018. Macrophages in bone fracture healing: Their essential role in endochondral ossification. *Bone,* 106**,** 78-89.

Schmidt-Bleek, K., Schell, H., Kolar, P., Pfaff, M., Perka, C., Buttgereit, F., Duda, G. & Lienau, J. 2009. Cellular composition of the initial fracture hematoma compared to a muscle hematoma: a study in sheep. *The Journal of Orthopaedic Research,* 27**,** 1147-1151.

Schmidt-Bleek, K., Schell, H., Schulz, N., Hoff, P., Perka, C., Buttgereit, F., Volk, H. D., Lienau, J. & Duda, G. N. 2012. Inflammatory phase of bone healing initiates the regenerative healing cascade. *Cell and Tissue Research,* 347**,** 567-73.

Schwartz, A. V., Vittinghoff, E., Bauer, D. C., Hillier, T. A., Strotmeyer, E. S., Ensrud, K. E., Donaldson, M. G., Cauley, J. A., Harris, T. B., Koster, A., Womack, C. R., Palermo, L. & Black, D. M. 2011. Association of BMD and FRAX score with risk of fracture in older adults with type 2 diabetes. *JAMA,* 305**,** 2184-2192.

Semeraro, F., Ammollo, C. T., Morrissey, J. H., Dale, G. L., Friese, P., Esmon, N. L. & Esmon, C. T. 2011. Extracellular histones promote thrombin generation through platelet-dependent mechanisms: involvement of platelet TLR2 and TLR4. *Blood,* 118**,** 1952-1961.

Seri, Y., Shoda, H., Suzuki, A., Matsumoto, I., Sumida, T., Fujio, K. & Yamamoto, K. 2015. Peptidylarginine deiminase type 4 deficiency reduced arthritis severity in a glucose-6-phosphate isomerase-induced arthritis model. *Scientific Reports,* 5**,** 13041.

Sharma, A., Muir, R., Johnston, R., Carter, E., Bowden, G. & Wilson-Macdonald, J. 2013. Diabetes is predictive of longer hospital stay and increased rate of complications in spinal surgery in the UK. *Annals of the Royal College of Surgeons of England,* 95**,** 275-279.

Shastry, B. S. 2007. SNPs in disease gene mapping, medicinal drug development and evolution. *Journal of Human Genetics,* 52**,** 871-880.

Simader, E., Beer, L., Laggner, M., Vorstandlechner, V., Gugerell, A., Erb, M., Kalinina, P., Copic, D., Moser, D., Spittler, A., Tschachler, E., Jan Ankersmit, H. & Mildner, M. 2019. Tissue-regenerative potential of the secretome of γ-irradiated peripheral blood mononuclear cells is mediated via TNFRSF1B-induced necroptosis. *Cell Death Dis,* 10**,** 729.

Sodré, F. M. C., Bissenova, S., Bruggeman, Y., Tilvawala, R., Cook, D. P., Berthault, C., Mondal, S., Callebaut, A., You, S., Scharfmann, R., Mallone, R., Thompson, P. R., Mathieu, C., Buitinga, M. & Overbergh, L. 2021. Peptidylarginine Deiminase Inhibition Prevents Diabetes Development in NOD Mice. *Diabetes,* 70**,** 516-528.

Soongsathitanon, J., Umsa-Ard, W. & Thongboonkerd, V. 2019. Proteomic analysis of peripheral blood polymorphonuclear cells (PBMCs) reveals alteration of neutrophil extracellular trap (NET) components in uncontrolled diabetes. *Molecular and Cellular Biochemistry,* 461**,** 1-14.

Sorvillo, N., Mizurini, D. M., Coxon, C., Martinod, K., Tilvawala, R., Cherpokova, D., Salinger, A. J., Seward, R. J., Staudinger, C., Weerapana, E., Shapiro, N. I., Costello, C. E., Thompson, P. R. & Wagner, D. D. 2019. Plasma Peptidylarginine Deiminase IV Promotes VWF-Platelet String Formation and Accelerates Thrombosis After Vessel Injury. *Circ Res,* 125**,** 507-519.

Speziale, P. & Pietrocola, G. 2021. Staphylococcus aureus induces neutrophil extracellular traps (NETs) and neutralizes their bactericidal potential. *Computational and Structural Biotechnology Journal,* 19**,** 3451-3457.

Stakos, D. A., Kambas, K., Konstantinidis, T., Mitroulis, I., Apostolidou, E., Arelaki, S., Tsironidou, V., Giatromanolaki, A., Skendros, P., Konstantinides, S. & Ritis, K. 2015. Expression of functional tissue factor by neutrophil extracellular traps in culprit artery of acute myocardial infarction. *European Heart Journal,* 36**,** 1405-1414.

Stefanowski, J., Lang, A., Rauch, A., Aulich, L., Köhler, M., Fiedler, A. F., Buttgereit, F., Schmidt-Bleek, K., Duda, G. N., Gaber, T., Niesner, R. A. & Hauser, A. E. 2019. Spatial Distribution of Macrophages During Callus Formation and Maturation Reveals Close Crosstalk Between Macrophages and Newly Forming Vessels. *Frontiers in Immunology,* 10.

Stegenga, M. E., Van Der Crabben, S. N., Blümer, R. M. E., Levi, M., Meijers, J. C. M., Serlie, M. J., Tanck, M. W. T., Sauerwein, H. P. & Van Der Poll, T. 2008. Hyperglycemia enhances coagulation and reduces neutrophil degranulation, whereas hyperinsulinemia inhibits fibrinolysis during human endotoxemia. *Blood,* 112**,** 82-89.

Sunahara, K. K. S., Sannomiya, P. & Martins, J. O. 2012. Briefs on Insulin and Innate Immune Response. *Cellular Physiology and Biochemistry,* 29**,** 1-8.

Suzuki, A., Yamada, R., Chang, X., Tokuhiro, S., Sawada, T., Suzuki, M., Nagasaki, M., Nakayama-Hamada, M., Kawaida, R., Ono, M., Ohtsuki, M., Furukawa, H., Yoshino, S., Yukioka, M., Tohma, S., Matsubara, T., Wakitani, S., Teshima, R., Nishioka, Y., Sekine, A., Iida, A., Takahashi, A., Tsunoda, T., Nakamura, Y. & Yamamoto, K. 2003. Functional haplotypes of PADI4, encoding citrullinating enzyme peptidylarginine deiminase 4, are associated with rheumatoid arthritis. *Nat Genet,* 34**,** 395-402.

Tang, Y., Wu, X., Lei, W., Pang, L., Wan, C., Shi, Z., Zhao, L., Nagy, T. R., Peng, X., Hu, J., Feng, X., Van Hul, W., Wan, M. & Cao, X. 2009. TGF-beta1-

induced migration of bone mesenchymal stem cells couples bone resorption with formation. *Nature Medicine,* 15**,** 757-65.

Tatsiy, O., Mayer, T. Z., De Carvalho Oliveira, V., Sylvain-Prévost, S., Isabel, M., Dubois, C. M. & Mcdonald, P. P. 2019. Cytokine Production and NET Formation by Monosodium Urate-Activated Human Neutrophils Involves Early and Late Events, and Requires Upstream TAK1 and Syk. *Frontiers in Immunology,* 10**,** 2996.

Tatsiy, O. & Mcdonald, P. P. 2018. Physiological Stimuli Induce PAD4-Dependent, ROS-Independent NETosis, With Early and Late Events Controlled by Discrete Signaling Pathways. *Front Immunol,* 9**,** 2036.

Tessaro, F. H. G., Ayala, T. S., Nolasco, E. L., Bella, L. M. & Martins, J. O. 2017. Insulin Influences LPS-Induced TNF-α and IL-6 Release Through Distinct Pathways in Mouse Macrophages from Different Compartments. *Cellular Physiology and Biochemistry,* 42**,** 2093-2104.

Thakur, S., Cattoni, D. I. & Nollmann, M. 2015. The fluorescence properties and binding mechanism of SYTOX green, a bright, low photo-damage DNA intercalating agent. *European Biophysics Journal,* 44**,** 337-348.

Thiam, H. R., Wong, S. L., Qiu, R., Kittisopikul, M., Vahabikashi, A., Goldman, A. E., Goldman, R. D., Wagner, D. D. & Waterman, C. M. 2020. NETosis proceeds by cytoskeleton and endomembrane disassembly and PAD4-mediated chromatin decondensation and nuclear envelope rupture. *proceedings of the national academy of sciences of the united states of america,* 117**,** 7326-7337.

Timlin, M., Toomey, D., Condron, C., Power, C., Street, J., Murray, P. & Bouchier-Hayes, D. 2005. Fracture Hematoma Is a Potent Proinflammatory Mediator of Neutrophil Function. *Journal of Trauma and Acute Care Surgery,* 58**,** 1223-1229.

Toben, D., Schroeder, I., El Khassawna, T., Mehta, M., Hoffmann, J. E., Frisch, J. T., Schell, H., Lienau, J., Serra, A., Radbruch, A. & Duda, G. N. 2011. Fracture healing is accelerated in the absence of the adaptive immune system. *Journal of Bone and Mineral Research,* 26**,** 113-24.

Tsourouktsoglou, T.-D., Warnatsch, A., Ioannou, M., Hoving, D., Wang, Q. & Papayannopoulos, V. 2020. Histones, DNA, and Citrullination Promote Neutrophil Extracellular Trap Inflammation by Regulating the Localization and Activation of TLR4. *Cell Reports,* 31**,** 107602.

Ulrich, S., Holle, R., Wacker, M., Stark, R., Icks, A., Thorand, B., Peters, A. & Laxy, M. 2016. Cost burden of type 2 diabetes in Germany: results from the population-based KORA studies. *BMJ Open,* 6**,** e012527.

Van Den Berghe, G., Wouters, P., Weekers, F., Verwaest, C., Bruyninckx, F., Schetz, M., Vlasselaers, D., Ferdinande, P., Lauwers, P. & Bouillon, R. 2001. Intensive insulin therapy in critically ill patients. *New England Journal of Medicine,* 345**,** 1359-67.

Varjú, I. & Kolev, K. 2019. Networks that stop the flow: A fresh look at fibrin and neutrophil extracellular traps. *Thrombosis Research,* 182**,** 1-11.

Veloso, C. A., Isoni, C. A., Borges, E. A., Mattos, R. T., Calsolari, M. R., Reis, J. S., Bosco, A. A., Chaves, M. M. & Nogueira-Machado, J. A. 2008. Inhibition of ROS production in peripheral blood mononuclear cells from

type 2 diabetic patients by autologous plasma depends on Akt/PKB signaling pathway. *Clinica Chimica Acta,* 394**,** 77-80.

Von Brühl, M.-L., Stark, K., Steinhart, A., Chandraratne, S., Konrad, I., Lorenz, M., Khandoga, A., Tirniceriu, A., Coletti, R., Köllnberger, M., Byrne, R. A., Laitinen, I., Walch, A., Brill, A., Pfeiler, S., Manukyan, D., Braun, S., Lange, P., Riegger, J., Ware, J., Eckart, A., Haidari, S., Rudelius, M., Schulz, C., Echtler, K., Brinkmann, V., Schwaiger, M., Preissner, K. T., Wagner, D. D., Mackman, N., Engelmann, B. & Massberg, S. 2012. Monocytes, neutrophils, and platelets cooperate to initiate and propagate venous thrombosis in mice in vivo. *journal of experimental medicine,* 209**,** 819-835.

Von Der Helm, K., Gürtler, L., Eberle, J. & Deinhardt, F. 1989. Inhibition of HIV replication in cell culture by the specific aspartic protease inhibitor pepstatin A. *FEBS Letters,* 247**,** 349-352.

Von Köckritz-Blickwede, M., Blodkamp, S. & Nizet, V. 2016. Interaction of Bacterial Exotoxins with Neutrophil Extracellular Traps: Impact for the Infected Host. *Frontiers in Microbiology,* 7**,** 402.

Vorobjeva, N. V. 2020. Neutrophil Extracellular Traps: New Aspects. *Moscow University Biological Sciences Bulletin,* 75**,** 173-188.

Vorobjeva, N. V. & Chernyak, B. V. 2020. NETosis: Molecular Mechanisms, Role in Physiology and Pathology. *Biochemistry (Moscow),* 85**,** 1178-1190.

Walters, G., Pountos, I. & Giannoudis, P. V. 2018. The cytokines and micro-environment of fracture haematoma: Current evidence. *J Tissue Eng Regen Med,* 12**,** e1662-e1677.

Wang, J., Li, Q., Yin, Y., Zhang, Y., Cao, Y., Lin, X., Huang, L., Hoffmann, D., Lu, M. & Qiu, Y. 2020. Excessive Neutrophils and Neutrophil Extracellular Traps in COVID-19. *Frontiers in Immunology,* 11**,** 2063.

Wang, L., Zhou, X., Yin, Y., Mai, Y., Wang, D. & Zhang, X. 2018. Hyperglycemia Induces Neutrophil Extracellular Traps Formation Through an NADPH Oxidase-Dependent Pathway in Diabetic Retinopathy. *Frontiers in Immunology,* 9**,** 3076.

Wang, S. & Wang, Y. 2013. Peptidylarginine deiminases in citrullination, gene regulation, health and pathogenesis. *Biochimica Biophysica Acta,* 1829**,** 1126-35.

Wang, Y.-N., Jia, T., Zhang, J., Lan, J., Zhang, D. & Xu, X. 2019. PTPN2 improves implant osseointegration in T2DM via inducing the dephosphorylation of ERK. *Experimental Biology and Medicine,* 244**,** 1493-1503.

Wasnik, S., Rundle, C. H., Baylink, D. J., Yazdi, M. S., Carreon, E. E., Xu, Y., Qin, X., Lau, K. W. & Tang, X. 2018. 1,25-Dihydroxyvitamin D suppresses M1 macrophages and promotes M2 differentiation at bone injury sites. *JCI Insight,* 3**,** e98773.

Weng, W., Häussling, V., Aspera-Werz, R. H., Springer, F., Rinderknecht, H., Braun, B., Küper, M. A., Nussler, A. K. & Ehnert, S. 2020. Material-Dependent Formation and Degradation of Bone Matrix-Comparison of Two Cryogels. *Bioengineering (Basel),* 7**,** 52.

Winterbourn, C. C. & Kettle, A. J. 2012. Redox Reactions and Microbial Killing in the Neutrophil Phagosome. *Antioxidants & Redox Signaling,* 18**,** 642-660.

Wintermeyer, E., Ihle, C., Ehnert, S., Schreiner, A. J., Stollhof, L., Stockle, U., Nussler, A., Fritsche, A. & Pscherer, S. 2019. Assessment of the Influence of Diabetes mellitus and Malnutrition on the Postoperative Complication Rate and Quality of Life of Patients in a Clinic Focused on Trauma Surgery. *Zeitschrift für Orthopädie und Unfallchirurgie,* 157**,** 173-182.

Wintermeyer, E., Ihle, C., Ehnert, S., Stockle, U., Ochs, G., De Zwart, P., Flesch, I., Bahrs, C. & Nussler, A. K. 2016. Crucial Role of Vitamin D in the Musculoskeletal System. *Nutrients,* 8**,** 319.

Wintges, K., Beil, F. T., Albers, J., Jeschke, A., Schweizer, M., Claass, B., Tiegs, G., Amling, M. & Schinke, T. 2013. Impaired bone formation and increased osteoclastogenesis in mice lacking chemokine (C-C motif) ligand 5 (Ccl5). *Journal of Bone and Minereral Research,* 28**,** 2070-2080.

Wittmann, A., Lamprinaki, D., Bowles, K. M., Katzenellenbogen, E., Knirel, Y. A., Whitfield, C., Nishimura, T., Matsumoto, N., Yamamoto, K., Iwakura, Y., Saijo, S. & Kawasaki, N. 2016. Dectin-2 Recognizes Mannosylated O-antigens of Human Opportunistic Pathogens and Augments Lipopolysaccharide Activation of Myeloid Cells*. *Journal of Biological Chemistry,* 291**,** 17629-17638.

Wong, S. L., Demers, M., Martinod, K., Gallant, M., Wang, Y., Goldfine, A. B., Kahn, C. R. & Wagner, D. D. 2015. Diabetes primes neutrophils to undergo NETosis, which impairs wound healing. *Nature Medicine,* 21**,** 815-819.

Wong, S. L. & Wagner, D. D. 2018. Peptidylarginine deiminase 4: a nuclear button triggering neutrophil extracellular traps in inflammatory diseases and aging. *FASEB Journal***,** 6358-6370.

Wright, F. A., Strug, L. J., Doshi, V. K., Commander, C. W., Blackman, S. M., Sun, L., Berthiaume, Y., Cutler, D., Cojocaru, A., Collaco, J. M., Corey, M., Dorfman, R., Goddard, K., Green, D., Kent, J. W., Lange, E. M., Lee, S., Li, W., Luo, J., Mayhew, G. M., Naughton, K. M., Pace, R. G., Paré, P., Rommens, J. M., Sandford, A., Stonebraker, J. R., Sun, W., Taylor, C., Vanscoy, L. L., Zou, F., Blangero, J., Zielenski, J., O'neal, W. K., Drumm, M. L., Durie, P. R., Knowles, M. R. & Cutting, G. R. 2011. Genome-wide association and linkage identify modifier loci of lung disease severity in cystic fibrosis at 11p13 and 20q13.2. *Nature Genetics,* 43**,** 539-546.

Xing, Z., Lu, C., Hu, D., Yu, Y. Y., Wang, X., Colnot, C., Nakamura, M., Wu, Y., Miclau, T. & Marcucio, R. S. 2010. Multiple roles for CCR2 during fracture healing. *Disease Models & Mechisms,* 3**,** 451-458.

Yang, L., Liu, Q., Zhang, X., Liu, X., Zhou, B., Chen, J., Huang, D., Li, J., Li, H., Chen, F., Liu, J., Xing, Y., Chen, X., Su, S. & Song, E. 2020. DNA of neutrophil extracellular traps promotes cancer metastasis via CCDC25. *Nature,* 583**,** 133-138.

Yang, S., Qi, H., Kan, K., Chen, J., Xie, H., Guo, X. & Zhang, L. 2017. Neutrophil Extracellular Traps Promote Hypercoagulability in Patients With Sepsis. *Shock,* 47**,** 132-139.

Yipp, B. G., Petri, B., Salina, D., Jenne, C. N., Scott, B. N. V., Zbytnuik, L. D., Pittman, K., Asaduzzaman, M., Wu, K., Meijndert, H. C., Malawista, S. E., De Boisfleury Chevance, A., Zhang, K., Conly, J. & Kubes, P. 2012. Infection-induced NETosis is a dynamic process involving neutrophil multitasking in vivo. *Nature Medicine,* 18**,** 1386-1393.

Yui, S., Osawa, Y., Ichisugi, T. & Morimoto-Kamata, R. 2014. Neutrophil Cathepsin G, but Not Elastase, Induces Aggregation of MCF-7 Mammary Carcinoma Cells by a Protease Activity-Dependent Cell-Oriented Mechanism. *Mediators of Inflammation,* 2014**,** 971409.

Zhang, J., Ji, C., Li, W., Mao, Z., Shi, Y., Shi, H., Ji, R., Qian, H., Xu, W. & Zhang, X. 2020. Tumor-Educated Neutrophils Activate Mesenchymal Stem Cells to Promote Gastric Cancer Growth and Metastasis. *Frontiers in Cell and Developmental Biology,* 8.

Zhang, Q., Raoof, M., Chen, Y., Sumi, Y., Sursal, T., Junger, W., Brohi, K., Itagaki, K. & Hauser, C. J. 2010. Circulating mitochondrial DAMPs cause inflammatory responses to injury. *Nature,* 464**,** 104-107.

Zhang, Y., Böse, T., Unger, R. E., Jansen, J. A., Kirkpatrick, C. J. & Van Den Beucken, J. 2017. Macrophage type modulates osteogenic differentiation of adipose tissue MSCs. *Cell and Tissue Research,* 369**,** 273-286.

Zhao, X., Gu, C. & Wang, Y. 2020. PAD4 selective inhibitor TDFA protects lipopolysaccharide-induced acute lung injury by modulating nuclear p65 localization in epithelial cells. *International Immunopharmacology,* 88**,** 106923.

Zheng, Y., Zhu, Y., Liu, X., Zheng, H., Yang, Y., Lu, Y., Zhou, H., Zheng, J. & Dong, Z. 2021. The screening of albumin as a key serum component in preventing release of neutrophil extracellular traps by selectively inhibiting mitochondrial ROS generation. *Can J Physiol Pharmacol,* 99**,** 427-438.

Zhou, Y., An, L. L., Chaerkady, R., Mittereder, N., Clarke, L., Cohen, T. S., Chen, B., Hess, S., Sims, G. P. & Mustelin, T. 2018. Evidence for a direct link between PAD4-mediated citrullination and the oxidative burst in human neutrophils. *Scietific Reports,* 8**,** 15228.

Zhu, Y., Li, Q., Zhou, Y. & Li, W. 2019. TLR activation inhibits the osteogenic potential of human periodontal ligament stem cells through Akt signaling in a Myd88- or TRIF-dependent manner. *Journal of Periodontology,* 90**,** 400-415.

8. Declaration of own contribution

The work was carried out in the Siegfried Weller Institute under the supervision of Prof. Dr. Andreas Nüssler and PD Dr. Sabrina Ehnert.

The study was designed in collaboration with Prof. Dr. Andreas Nüssler and PD Dr. Sabrina Ehnert.

All experiments were performed after familiarization by laboratory members by me independently. ARMS-PCRs were performed by Sabrina Ehnert and Bianca Braun. Bio-impedance measurements were performed under the guidance of Dr. Markus Burkard and Christian Leischner.

Statistical analysis was performed under the guidance of PD Dr. Sabrina Ehnert.

I certify that I have written the manuscript independently and that I have not used any sources other than those indicated by me.

The manuscript was under review by a paid professional English editing service (proof-reading-service.com). A version with all comments and a certificate from the service was sent to the doctoral office.

Tübingen, the 4th February 2022

Caren Linnemann

9. Publications

Y. Chen, M. M. Menger, B. J. Braun, S. Schweizer, **C. Linnemann**, K. Falldorf, M. Ronniger, H. Wang, T. Histing, A. K. Nussler, and S. Ehnert (2021) “Modulation of macrophage activity by pulsed electromagnetic fields in the context of fracture healing” Bioengineering **8** (167).

Linnemann, C., L. Savini, M. F. Rollmann, T. Histing, A. K. Nussler and S. Ehnert (2021). "Altered Secretome of Diabetic Monocytes Could Negatively Influence Fracture Healing—An In Vitro Study." Int J Mol Sci **22**(17). IF 4.556

Ehnert, S., B. Relja, K. Schmidt-Bleek, V. Fischer, A. Ignatius, **C. Linnemann**, H. Rinderknecht, M. Huber-Lang, M. Kalbitz, T. Histing and A. K. Nussler (2021). "Effects of immune cells on mesenchymal stem cells during fracture healing." World J Stem Cells **13**(11): 1667-1695. IF 3.231

Rinderknecht, H., S. Ehnert, B. Braun, T. Histing, A. K. Nussler and **C. Linnemann** (2021). "The Art of Inducing Hypoxia." Oxygen **1**(1).

Linnemann, C., S. Venturelli, F. Konrad, A. K. Nussler and S. Ehnert (2020). "Bio-impedance measurement allows displaying the early stages of neutrophil extracellular traps." Excli j **19**: 1481-1495. IF 2.837

Ehnert, S., **C. Linnemann**, R. H. Aspera-Werz, V. Häussling, B. Braun, W. Weng, S. Zhu, K. C. Ngamsri and A. Nussler (2020). "Feasibility of Cell Lines for In Vitro Co-Cultures Models for Bone Metabolism." SciMedicine Journal **2**(3): 157-181.

Ehnert, S., **C. Linnemann**, B. Braun, J. Botsch, K. Leibiger, P. Hemmann and A. A. K. Nussler (2019). "One-Step ARMS-PCR for the Detection of SNPs-Using the Example of the PADI4 Gene." Methods Protoc **2**(3).

Ruoss, M., V. Kieber, S. Rebholz, **C. Linnemann**, H. Rinderknecht, V. Haussling, M. Hacker, L. H. H. Olde Damink, S. Ehnert and A. K. Nussler (2019). "Cell-Type-Specific Quantification of a Scaffold-Based 3D Liver Co-Culture." Methods Protoc **3**(1).

Geisler, S., L. Jager, S. Golombek, E. Nakanishi, F. Hans, N. Casadei, A. L. Terradas, **C. Linnemann** and P. J. Kahle (2019). "Ubiquitin-specific protease USP36 knockdown impairs Parkin-dependent mitophagy via downregulation of Beclin-1-associated autophagy-related ATG14L." Exp Cell Res **384**(2): 111641. IF 3.905

Reumann, M. K., **C. Linnemann**, R. H. Aspera-Werz, S. Arnold, M. Held, C. Seeliger, A. K. Nussler and S. Ehnert (2018). "Donor Site Location Is Critical for Proliferation, Stem Cell Capacity, and Osteogenic Differentiation of Adipose Mesenchymal Stem/Stromal Cells: Implications for Bone Tissue Engineering." Int J Mol Sci **19**(7). IF 4.556

Ehnert, S., **C. Linnemann**, R. H. Aspera-Werz, D. Bykova, S. Biermann, L. Fecht, P. M. De Zwart, A. K. Nussler and F. Stuby (2018). "Immune Cell Induced Migration of Osteoprogenitor Cells Is Mediated by TGF-beta Dependent Upregulation of NOX4 and Activation of Focal Adhesion Kinase." Int J Mol Sci **19**(8). IF 4.556

Acknowledgement

I would like to sincerely thank Prof. Nüssler who gave me the opportunity to do my PhD at the Siegfried Weller Institute. He strongly encouraged me and helped me become a better scientist. Special thanks to Sabrina Ehnert who was supporting me and my project a lot, always sharing my enthusiasm for the work, and bringing new ideas.

I would like to thank my fellow PhD colleagues Romina, Marc, Helen, and Victor who always had good advice and knew how to deal with setbacks in PhD life. Special thanks to Helen who was always the one to ask for quick advice just across the table. Also, great thanks to my Chinese fellows (Lu, Liu, Weidong, Yangmengfan, and Tao) with whom I had some great experiences, shared a lot of laughter, and learned a lot about the Chinese and also the German culture.

I would like to thank all the students (Ronja, Sara, Annick, Alicia, Lina, Umut, Jonas, Heiko, Andrè, Josefine) who joined me in parts of the project and always brought new enthusiasm into it. Special thanks to Jonas, Sara, and Charlotte for giving me the chance to learn a lot about teaching and motivating others.

I would like to thank Melanie, Wiebke Eisler, and Franziska Konrad with whom I had the chance to participate in an interesting collaboration. Thanks to Sascha Venturelli, Markus Burkhard, and Christian Leischner for giving me the opportunity to perform my bio-impedance measurements.

I am severely grateful for the support of the Studienstiftung des deutschen Volkes which financed my work and gave me the opportunity to be part of a nice community.

Lastly, I would like to give my severe thanks to all those who supported me during my thesis and reminded me that distraction is sometimes useful: my family, my friends, and my tennis team.

Supplementary information

I. Confirmation of neutrophil isolation

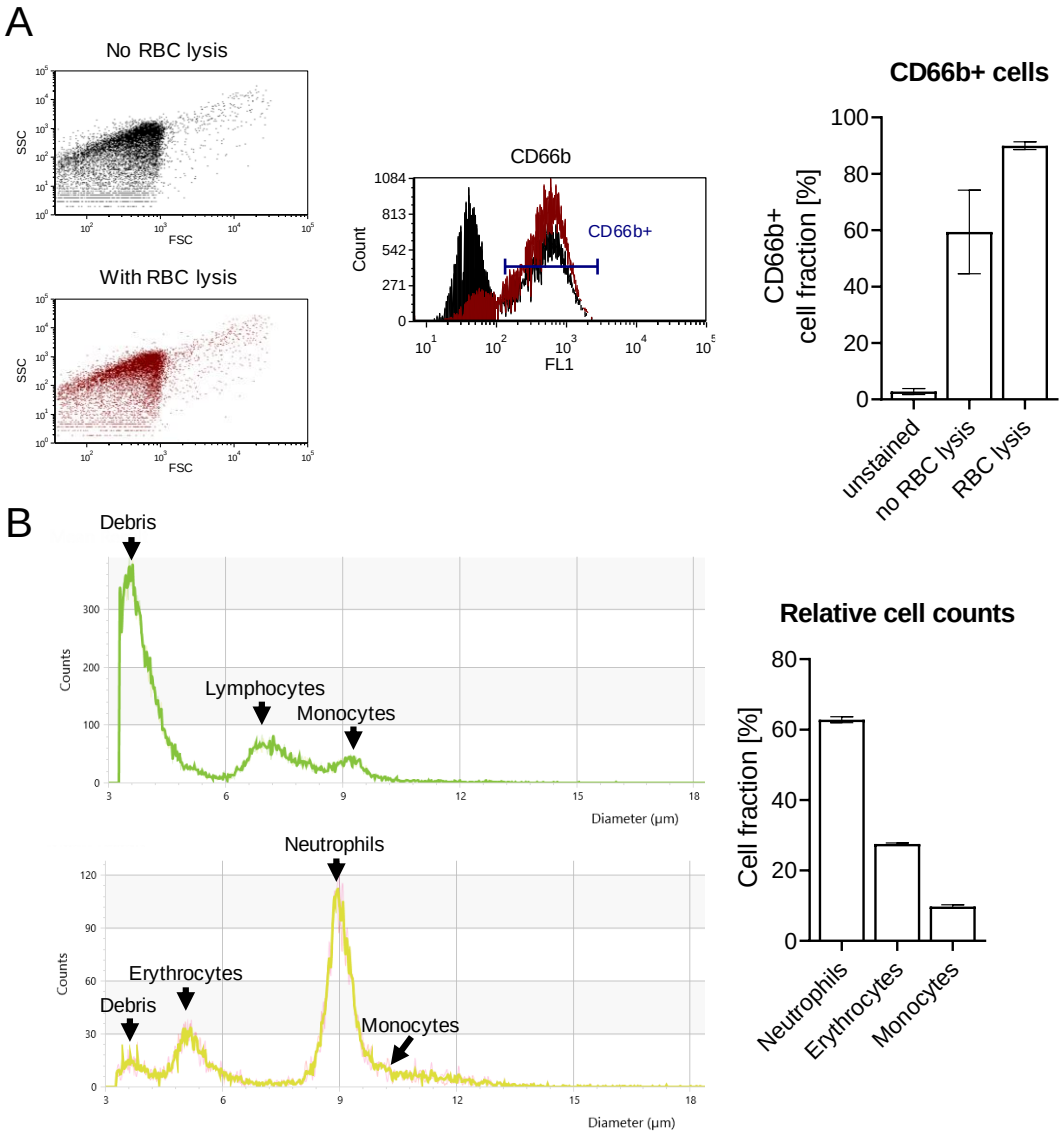

Supplementary Figure 1: Flow cytometry of isolated neutrophils with and without red blood cell lysis and analysis of isolated neutrophils in the CASY device (Omni Life Sciences, OLS, Bremen, Germany). **(A)** Flow cytometry analysis for CD66b. Neutrophils were isolated and stained with the FITC-CD66b antibody (Miltenyi Biotech, Bergisch Gladbach, Germany) in flow cytometry buffer (PBS with 0.5% BSA, 2 mM EDTA). Immediately after staining, cells were measured in a CyFlow Cube 8 (Sysmex, Norderstedt, Germany). Cell size was determined by SSC against FCS (left panel). Red indicates neutrophils with RBC lysis; black indicates no RBC lysis. RBC were lysed by hypotonic lysis (2 min in $(NH_4)_2HCO_3$ buffer). CD66b+ cells were measured in the FL1 channel (Ex. 488 nm, middle panel), and the positive fraction was determined as indicated. The percentage of CD66b+ cells is shown in the right panel. N=2, n=2. **(B)** Cellular fractions were analyzed after isolation with Lympholyte-poly medium and subsequent washing in the CASY device. Ten microliters of freshly isolated cells were measured, and cellular fractions were determined according to size. The upper panel shows the PBMC fraction, and the lower panel shows the neutrophil fraction. The right panel shows the relative cell counts in the neutrophil fraction. N=3, n=3.

II. Test of different housekeeping genes in stimulated neutrophils

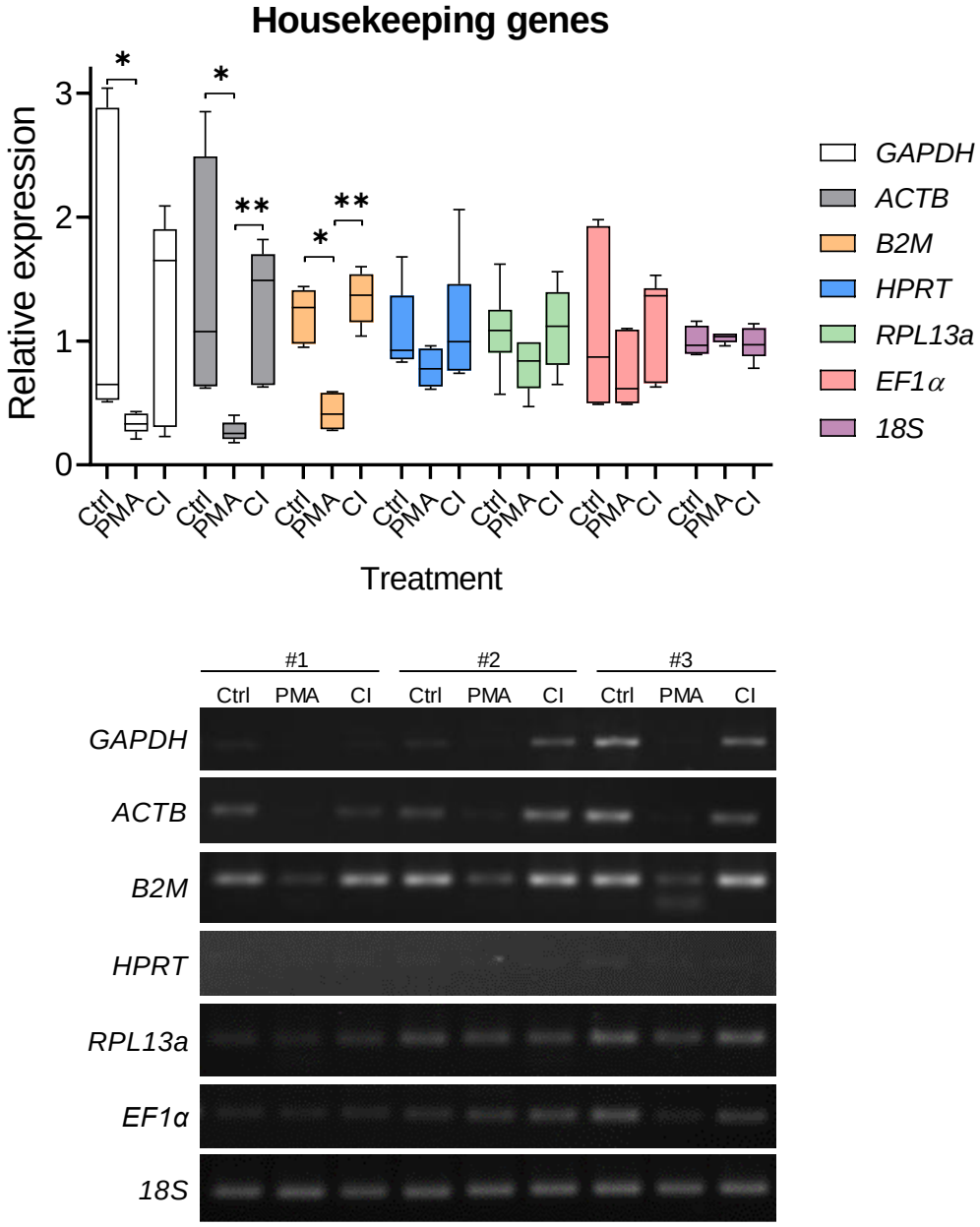

Supplementary Figure 2: Test of different housekeeping genes in stimulated neutrophils. Neutrophils were stimulated with 100 PMA or 4 µM CI for 3 h, and then RNA was isolated. Complementary DNA (cDNA) was synthesized by using the First Strand cDNA Synthesis Kit (Thermo Fisher Scientific) according to the manufacturer's instructions. PCR was done with Biozym Red HS Mastermix with previously established PCR conditions. *p<0.05, **p<0.01. N=3, n=3.

III. Determining the appropriate non-toxic concentration of DNase, protease inhibitors, and proteinase K for SCP-1 treatment

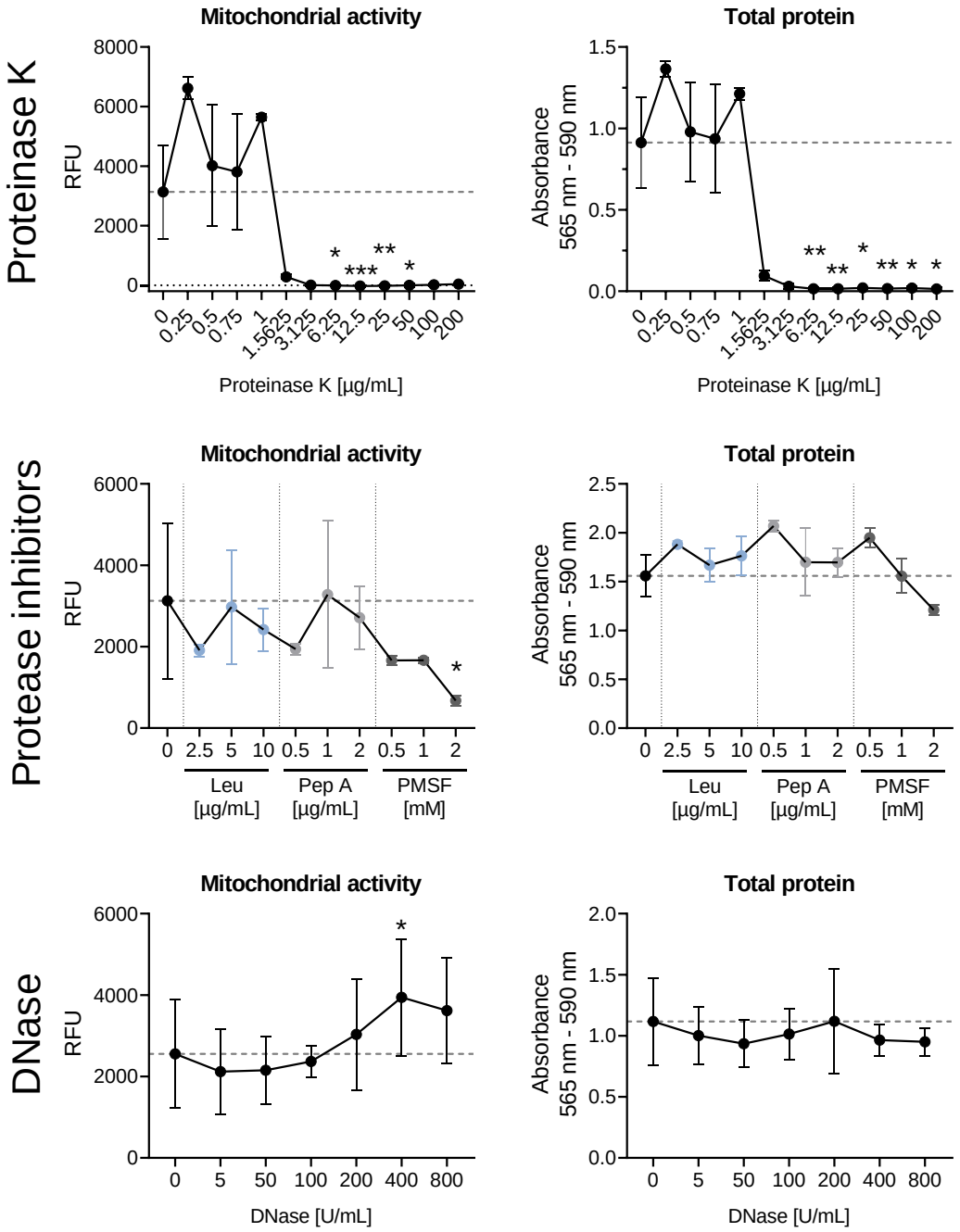

Supplementary Figure 3: Supplementary Figure 4: Determination of the appropriate DNase, protease inhibitor, and proteinase K concentrations that do not exert toxicity on SCP-1 cells. SCP-1 cells were treated with the indicated concentrations of proteinase K (upper panel), protease inhibitors (middle panel), or DNase (lower panel) and incubated for 48 h. Mitochondrial activity was measured by resazurin conversion (left panel), and total protein content was determined by SRB staining (right panel). N=3, n=3. *p<0.05, **p<0.01, ***p<0.001. Data are shown as the mean ± standard deviation.

IV. Analysis of HL-60 cells as a model system for NET formation of neutrophils

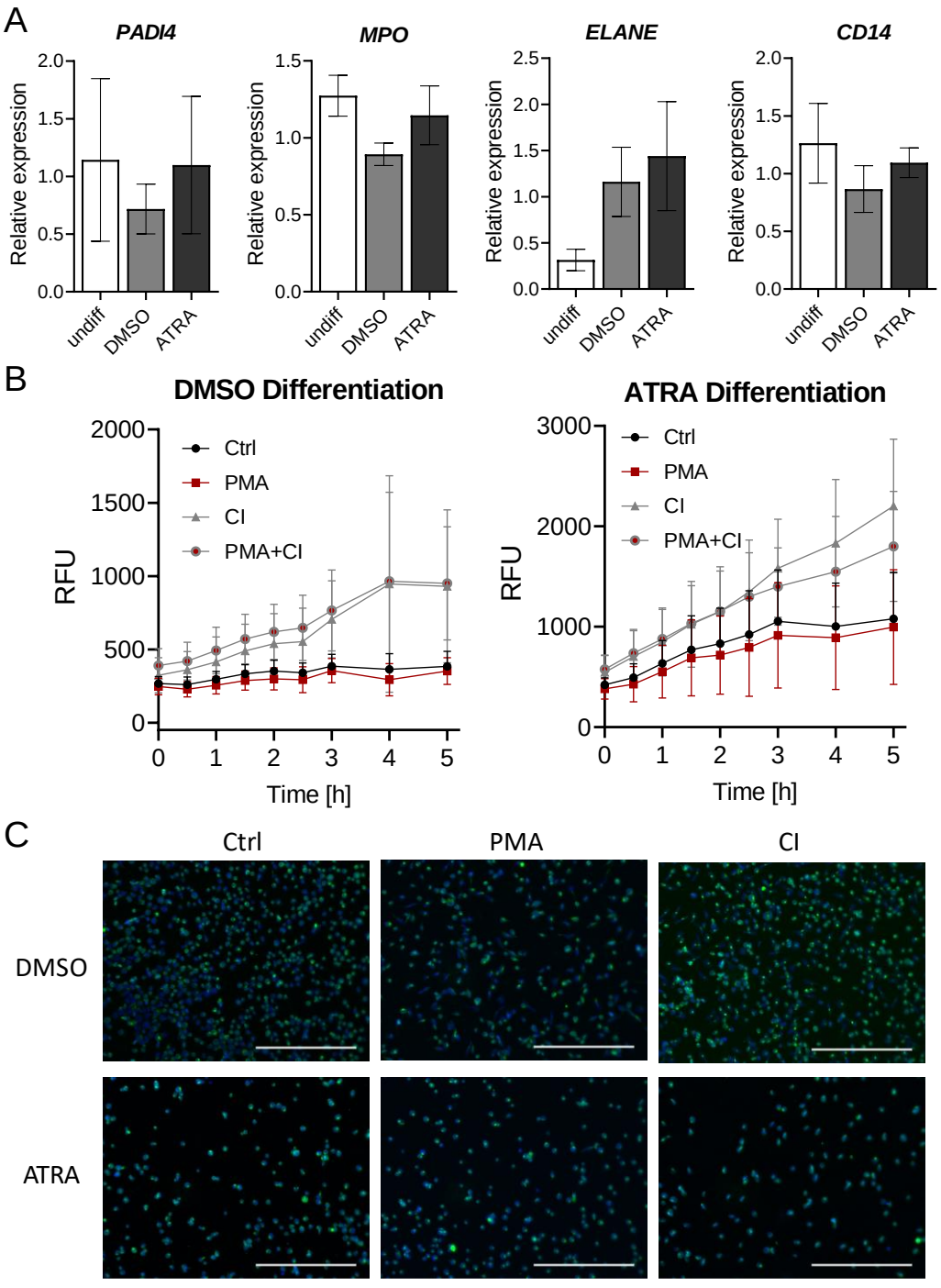

Supplementary Figure 5: Differentiation of HL-60 cells with DMSO or ATRA. HL-60 cells were differentiated into granulocytes and tested for their granulocyte markers and ability to release NETs. **(A)** Expression of different neutrophil (*PAD4*, *MPO*, *ELANE*) and monocyte (*CD14*) markers after 6 days of differentiation with 1.25% DMSO or 1 µM ATRA or no differentiation (undiff); N=3, n=3. **(B)** Analysis of NET release by the Sytox Green Assay of DMSO (left) and ATRA (right) differentiated HL-60 cells. (C) Analysis of NET formation by immunofluorescence analysis. Green: MPO; blue: Hoechst 3342 (DNA). The scale bar is 200 µm. Data are shown as the mean ± standard deviation.

V. Macros for NET formation analysis *via* immunofluorescence

Macro DAPI:

```
run("8-bit");
run("Auto Local Threshold", "method=Bernsen radius=7.5 parameter_1=35 parameter_2=0 white");
run("Analyze Particles...", "size=20-Infinity display exclude summarize");
```

Macro GFP:

```
run("8-bit");
run("Auto Local Threshold", "method=Bernsen radius=8 parameter_1=10 parameter_2=0 white");
run("Analyze Particles...", "size=80-Infinity circularity=0.00-0.2 display exclude summarize");
```

VI. EC_{50} calculation of NETs on SCP-1

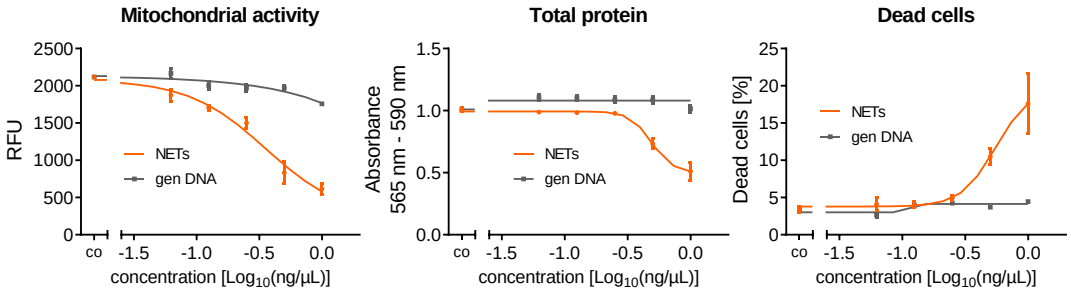

Supplementary Figure 6: EC_{50} calculation for the effects of NETs on SCP-1 cells. The graphs represent mitochondrial activity (resazurin conversion after 48-h incubation), total protein content (SRB staining), and percentage of dead cells (LDH release) plotted against the log_{10} of the concentration of NETs in ng/µL. EC_{50} was determined with GraphPad Prism 8. N=3, n=3. Data are shown as the mean ± standard error of the mean.

VII. Effect of NETs from high glucose conditions on SCP-1 cells

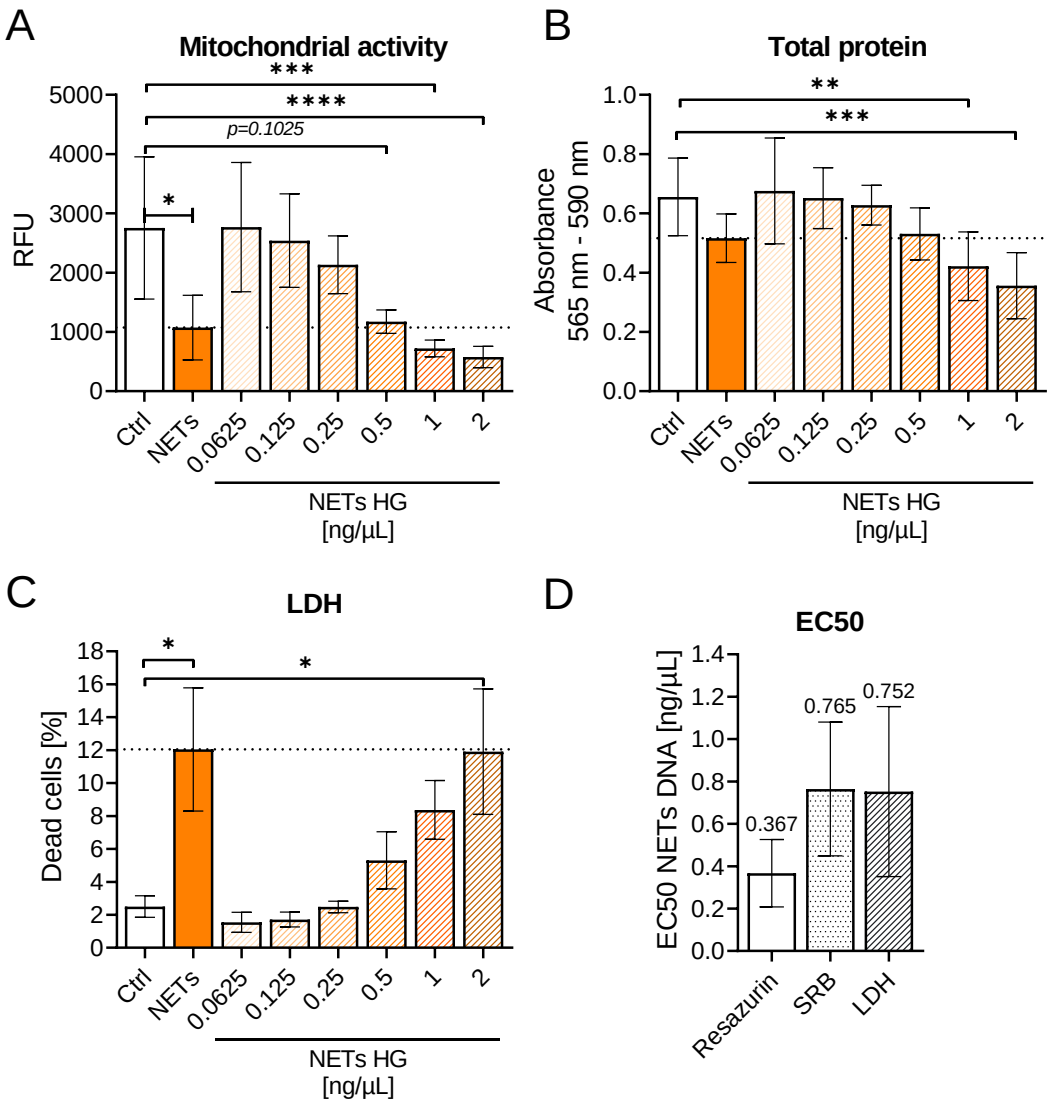

Supplementary Figure 7: NETs from HG conditions show no difference to NETs from normal glucose conditions. NETs were prepared from neutrophils of healthy volunteers with stimulation in HG (25 mM) conditions. NETs were isolated as described, and SCP-1 cells were incubated for 48 h with the HG NETs (NETs HG) and an appropriate control (NETs). **(A)** Mitochondrial activity determined by resazurin conversion. **(B)** Total protein content determined by SRB staining. **(C)** The dead cell content determined by measuring released LDH. **(D)** Calculated EC_{50} for HG NETs. N=3, n=3. *p<0.05, **p<0.01, ***p<0.001, ****p<0.0001. Data are shown as the mean ± standard deviation.

.

VIII. Effect of SCP-1 supernatant on NET formation

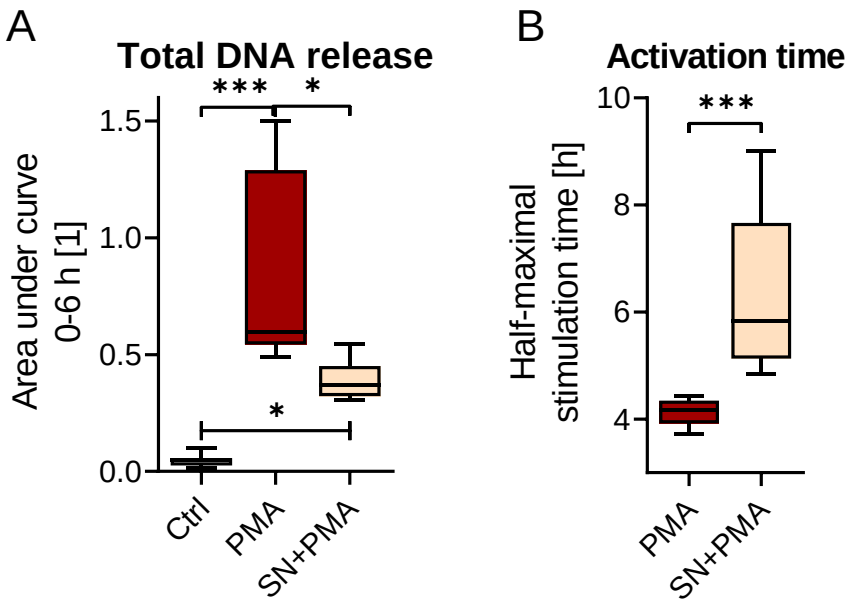

Supplementary Figure 8: Effect of SCP-1 supernatant on PMA-induced NET formation. NET release was measured by the Sytox Green Assay. SCP-1 supernatant was collected after 48-h incubation in differentiation medium. Neutrophils were stimulated with 50% RPMI medium with 50% conditioned medium/MEM-α as well as 100 nM PMA (PMA, SN+PMA). DNA release was measured for 6 h. **(A)** Total DNA release was measured by calculating the AUC. **(B)** Activation time was calculated from the half-maximal stimulation time of the Sytox Green time course. N=3, n=3. *p<0.05, ***p<0.001.